Topological states of matter in low dimensions

Christian Spånslätt

Academic dissertation for the Degree of Doctor of Philosophy in Theoretical Physics at Stockholm University to be publicly defended on Wednesday 30 May 2018 at 13.00 in lecture room FB42, AlbaNova universitetscentrum, Roslagstullsbacken 21.

Abstract

A central theme in condensed matter physics is the classification and characterization of states of matter. In the recent decades, it has become evident that there exists a large class of quantum mechanical systems that must be classified according to properties deeply rooted in the mathematical field of topology, rather than in terms of which symmetries they break. Together with rapid technological developments, such topological states of matter pose a promising path for a fundamentally new generation of quantum devices and exotically engineered materials, with applications in quantum metrology, quantum sensing, and quantum computations.

This doctoral thesis comprises a study of a general theoretical framework describing topological states of matter, followed by applications in systems of low dimension. Together, these two parts form the foundation for the following accompanying papers:

PAPERS I-II concerns Majorana zero modes in various Josephson junction setups of one-dimensional topological superconductors. In addition to determining the mathematical conditions for the existence of such exotic states, the papers also provide experimental proposals for their detection.

PAPER III deals with the nature of a widely used model of a synthetically engineered one-dimensional topological superconductor. It is shown that in a certain parameter limit, the superconducting order parameter obtains a geometric contribution, which originates from the directional nature of the Rashba spin-orbit coupling. This geometrical dependence is argued to manifest itself in various Josephson junction setups, and in particular as a direct connection between the charge current density and the local curvature.

PAPER IV proposes a method of constructing non-local order parameters for two-dimensional Chern insulators, and describes how such operators can be used to distinguish between different topological sectors.

Stockholm 2018
http://urn.kb.se/resolve?urn=urn:nbn:se:su:diva-155166

ISBN 978-91-7797-153-5
ISBN 978-91-7797-154-2

Department of Physics

Stockholm University, 106 91 Stockholm

TOPOLOGICAL STATES OF MATTER IN LOW DIMENSIONS

Christian Spånslätt

Stockholm University

Topological states of matter in low dimensions

Christian Spånslätt

ISBN print 978-91-7797-153-5
ISBN PDF 978-91-7797-154-2

Printed in Sweden by Universitetsservice US-AB, Stockholm 2018
Distributor: Department of Physics, Stockholm University
Cover art: Bedlam of bound states

For Elin, Edith and Sam...

Abstract

A central theme in condensed matter physics is the classification and characterization of states of matter. In the recent decades, it has become evident that there exists a large class of quantum mechanical systems that must be classified according to properties deeply rooted in the mathematical field of topology, rather than in terms of which symmetries they break. Together with rapid technological developments, such topological states of matter pose a promising path for a fundamentally new generation of quantum devices and exotically engineered materials, with applications in quantum metrology, quantum sensing, and quantum computations.

This doctoral thesis comprises a study of a general theoretical framework describing topological states of matter, followed by applications in systems of low dimension. Together, these two parts form the foundation for the following accompanying papers:

PAPERS I-II concerns Majorana zero modes in various Josephson junction setups of one-dimensional topological superconductors. In addition to determining the mathematical conditions for the existence of such exotic states, the papers also provide experimental proposals for their detection.

PAPER III deals with the nature of a widely used model of a synthetically engineered one-dimensional topological superconductor. It is shown that in a certain parameter limit, the superconducting order parameter obtains a geometric contribution, which originates from the directional nature of the Rashba spin-orbit coupling. This geometrical dependence is argued to manifest itself in various Josephson junction setups, and in particular as a direct connection between the charge current density and the local curvature.

PAPER IV proposes a method of constructing non-local order parameters for two-dimensional Chern insulators, and describes how such operators can be used to distinguish between different topological sectors.

Svensk sammanfattning

Ett centralt tema inom den kondenserade materiens fysik är beskrivningen av hur materia är organiserad, det vill säga vilket tillstånd materian befinner sig i. De tre i särklass vanligaste förekommande aggregationstillstånden är gasform, vätskeform och fast form, men inom dessa tillstånd förutsäger kvantmekaniken vid extremt låga temperaturer existensen av en hel värld med mer exotiska faser såsom supraledare, vissa typer av magneter och Bose-Einstein-kondensat.

De senaste årens forskning på kvantmekaniska materiefaser har påvisat existensen av en viss typ av faser med egenskaper relaterade till det matematiska området topologi. Detta innebär att faserna är extremt tåliga mot många sorters störningar och kan därför antas vara mycket användbara inom flertalet områden, exemeplvis metrologi, lagrandet av kvantinformation eller utforskandet av kvantmekanikens grunder.

Denna doktorsavhandling handlar om det teoretiska ramverket för beskrivningen av sådana topologiska materiefaser, följt av en beskrivning om hur dessa kan förverkligas genom att manipulera fysikaliska system på nanonivå. Tillsammans utgör dessa avsnitt bakgrunden till fyra medföljande artiklar:

ARTIKLAR I-III handlar om topologiskt supraledande nanotrådar ihopkopplade i Josephson-övergångar. Sådana system förutspås innehålla en speciell typ av kvanttillstånd, “Majorana-noll-tillstånd”, som har egenskaper väldigt användbara för en potentiell kvantdator. I artiklarna härleds matematiska villkor för existensen av Majorana-tillstånden och förslag på experimentuppställningar för att påvisa deras existens.

ARTIKEL IV berör en viss typ av fysikaliska system som uppvisar kvanthalleffekten och hur de topologiska egenskaperna hos dessa kan särskiljas genom icke-lokala kvantoperatorer.

List of accompanying papers and the author's contribution

The following papers, referred to in the text by their Roman numerals, are included in this thesis.

I **Topological aspects of π phase winding junctions in superconducting wires**
C. Spånslätt, E. Ardonne, J.C. Budich, and T.H. Hansson,
J. Phys.: Condens. Matter, **27**, 405701 (2015).

I performed a large fraction of the analytical calculations in Sec. II and III, a minor part of the calculations in Sec. IV., and all of the numerical calculations. I wrote a significant part of the manuscript, except Sec. I, VI and App. C

II **Extended Majorana zero modes in a topological superconducting-normal T-junction**
C. Spånslätt and E. Ardonne,
J. Phys.: Condens. Matter, **29**, 105602 (2017).

I performed most of the analytical calculations, all of the numerical work and wrote the manuscript.

III **Geometric Josephson effects in chiral topological nanowires**
C. Spånslätt
arXiv preprint: arXiv:1804.06901, (2018).

Single author paper.

IV **Monopole response and a non-local order parameter for the Chern insulators**
T. Kvorning, C. Spånslätt, A. P. O. Chan, and S. Ryu,
Manuscript in preparation, (2018).

I performed some of the calculations in Sec. III, V, and VI, wrote parts of Sec. I, III, and V, and also contributed to the over all structure of the manuscript.

Reprints were made with permission from the publishers.
Note: Parts of this thesis are based on previous work in Spånslätt (2015).

Contents

1. Introduction

THE ADVENT OF QUANTUM MECHANICS in the early twentieth century was followed by a paradigmatic shift in how nature could be described and it also opened doors to novel worlds awaiting exploration. One extraordinary such world is accessible in systems of constant density, such as solids and liquids, in the energy range corresponding roughly to room temperature and below. Here lies the realm of *condensed matter*. The possibility to describe and understand condensed matter systems is of great importance, not only because it increases mankind's knowledge about nature, but also from a practical point of view.

Condensed matter physics is one of the most successful branches in physics, both in terms of widely applicable theoretical models but also since it has provided modern society with a huge number of important technological applications, such as the *transistor* (Bardeen and Brattain, 1948), *magnetic resonance imaging* (MRI) (Lauterbur, 1973), *superconducting magnets* (Yntema, 1955) and the *light emitting diodes* (LEDs) (Zheludev, 2007).

1.1 Principles of condensed matter physics

The great success of the theoretical description of condensed matter can be attributed to the formulation of a few but very strong principles (Altland and Simons, 2010):

Emergence is the concept that knowledge of the constituents of a system by no means implies that the system behaviour itself is fully understood. On the contrary, a physical system is most often far more than a stack of fundamental building blocks and depending on the detail of study, new features in terms of new physical laws and behaviour can arise. This is fortunate, since even though there might exist an underlying microscopic model that is impossible to solve exactly (which is usually the case), it is still possible to formulate effective theories relevant for the level of study, thereby reducing the complexity of the system in question by ignoring effects that are beyond said level.

Universality means that many microscopically different systems demonstrate common collective behaviour and are therefore describable with the same effective model. In addition to unifying seemingly different systems,

universality implies that many layers of complexity are irrelevant and can be ignored, and motivates the use of simple models.

Symmetry is deeply rooted in the language of all physics. A physical system is said to exhibit a symmetry if it does not change under certain manipulations or transformations of its constituents. Symmetries are typically related to some conserved quantity, which greatly simplifies many problems, and can also be responsible for the stability of physical systems.

Adiabatic continuity states that given some fundamental symmetries, the theoretical description of an interacting system often may be viewed as emerging *adiabatically* (in this context meaning slowly with respect to some relevant energy scale) by imagining turning on the interactions in the corresponding non-interacting system provided the symmetries remain intact. Related to this adiabatic continuity is the emergence of *quasiparticles*, weakly interacting particles "dressed" by effects from interactions. This principle is the reason why seemingly "wrong" theories of non-interacting systems accurately can describe systems where interactions are known to be strong.

One of the most successful results of condensed matter physics is the classification and identification of the ways matter can organize itself: the *phases of matter*. The most well-known phases are solids, liquids and vapours, but quantum mechanics predicts a plethora of additional phases, for instance various magnets or superconductors.

The classification of matter phases has been extremely successful due to *Landau's theory of symmetry breaking* (Landau, 1937; Landau and Lifshitz, 1980). Within this framework, a phase transition – which is the occasion when matter reorganizes – is described by a quantity called the *local order parameter*. The order parameter takes a non-zero value only below some transition temperature and is associated with the breaking of some underlying symmetry of the system. For example, a ferromagnet exhibits a spontaneous magnetization below the Curie temperature, where rotational invariance is broken as the microscopic dipoles, arising from internal electronic motion, all align in a single random but fixed direction. The notion of locality is important, because it means that symmetry breaking phases are revealed by a local measurement, for instance the local magnetization. One of the great strengths of Landau's theory is that it can be formulated on quite general premises, requiring only an expansion of the free energy in terms of the local order parameter.

This thesis discusses systems that are outside the scope of Landau's theory. There exists phases of matter, known as *topological phases of matter*, which cannot be assigned any local order parameter, and the information about the phase is instead encoded in its global features. The mathematical field dealing with such properties is *topology*.

While topology has been part of quantum mechanics almost since its foundation, its integration into condensed matter physics has increased rapidly in the recent years.

1.2 From symmetry to topology

Already in 1931, with Dirac's quantum mechanical treatment of the magnetic monopole (Dirac, 1931), the concept of topology seriously entered the realm of theoretical physics. But it was not until around 50 years later that it made its grand appearance in condensed matter physics, with the discovery of the integer- (von Klitzing *et al.*, 1980) and fractional quantum Hall effects (Tsui *et al.*, 1982; Laughlin, 1983) (IQH and FQH effects respectively).

These effects occur when a two-dimensional electron gas, trapped in a semiconducting heterostructure at low temperature is exposed to a strong magnetic field. Driving a current through the electron gas and measuring the resulting transverse- or Hall conductance as the magnetic field is changed, results in plateaux of integer (IQH effect) or fractional (FQH effect) multiples of e^2/h independently of any microscopical details, to nearly one part in a billion. Due to this astonishing accuracy, the *von Klitzing constant* $R_K = h/e^2 = 25\,812.807\,4555(59)\ \Omega$ is today used as a resistance standard.

The quantum Hall setup was the first experimental example of a state that was not describable within Landau's framework of symmetry breaking. Phases of matter that exhibit a quantized Hall conductance can not be assigned any local order parameter (Thouless *et al.*, 1982; Niu *et al.*, 1985; Kohmoto, 1985) since there is no difference in symmetries between configurations with different values of the Hall conductance. Systems that have this property are usually said to be *topologically ordered* (Wen, 1990), and constitute phases of matter whose low energy effective field theories are *topological field theories*. Such theories, as the name suggests, depend on concepts from the mathematical field of *topology* and it is the topological properties of the underlying mathematical structure that explains the origin of the precise Hall conductance quantization.

There is another important feature of the quantum Hall state. The interior, or bulk, is insulating while the edges are conducting (Halperin, 1982). These current carrying edge states are *chiral*, which means that they travel in a single direction for a given edge, and become immune to many types of scattering. The chiral edge states therefore transfer charge across the sample through ideal conducting channels which results in the perfectly quantized Hall conductance. One may say that the internal topology of the quantum Hall system is made manifest holographically by the edge states.

Theoretical models describing topologically ordered systems are usually complicated, due to the need of describing strong interactions and correla-

tions that typically arise. The condensed matter physics community was therefore surprised when it became apparent that phases or states[1] formed in non-interacting fermion systems, despite seeming trivial and being exactly solvable, also exhibit interesting properties rooted in topology. To distinguish between topologically ordered states and the free fermion states, the latter will be called *topological states of matter*[2] (TSM) and is the main topic of this thesis. The IQH state turned out to be the first known example of a TSM, while the FQH state can not be described by any free fermion model since it is a highly correlated and interacting system. It was later discovered that the theory of electronic band structure in solids, which had been around since the early days of quantum mechanics, had an un-explored topological structure. This enhanced band theory is called *topological band theory* and lies at the heart of TSM.

One very important step in the understanding of TSM came in 1988, when Haldane showed that in a graphene-like model with non-interacting spin-less fermions, there could be a quantized Hall conductance although the net magnetic field was zero (Haldane, 1988). This was considered quite remarkable, since the magnetic field was thought to be a crucial ingredient for the topological properties in the IQH state. Instead, it became apparent that it was the breaking of time-reversal symmetry, which a magnetic field manifestly imposes on a system, that was the crucial ingredient for the topological state. Haldane's model is usually referred to as a *Chern insulator* or the *quantum anomalous Hall effect* and has recently been experimentally realized in cold atom traps (Jotzu *et al.*, 2014).

Almost twenty years later, in 2005, Kane and Mele predicted that graphene should exhibit the *quantum spin Hall* (QSH) effect (Kane and Mele, 2005a,b). In their model, two copies of Haldane's model, one for each spin direction, were coupled via spin-orbit interactions. For symmetry reasons, this construction leads to a zero Hall conductance, but along the edges, states with opposite *helicity* forms, which in this case are stable due to the absence of any magnetic field. The edge states are said to be protected by time-reversal symmetry.

Unfortunately, the QSH effect turned out to be too small for detection in graphene. But one year later, Bernevig, Hughes and Zhang developed another model of the QSH effect, appropriate for two-dimensional HgTe/CdTe quantum wells (Bernevig *et al.*, 2006). In this system, the QSH effect was indeed detectable and its state was verified as the first symmetry protected TSM (König *et al.*, 2007). The QSH effect was soon thereafter generalized to

[1] The notions of a *phase* of matter and a *state* of matter are frequently used interchangeably in this thesis.

[2] Different naming conventions can be found in the literature, for instance *symmetry protected topological* (SPT) phases or short range entangled states.

three dimensional systems, where exotic surface states appear on slabs of certain heavy element materials (Fu *et al.*, 2007; Moore and Balents, 2007; Hsieh *et al.*, 2008; Roy, 2009).

Meanwhile, Kitaev presented in 2001 a seminal paper where a model for a topological superconductor was constructed (Kitaev, 2001). This deceptively simple model featured a peculiar quasiparticle excitation, known as a Majorana zero mode (MZM), exhibiting *non-Abelian statistics*, a property of immense interest in the field of topological quantum computation (Nayak *et al.*, 2008). Kitaev's paper launched a huge effort to realize MZMs experimentally, and pioneering work by Fu and Kane (2008) has led to a field of research where already existing building blocks of nanotechnology are combined into synthetically engineered devices with topological superconductivity and the exotic MZMs (Alicea, 2012). The first experimental results on such devices (Mourik *et al.*, 2012; Deng *et al.*, 2012; Das *et al.*, 2012) were unsatisfactory in several aspects, but with impressive technological improvement, recent experiments have shown strong support for the existence of MZMs (Zhang *et al.*, 2017).

Around 2010, it was found that the IQH effect, the QSH effect, topological superconductors and many other systems exhibiting topological behaviour could be described within a common framework, now known under various names as *The ten-fold way*, *The periodic table of topological insulators and superconductors* or *The Cartan-Altland-Zirnbauer classification table* (Altland and Zirnbauer, 1997; Schnyder *et al.*, 2008; Kitaev, 2009; Ryu *et al.*, 2010). This framework describes a general setting where insulating and superconducting band structures, symmetry, topology and spatial dimensions generates a quite general classification of all possible non-interacting fermionic TSM.

Most interestingly, in the last couple of decades, condensed matter physics has seen a rapid technological development due to groundbreaking new technology including cold atom traps, the ability to fabricate nano-scale devices with atom precision and superconducting circuits and heterostructures. These advances, in combination with new and exciting topological models, outline a promising path towards a fundamentally new generation of quantum devices and exotically engineered materials.

1.3 Outline

The purpose of this thesis is to provide an accessible introduction to topological states of matter, to demonstrate some applications in low dimensional systems, and to act as a foundation for the accompanying papers. The papers are meant to be quite self-contained and are therefore only briefly summarized.

The remainder of this thesis is organized as follows:

Chapter 2 sets the stage for a general discussion of topological states of matter. Together with a brief introduction to important concepts, the chapter summarizes the tight-binding formalism which is a convenient language for describing topological band theory. The chapter continues with a discussion of quantum mechanical symmetries which are the basic ingredients for a classification of non-interacting fermionic topological states of matter. This classification is outlined together with a discussion of its applications, limitations and extensions.

Chapter 3 is devoted to applications of the earlier framework within the context of one-dimensional topological superconductors. Such systems are characterized by the presence of a remarkable kind of edge states known as Majorana zero modes. These modes and their properties are introduced on a general level which is followed by a discussion on their detection in mesoscopic devices, in particular Josephson junctions. This chapter forms the basis for PAPERS I-III.

Chapter 4 summarizes the well-known theory of the IQH effect and its more recent descendants, the Chern insulators and time-reversal protected topological insulators. It is then argued that the defining properties of these systems can be captured in a quantum field theory description, specifically that of topological field theory. The power of such a description is further shown to provide important insights that go beyond the previously described framework of free fermions. This chapter provides the necessary background for PAPER IV.

Chapter 5 concludes the thesis with a summary and some speculations on future directions.

Note: Chapters 1, 2 and 3 are partially based on Spånslätt (2015).

2. Topological states of matter

In this chapter, the concept of *topological insulators and superconductors*, collectively called *Topological States of Matter* (TSM), are introduced. To describe such TSM, the chapter continues by providing an accessible introduction to the tight-binding formalism, which will be used frequently in this thesis to describe various models which host TSM. Following is a brief description of the concept of quantum mechanical symmetries which are of paramount importance in the field of TSM. These symmetries will be shown to form the foundation of a classification of non-interacting TSM in different spatial dimensions. The chapter concludes with a discussion regarding the limitations of the presented framework and highlights some extensions which are in focus of contemporary research.

2.1 Topological insulators and superconductors

The mathematical field of *topology* deals with the question whether certain mathematical objects can be deformed into each other. The deformations are restricted to being continuous, which includes bending, stretching and twisting but not tearing, cutting or gluing. A natural follow-up question is: which global properties are preserved during such allowed deformations?

As an example, a sphere can be continuously deformed into a cube but not into a torus, because that would require cutting holes and using glue, which the prescribed rules do not allow. The sphere and the cube are therefore said to be topologically equivalent, or *homeomorphic*, while the sphere and the torus are topologically distinct.

Applied to the setting of condensed matter physics, the relevant question is whether two quantum systems, represented by their Hamiltonians (or equivalently their ground states), can be transformed, by continuously changing some parameters $\{\lambda_i\}$, into each other given some constraint on the deformation (Hasan and Kane, 2010; Akhmerov *et al.*, 2015). If this is possible, the systems are said to be topologically equivalent, otherwise they are topologically distinct. The type of constraint is very important, for without it the above notion would be meaningless, since any Hamiltonian can in some, perhaps extreme, way be deformed to any other. Compare with the rule of "no

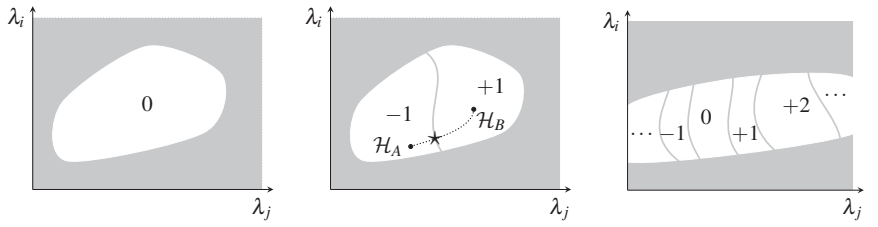

(a) Trivial **(b)** Topological $\mathbb{Z}_2$ **(c)** Topological $\mathbb{Z}$

Figure 2.1: A sketch of three typical phase diagrams of gapped fermionic Hamiltonians depending on some set of parameters $\{\lambda_i\}$. Gray/white regions correspond to gapless/gapped Hamiltonians. In **(a)**, there is only one gapped region and all Hamiltonians are topologically equivalent and trivial. In **(b)**, there are two topologically distinct classes of Hamiltonians distinguished by a $\mathbb{Z}_2$ invariant ν. The Hamiltonian $\mathcal{H}_A$ with $\nu = -1$ can be deformed into $\mathcal{H}_B$ with $\nu = +1$ only by passing through a gap-closing region $\star$. In **(c)**, there is an infinite set of distinct Hamiltonians, labelled by a $\mathbb{Z}$ invariant, separated by gapless regions. Figure adapted from Stanescu (2017).

cutting" above. This thesis deals with the constraint that the Hamiltonians must be gapped during the deformation, meaning that they always have an associated energy gap. Gapped fermionic Hamiltonians have between occupied and unoccupied energy eigenstates a finite energy region where no states exist. This gap must exist regardless of the system size and with this requirement, the prescribed Hamiltonians describe insulators and mean field superconductors.

Related to the deformation of Hamiltonians is a quantity called the *topological invariant*. This invariant, as the name suggests, does not change during deformations between two topologically equivalent Hamiltonians, but will generally do so whenever a deformation forces the energy gap to close. When this happens, the system is said to undergo a *topological phase transition*. To connect to the example of the sphere-torus deformation above, the number of holes, called the *genus* or the *Euler characteristic*, would be a relevant quantity for a topological invariant in that specific problem. The genus does not change as the sphere is deformed into the cube, but it does so when the sphere is turned into a torus, which requires forbidden cutting and gluing processes.

In this thesis, the invariants typically come in two flavours. One invariant is usually called the $\mathbb{Z}_2$, *parity* or *Pfaffian* invariant and takes one of two possible values, often labelled -1 and $+1$. The other invariant is known as the $\mathbb{Z}$, *Chern number* or *winding number* invariant and takes integer values $0, \pm 1, \pm 2, \ldots$. Together with the possibility of the non-existence of a meaningful invariant, the three cases are depicted in Fig. 2.1.

There is an additional constraint to the deformations which is important

for TSM. Imposing symmetries may reduce the allowed set of deformations between Hamiltonians. This leads naturally to the definition of a *(symmetry protected) topological state of matter* which may be formulated as:

> *"As long as a certain symmetry is present, a symmetry protected topological state can not be deformed into a trivial state unless the gap closes."*

A *trivial state* is equivalent to an ordinary insulator, which can be continuously deformed into an insulating state of isolated atoms, or in the case of superconductors, simply an ordinary superconductor. The trivial states can also be defined to be those that have trivial values of their topological invariants.

Having defined what a TSM is, the next relevant question is to ask how they can be found, at least theoretically. As will be shown in coming sections, recent progress in the field of condensed matter theory has allowed for a broad classification of possible TSM. However, before discussing such a classification, it is useful to introduce a few more useful tools and concepts.

2.2 The tight-binding method and bulk Hamiltonians

The tight-binding description of quantum systems is a powerful method to model the band structure of non-interacting electrons (see for instance Ashcroft and Mermin (1976); Yu and Cardona (2010) for a detailed description). The method captures the lattice structure of the system and allows for a straightforward implementation of symmetry constraints, various internal degrees of freedom, impurities or external fields. Importantly in the context of TSM, it contains a natural high energy cutoff which is crucial to assign well behaved topological properties to the system. For a model lacking this cutoff, various regularization and compactification schemes have to be implemented which can turn out to be complicated. Due to its power and simplicity, many models of TSM are formulated within the tight-binding description.

A general tight-binding model has a Hamiltonian

$$\mathcal{H} = \sum_{ij\alpha\beta} c^{\dagger}_{i\alpha} H^{\alpha\beta}_{ij} c_{j\beta}, \tag{2.1}$$

where i, j denotes lattice sites in some spatial dimension d and α, β represents internal degrees of freedom, for example spin, orbitals or electron-hole labels. The second quantization operator $c^{\dagger}_{i\alpha}$ ($c_{i\alpha}$) creates (annihilates) a particle with internal degree of freedom α on lattice site i. As will be shown in Sec. 2.3, the coefficients $H^{\alpha\beta}_{ij}$ capture the symmetries of the system.

By imposing translational invariance, typically through periodic boundary conditions, the Hamiltonian can be Fourier transformed into

$$\mathcal{H} = \sum_{k\alpha\beta} c^{\dagger}_{k\alpha} h^{\alpha\beta}(k) c_{k\beta}, \tag{2.2}$$

where $h^{\alpha\beta}(k)$ is an element of the *Bloch* (or in the superconducting case, the Bogoliubov - de Gennes or *BdG*) *Hamiltonian*. The notion of the *bulk Hamiltonian*, in the sense that it describes a system without a border, is also frequently used. The quantity $k = (k_1, k_2, \ldots, k_d)$ is the Bloch or crystal momentum, which takes values in the first Brillouin zone (BZ): the d-dimensional torus $T^d = \bigotimes_{j=1}^{d} S^1_j$, where each S^1_j is a unit circle. Frequently, the thermodynamic limit is taken, in which k can be viewed as a continuous variable.

The Bloch Hamiltonian is a matrix in the internal degrees of freedom with elements $h^{\alpha\beta}(k)$ related to $H^{\alpha\beta}_{ij}$ by

$$h^{\alpha\beta}(k) = \sum_{\delta} H^{\alpha\beta}_{\delta} e^{-i\delta\cdot k}, \tag{2.3}$$

where δ is a vector connecting the lattice sites. Most often, δ is restricted to the set of nearest neighbour vectors.

Another useful advantage of the tight-binding model is that it can be straightforwardly implemented numerically. To see this, recall the notion of matrix representation of quantum mechanics, and let $\{|i\rangle\}_i$ be an orthonormal and complete basis set of the Hilbert space, fulfilling $\sum_i |i\rangle\langle i| = \mathbb{1}$ with inner product $\langle i|j\rangle = \delta_{ij}$. Any operator, $\mathcal{A}$, on the Hilbert space, can then be written as

$$\mathcal{A} = \mathbb{1}\cdot\mathcal{A}\cdot\mathbb{1} = \Big[\sum_i |i\rangle\langle i|\Big]\cdot\mathcal{A}\cdot\Big[\sum_j |j\rangle\langle j|\Big] = \sum_{ij} A_{ij}|i\rangle\langle j|, \tag{2.4}$$

with $A_{ij} = \langle i|\mathcal{A}|j\rangle \in \mathbb{C}$, being an element of the matrix A which is a representation of the abstract operator $\mathcal{A}$ in the given basis. This procedure can also be performed on a state vector yielding the representation

$$|\psi\rangle = \mathbb{1}|\psi\rangle = \sum_i |i\rangle\langle i|\psi\rangle = \sum_i \psi_i |i\rangle, \tag{2.5}$$

with $\psi_i = \langle i|\psi\rangle \in \mathbb{C}$, being the basis element of the vector $\vec{\psi}$ which represents $|\psi\rangle$ in the given basis.

The abstract entities $\mathcal{A}$ and $|\psi\rangle$ associated with the Hilbert space have thus been converted to the matrix A and the vector $\vec{\psi}$ which are sets of complex numbers that can be calculated on a computer.

Consider now the time independent Schrödinger equation $\mathcal{H}|\psi\rangle = \varepsilon|\psi\rangle$, for some state $|\psi\rangle$ with eigenvalue ε. Using the representations (2.4) and (2.5)

above gives

$$\Big[\sum_{ij} H_{ij}\,|i\rangle\,\langle j|\Big]\Big[\sum_{k}\psi_k\,|k\rangle\Big] = \varepsilon\Big[\sum_{i}\psi_i\,|i\rangle\Big]$$
$$\Rightarrow \sum_{ij} H_{ij}\psi_j\,|i\rangle = \varepsilon\sum_{i}\psi_i\,|i\rangle\,. \tag{2.6}$$

Multiplying with $\langle k|$ from the left and using the orthonormality of the basis leads to the equation

$$\sum_{kj} H_{kj}\psi_j = \varepsilon\psi_k \quad \text{or} \quad H\vec{\psi} = \varepsilon\vec{\psi}, \tag{2.7}$$

which is just the eigenvalue equation of the matrix H. Solving it will give the energy eigenvalues $\{\varepsilon_i\}$, and the eigenvectors $\{\vec{\psi}_i\}$. The elements of the eigenvectors are coefficients of the basis expansion (2.5). The procedure can be extended to time-dependent systems, but will not be considered in this thesis.

To clarify the concepts above, consider a one-dimensional chain consisting of N sites with particles hopping back and forth. There is an on-site chemical potential μ and a nearest neighbouring hopping amplitude t. This system has the Hamiltonian

$$\mathcal{H} = \sum_{i=1}^{N}\Big[-t(c_i^\dagger c_{i+1} + c_{i+1}^\dagger c_i) - \mu c_i^\dagger c_i\Big], \tag{2.8}$$

which can be implemented numerically by defining a sparse $N\times N$ matrix H with non-zero elements

$$H_{ii} = -\mu, \quad H_{i,i+1} = H_{i+1,i} = -t. \tag{2.9}$$

The basis states are chosen to $|i\rangle \equiv c_i^\dagger|0\rangle = (0,\ldots,1,\ldots,0)^T$, where $|0\rangle$ is the vacuum state containing no particles, the 1 is in the i-th position, and the superscript T denotes transposition. Solving the eigenvalue equation for the matrix H gives the spectrum of the model and the eigenstates, where the latter will be linear combinations of the basis states, the *Bloch states*, appearing in any periodic crystal structure.

Requiring periodic boundary conditions, $c_{N+1} = c_1$ and $c_{N+1}^\dagger = c_1^\dagger$, allows for a Fourier transform which in this specific problem directly yields the one-dimensional Bloch Hamiltonian and energies $h(k) = \varepsilon(k) = -2t\cos(k) - \mu$ where a unit lattice constant is assumed. The crystal momentum k takes the values $k = \frac{2\pi n}{L}$ where $n = 0,1,2,...,N-1$. Inserting these values into the dispersion relation gives the same numbers as the eigenvalues of the matrix H with the additional periodic boundary conditions $H_{1N} = H_{N1} = -t$.

With the tight-binding formalism as the basic formalism, the next step in understanding TSM is to investigate the influence of symmetries.

2.3 Symmetries

In quantum mechanics, symmetries are represented by unitary operators that commute or anticommute[1] with the Hamiltonian. An ordinary symmetry is said to exist if the system Hamiltonian commutes with a corresponding unitary operator

$$[\mathcal{H}, U] = 0 \Leftrightarrow U^\dagger \mathcal{H} U = \mathcal{H}. \tag{2.10}$$

Typical examples of such ordinary symmetries are the spin projection or linear momentum operators.

A unitary symmetry allows for a reduction of the Hamiltonian into blocks. As an example, a spin Hamiltonian commuting with σ_z can be written in separate spin-up and spin-down blocks. Due to the commutativity with the Hamiltonian and by the Heisenberg equation of motion, these spins are separately conserved and the blocks will therefore be completely disconnected. Each block on its own will not posses the spin symmetry since that degree of freedom has been eliminated in each block.

Every sub-block may in turn be analyzed further until no symmetry is left and one has reached an *irreducible* representation of the full symmetry group of the Hamiltonian. But each sub-block can be classified further with a second kind of symmetry operators. These are the so-called antiunitary operators which work in a somewhat different way. They impose spectral constraints on the Hamiltonian which is of utter importance when topological band structure is concerned. Another important aspect of antiunitary symmetries is that they are the only ones that remain exact when randomness or disorder is implemented in a Hamiltonian.

For TSM there are two important antiunitary symmetries (Bernevig and Hughes, 2013; Stanescu, 2017). A Hamiltonian is defined to be *time-reversal symmetry* (TRS) or *particle-hole symmetry* (PHS)[2] invariant if there can be found antiunitary operators that commute respectively anticommute with the Hamiltonian:

$$\mathcal{T}\mathcal{H}\mathcal{T}^{-1} = \mathcal{H}, \quad \mathcal{P}\mathcal{H}\mathcal{P}^{-1} = -\mathcal{H}. \tag{2.11}$$

TRS is the notion that a system looks the same if all motion would be reversed. PHS is a bit more subtle and is harder to interpret physically. Furthermore, in some situations, notably in mean field superconductivity, PHS arises automatically from an artificial doubling of the degrees of freedom. For this reason

[1] Anticommuting operators do not respect a strict definition of a quantum mechanical symmetry. However, such operators will be treated on the same footing as commuting operators in this thesis.

[2] Also known as *charge conjugation symmetry.*

PHS might not always be a physical symmetry, but will nonetheless be treated on the same footing as any other symmetry in this thesis.

According to Wigner's theorem (see for instance Sakurai and Napolitano (2011)), every antiunitary operator can be written as the product of some unitary operator and the complex conjugation operator $\mathcal{K}$. For example, the TRS operator for a spin-$\frac{1}{2}$ system in the basis of σ_z-eigenstates, can be written as $\mathcal{T} = i\sigma_y\mathcal{K}$ with $i\sigma_y$ unitary (it is important to note that the representation of any operator can depend on the choice of basis). Applying $\mathcal{T}$ to the spin operator flips all spin components,

$$\mathcal{T}\sigma_i\mathcal{T}^{-1} = -\sigma_i, \quad i \in \{x,y,z\} \tag{2.12}$$

as time-reversal intuitively should do. By virtue of Wigner's theorem, a notational convention $\mathcal{T} = T\mathcal{K}$ and $\mathcal{P} = P\mathcal{K}$ with T and P being unitary operators, is useful.

TRS and PHS each come in two distinct versions. Squaring any of the operators, there are the possibilities $\mathcal{T}^2 = \pm 1$ and $\mathcal{P}^2 = \pm 1$. This difference is important and may drastically affect the energy spectrum. A well-known example is the $\mathcal{T}^2 = -1$ operator for spin-$\frac{1}{2}$ particles, resulting in *Kramers theorem*: in the presence of TRS, all energy states are at least two-fold degenerate.

For Bloch or BdG Hamiltonians $h(k)$ (remember that this object is typically a matrix), TRS and PHS in Eq. (2.11) translate into the the following spectral constraints (Bernevig and Hughes, 2013)

$$Th^T(k)T^\dagger = h(-k), \quad Ph^T(k)P^\dagger = -h(-k), \tag{2.13}$$

where the hermicity of $h(k)$ has been used. As a direct consequence of TRS and PHS, the energy eigenvalues come in $\{\varepsilon_k, \varepsilon_{-k}\}$ and $\{\varepsilon_k, -\varepsilon_{-k}\}$ pairs, respectively.

The combination of TRS and PHS is called *chiral symmetry* (CS), and may be represented by the operator $\mathcal{C} = T\mathcal{K}P\mathcal{K} = TP^* \equiv C$. CS imposes the constraint:

$$\mathcal{C}\mathcal{H}\mathcal{C}^{-1} = -\mathcal{H}, \tag{2.14}$$

and for the Bloch Hamiltonian

$$Ch(k)C^\dagger = -h(k). \tag{2.15}$$

Hence, CS is represented by a unitary operator that anticommutes with the Hamiltonian. Sometimes CS is called *sublattice symmetry* since the same type of symmetry exists in systems where one can make a division between two

sublattices, a and b. The Hamiltonian can then always be written in a basis such that the Bloch Hamiltonian is off-diagonal

$$h(k) = \begin{pmatrix} 0 & h_{ab} \\ h_{ab}^{\dagger} & 0 \end{pmatrix}. \tag{2.16}$$

Using Eq. (2.15), it is straightforward to show that for systems with CS, eigenstates come in $\{\varepsilon_k, -\varepsilon_k\}$ pairs.

As will be presented next, analysis of the three symmetries discussed in this section serves as the foundation to the classification of TSM Hamiltonians.

2.4 Symmetry classification of non-interacting fermion Hamiltonians

The topological classification of all non-interacting and gapped fermionic Hamiltonians essentially boils down to two basic sets of problems.

1. Given a set of antiunitary symmetries and some specified spatial dimension d, what is the set of topologically distinct Hamiltonians, how many different topological phases are there and what kind of object is the topological invariant?

2. Given a Hamiltonian, in some class, with certain fixed parameters, which topological phase is the system in, and what is the value of the topological invariant?

The first of these problems is discussed at a very basic conceptual level in this section. The second problem is a bit more context dependent and will be addressed in more detail for some specific cases later in the thesis.

2.4.1 General outline of the classification

The main idea behind the classification is that physical systems in any spatial dimension having an insulating bulk gap can be divided into different classes distinguished by the symmetries TRS, PHS and CS. Both TRS and PHS can either be present and square to ± 1, or be absent. This directly yields nine different possibilities. The CS is always fixed by the other two symmetries except for one specific case. When both TRS and PHS are absent, there is still the possibility of a CS[1]. This yields a grand total of ten distinct classes.

[1]The CS operator always squares to +1.

	Cartan label	TRS	PHS	CS
Standard classes (Wigner-Dyson)	$\mathcal{A}$ (unitary)	0	0	0
	$\mathcal{AI}$ (orthogonal)	$+1$	0	0
	$\mathcal{AII}$ (symplectic)	-1	0	0
Chiral/sublattice classes	$\mathcal{AIII}$ (chiral unitary)	0	0	1
	$\mathcal{BDI}$ (chiral orthogonal)	$+1$	$+1$	1
	$\mathcal{CII}$ (chiral symplectic)	-1	-1	1
Bogoliubov-de Gennes classes	$\mathcal{D}$	0	$+1$	0
	$\mathcal{C}$	0	-1	0
	$\mathcal{DIII}$	-1	-1	1
	$\mathcal{CI}$	$+1$	-1	1

Table 2.1: The ten different symmetry classes of gapped non-interacting fermionic Hamiltonians. The classes are defined by the presence or absence of TRS, PHS and CS. For TRS and PHS, ± 1 describes the squared symmetry operator. For CS, 1 means presence. A zero entry means the absence of a symmetry.

This result was obtained by Altland and Zirnbauer in the context of disordered mesoscopic hybrid structures (Altland and Zirnbauer, 1997) and is presented in Tab. 2.1. The classes are, for historical reasons, typically divided into three broad categories of which the first, the standard classes, were originally treated by Wigner and Dyson within *random matrix theory* (Dyson, 1962). The second category are the chiral or sublattice classes, characterized by the presence of CS. That symmetry is also present in some of the Bogoliubov-deGennes classes, related to mean field superconductors, but the main property of these is the PHS of superconductivity.

Each class is given a name that can be traced back to the classification of *compact symmetric spaces*, performed by Cartan in the early twentieth century (Cartan, 1926; Stanescu, 2017). For a generic $N \times N$ hermitian Hamiltonian $\mathcal{H}$, the corresponding time-evolution operator $\mathcal{U} = \exp[it\mathcal{H}]$ belongs to the group of unitary matrices $U(N)$ which Cartan labels as class $\mathcal{A}$. If for example there is an additional TRS squaring to $= +1$, the Hamiltonian can aways be chosen to be real and symmetric, and correspondingly $\mathcal{U} \in U(N)/O(N)$, ($O(N)$ is the orthogonal group), which is called $\mathcal{AI}$. The remaining classes are labelled in a similar manner.

The next step in the classification procedure is to determine how many topologically distinct Hamiltonians there are for each symmetry class. For

simplicity and brevity, this procedure will be performed only for a few classes.

The relevant quantity for the topological classification of an insulating band structure in class $\mathcal{A}$, is the operator that projects onto the subspace of occupied bands (Schnyder *et al.*, 2008; Kitaev, 2009; Ryu *et al.*, 2010; Stanescu, 2017). This operator may be written as

$$P(k) = \sum_{j=1}^{n} |u_j(k)\rangle \langle u_j(k)|, \tag{2.17}$$

where $|u_j(k)\rangle$ is the j-th Bloch state. It is assumed that n out of $n+m$ bands are occupied, equivalent to placing the Fermi energy between band n and $n+1$.

Since it is only the global properties of the band structure that are relevant, the band structure can be continuously deformed as long as the gap separating occupied and empty bands is maintained. The insulator can therefore conveniently be transformed into a *flat band insulator*, where all occupied bands have energy $\varepsilon_- = -1$ and all empty bands have energy $\varepsilon_+ = +1$. After this procedure, one obtains the corresponding flat band Hamiltonian:

$$q(k) = (+1)(1-P(k)) + (-1)P(k) = 1 - 2P(k). \tag{2.18}$$

Note that $q(k)^2 = 1$ due to the idempotence of projection operators and also that $\mathrm{Tr}\,[q(k)] = m-n$. Generally, $q(k)$ will be a $U(n+m)$ matrix defined up to a $U(n)\times U(m)$ "rotational" or redundancy degree of freedom corresponding to independent basis rotations in the occupied and empty band subspaces. With these restrictions, the flat band Hamiltonian, and the original Hamiltonian too as far as topology is concerned, belongs to the coset space

$$G_{n+m,m}(\mathbb{C}) = G_{n+m,n}(\mathbb{C}) = U(n+m)/(U(n)\times U(m)), \tag{2.19}$$

which is called the *complex Grassmannian* and is a generalization of the projective spaces. The set of topologically distinct Hamiltonians is determined by the *homotopy classes* of the mappings

$$\begin{aligned} q\colon BZ &\to G_{n+m,m}(\mathbb{C}) \\ k &\mapsto q(k). \end{aligned} \tag{2.20}$$

Here, BZ, corresponds either to T^d, the d-dimensional torus in the case of lattice models, or for a continuum model, the d-sphere S^d. If two maps $k \mapsto q_1(k)$ and $k \mapsto q_2(k)$ can be continuously deformed into each other, the corresponding Hamiltonians $h_1(k)$ and $h_2(k)$ can as well and are therefore considered equivalent. The set of inequivalent maps label the topologically distinct Hamiltonians.

For $BZ = S^d$, the problem reduces to finding the d-th homotopy group, denoted by $\pi_d[G_{n+m,m}(\mathbb{C})]$. It is a well-known mathematical result (see for instance Nakahara (2003)) that

$$\begin{aligned} \pi_d[G_{n+m,m}(\mathbb{C})] &= \mathbb{Z} \qquad \text{for } d \text{ even}, \\ \pi_d[G_{n+m,m}(\mathbb{C})] &= \{1\} \quad \text{for } d \text{ odd}. \end{aligned} \tag{2.21}$$

An immediate consequence of this result is a prediction of an infinite number of topologically distinct $d = 2$ IQH states, each classified by an integer (see Fig. 2.1c). This prediction has strong experimental support and the integer *Chern number* (see Sec. 4.3.1) is precisely the value of the Hall conductance in units of e^2/h. The result further implies that IQH states only can exist in even spatial dimensions.

Assigning additional symmetries to the Hamiltonian (2.18) alters the mapping target space in Eq. (2.20) so that the homotopy group may change as well. If for instance CS is imposed, corresponding to class $\mathcal{AIII}$, the target space becomes $U(n)$, resulting in

$$\begin{aligned} \pi_d[U(n)] &= \{1\} \quad \text{for } d \text{ even}, \\ \pi_d[U(n)] &= \mathbb{Z} \qquad \text{for } d \text{ odd}. \end{aligned} \tag{2.22}$$

In both the examples given, the base space for the mappings were taken to be S^d. The same result is often obtained by taking T^d instead, but sometimes this is not the case. When this happens the corresponding system is said to be *weakly topological* and the system is unstable to breaking of translational invariance, typically due to disorder (Ryu *et al.*, 2010).

General strategies to determine all possible mappings for every symmetry class is quite complicated and to fully describe the various methods is out of scope of this thesis. The mathematically inclined reader is referred to Qi *et al.* (2008); Schnyder *et al.* (2008); Kitaev (2009); Ryu *et al.* (2010).

2.4.2 The periodic table of topological insulators and superconductors

The result of classifying all gapped non-interacting fermionic Hamiltonians is summarized in Tab. 2.2. This table is known under various names of which the most commonly used are: *The ten-fold way*, *The Cartan-Altland-Zirnbauer classification table* or *the periodic table of topological insulators and superconductors*. In this thesis, the latter of these names will be used.

In the left column of the table are listed the ten different symmetry classes as defined in Tab. 2.1. The main space of the table consists of the homotopy group corresponding to every class for spatial dimensions $d = 0$ to $d = 7$.

To summarize the discussion in the beginning of this chapter, a $\mathbb{Z}$ invariant means that there is an infinite number of topologically distinct Hamiltonians,

Class	$d=0$	1	2	3	4	5	6	7
$\mathcal{A}$	$\mathbb{Z}$	0	$\mathbb{Z}$	0	$\mathbb{Z}$	0	$\mathbb{Z}$	0
$\mathcal{AIII}$	0	$\mathbb{Z}$	0	$\mathbb{Z}$	0	$\mathbb{Z}$	0	$\mathbb{Z}$
$\mathcal{AI}$	$\mathbb{Z}$	0	0	0	$2\mathbb{Z}$	0	$\mathbb{Z}_2$	$\mathbb{Z}_2$
$\mathcal{BDI}$	$\mathbb{Z}_2$	$\mathbb{Z}$	0	0	0	$2\mathbb{Z}$	0	$\mathbb{Z}_2$
$\mathcal{D}$	$\mathbb{Z}_2$	$\mathbb{Z}_2$	$\mathbb{Z}$	0	0	0	$2\mathbb{Z}$	0
$\mathcal{DIII}$	0	$\mathbb{Z}_2$	$\mathbb{Z}_2$	$\mathbb{Z}$	0	0	0	$2\mathbb{Z}$
$\mathcal{AII}$	$2\mathbb{Z}$	0	$\mathbb{Z}_2$	$\mathbb{Z}_2$	$\mathbb{Z}$	0	0	0
$\mathcal{CII}$	0	$2\mathbb{Z}$	0	$\mathbb{Z}_2$	$\mathbb{Z}_2$	$\mathbb{Z}$	0	0
$\mathcal{C}$	0	0	$2\mathbb{Z}$	0	$\mathbb{Z}_2$	$\mathbb{Z}_2$	$\mathbb{Z}$	0
$\mathcal{CI}$	0	0	0	$2\mathbb{Z}$	0	$\mathbb{Z}_2$	$\mathbb{Z}_2$	$\mathbb{Z}$

Table 2.2: The periodic table of possible topological phases of gapped non-interacting fermionic Hamiltonians. For every class in spatial dimension d, there is a corresponding topological invariant. An entry of $\mathbb{Z}_2$, $\mathbb{Z}$ or $2\mathbb{Z}$ indicates that there are topologically distinct Hamiltonians for the corresponding class to the left. An entry of 0 means that all Hamltonians are topologically trivial.

labelled by the set of integers. The $\mathbb{Z}$ archetype is the IQH- or Chern insulator states in class $\mathcal{A}$ for $d=2$. A $2\mathbb{Z}$ entry is similar, but only even integers are realized by the topological invariant because of some doubling of the degrees of freedom. For example, a spin-$\frac{1}{2}$ quantum dot with TRS, and thereby Kramer's degeneracy, has an invariant equal to the number of filled levels which is even (Akhmerov *et al.*, 2015). This system belongs to class $\mathcal{AII}$ with $d=0$. An entry of $\mathbb{Z}_2$ indicates two topologically distinct classes of Hamiltonians: trivial or topological. One example such a system is the Kitaev chain model (Kitaev, 2001) which is a topological superconductor belonging to class $\mathcal{D}$ with $d=1$. This invariant will be derived explicitly later in this thesis. Finally, a zero entry means that all gapped Hamiltonians with the given symmetries and dimensionality can be deformed into each other without closing the gap or breaking any symmetries. In that case, no meaningful topological invariant can be defined.

There several additional interesting features of the periodic table that are worth mentioning (Stanescu, 2017). First, for each spatial dimension d, there are exactly five classes of topological insulators or superconductors. Out of these, there are three with winding or Chern number invariants and two with $\mathbb{Z}_2$ invariants. Systems with $d>3$ might seem unrealistic, but models with periodic parameters that act as additional momenta typically exist in the table for these entries. Moreover, high-dimensional systems are often useful for deriving topological invariants for low-dimensional systems, a procedure knowns

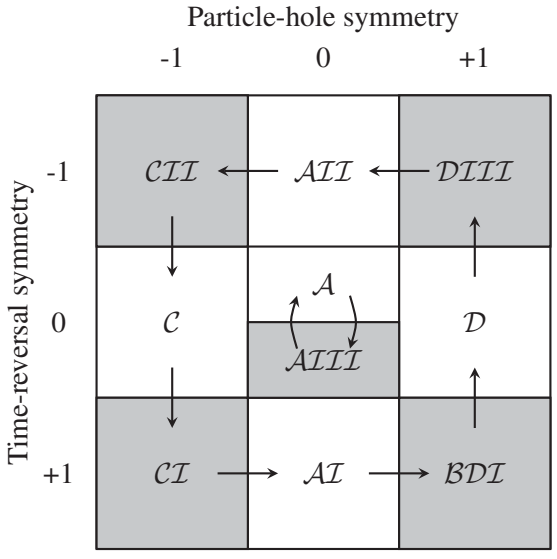

Figure 2.2: The periodicity obtained upon dimensional extension of the symmetry classes is known as the "Bott Clock". Chiral classes are coloured grey and the arrows depict the direction in which dimensional extension conserves the topological invariant. The periodicity is eight for the real, outer classes and two for the inner complex classes. Figure adapted from Fulga *et al.* (2012).

as *dimensional reduction*, which will be discussed briefly in the next section.

The observant reader notes that the classes have been rearranged with respect to Tab. 2.1 which reveals a periodicity in the topological invariants when the dimension d is changed. The two topmost classes, $\mathcal{A}$ and $\mathcal{AIII}$, known as the complex classes, since they do not have any antiunitary symmetry imposing reality constraints, have a period of two. The remaining eight classes, called the real classes due to reality constraints from the symmetries, exhibits a periodicity when the dimension is changed by eight. These two features are collectively known as *Bott periodicity* and will be discussed in some more detail next.

2.4.3 Dimensional extension and the Bott Clock

The periodicity in the occurrence of topological invariants in the periodic table 2.2 is quite subtle and requires the mathematics of vector bundles to explain. But parts of the periodicity, specifically the staggered pattern of the complex classes $\mathcal{A}$ and $\mathcal{AIII}$ can be explained in a more accessible manner. The following discussion is to large extent based on Akhmerov *et al.* (2015).

For the complex classes, there is the possibility of either presence or ab-

sence of CS. Assume first that there exists a Bloch Hamiltonian in dimension d, denoted by h_d (the k-dependence is suppressed for simplicity), with CS represented by the operator $\mathcal{C}$. Then h_d belongs to class $\mathcal{AIII}$. The energies $\pm\varepsilon_d^n$ are symmetrically distributed around zero energy and depend on d Bloch momenta. One may then form the *dimensionally extended* Hamiltonian

$$h_{d+1} = h_d \cos(k_{d+1}) + \mathcal{C} \sin(k_{d+1}), \tag{2.23}$$

with energies

$$\varepsilon_{d+1}^n = \pm \left[(\varepsilon_d^n)^2 \cos^2(k_{d+1}) + \sin^2(k_{d+1}) \right]^{1/2}. \tag{2.24}$$

Here, $\mathcal{C}^2 = 1$ has been used and it follows that h_d and h_{d+1} have the same number of bands, although the latter depends on one more Bloch momentum. The expression (2.23) ensures, by construction, that the gap of h_{d+1} closes if and only if that of h_d closes. This implies that their topological invariant must be the same. The construction further ensures that h_{d+1} breaks the CS since the term that was added contains $\mathcal{C}$ and consequently cannot anticommute with $\mathcal{C}$. Hence, it follows that the topological classification of a class $\mathcal{AIII}$ Hamiltonian in dimension d is the same as that for a class $\mathcal{A}$ Hamiltonian in dimension $d+1$. This observation is abbreviated by $\mathcal{AIII} \to \mathcal{A}$.

Next, assume that h_d does not have any CS, thus being in class $\mathcal{A}$. One may then construct

$$h_{d+1} = h_d \cos(k_{d+1})\tau_x + \sin(k_{d+1})\tau_y, \tag{2.25}$$

having twice the number of bands compared to h_d and with energies given by Eq. (2.24). By the same argument as above, h_{d+1} must have the same topological invariant as h_{d+1} but it has now a CS given by $\mathcal{C} = \tau_z$. One concludes that $\mathcal{A} \to \mathcal{AIII}$.

These two procedures, adding one extra dimension and breaking or imposing a symmetry go under the name of *dimensional extension*. It explains the staggered pattern in the upper part of Tab. 2.2: $\mathcal{A} \to \mathcal{AIII} \to \mathcal{A}$. It is possible to apply dimensional extension to the other classes too. The strategy is the same but at the same time a bit more complicated since more symmetries must be considered. The end result is

$$\mathcal{AI} \to \mathcal{BDI} \to \mathcal{D} \to \mathcal{DIII} \to \mathcal{AII} \to \mathcal{CII} \to \mathcal{C} \to \mathcal{CII} \to \mathcal{C} \to \mathcal{AI}, \tag{2.26}$$

and one notes that the pattern for the real classes repeats itself after eight dimensional extensions. This is called *Bott periodicity* (Bott, 1959) and is a property of an underlying mathematical structure known as *K-theory* (Kitaev, 2009).

The Bott periodicity of the periodic table can conveniently be presented in the form of a *Bott clock* depicted in Fig. 2.2. The different classes are arranged in a 3×3 grid according to their symmetries. Chiral classes are displayed in gray. The arrows tells which classes that have the same topological invariant when performing the dimensional extension $d \to d+1$. The two complex classes are situated in the middle and are isolated from the real classes positioned around the "clock". One revolution around the clock brings back the same class after eight dimensional extensions.

There are many more interesting symmetry properties of the periodic table, for instance the $\mathbb{Z}_2 \to \mathbb{Z}_2 \to \mathbb{Z}$ occurrence in all rows. The interested reader is referred to Schnyder *et al.* (2008); Kitaev (2009); Ryu *et al.* (2010) for a more detailed discussion.

This section concludes the description of how topological insulators and superconductors are classified, but before analyzing the limitations and extensions of the presented framework, there is one more important concept that needs to be discussed.

2.5 The bulk-boundary correspondence

One question that naturally arises in the discussion of TSM is how to identify which side of the topological phase transition that is topological. In particular, it is desirable to connect the topological invariant to an observable quantity, accessible in an experiment. One answer to this question is given by *the bulk-boundary correspondence* which is the topic of this section.

The essence of this correspondence is that the topology of a closed bulk Hamiltonian will result in edge states for the corresponding open system. It can be understood in the following intuitive way.

Since a topological invariant only can change if the bulk gap closes (as long as no important symmetry is broken), any spatial region where some parameter changes such that it forces a topological phase transition must be accompanied with a local closing of the gap (see Fig. 2.3). This relation holds especially at an edge, which borders the (by definition) trivial vacuum. The edges of a topological insulator or superconductor will therefore generally host some exotic edge states whose properties will follow from the symmetries of the bulk.

As a rule of thumb, a system satisfying TRS will generally host *helical edge modes*, meaning that there are two separate species of modes travelling in opposite directions, PHS implies *Majorana zero modes* which are equally weighted superpositions of particles and holes and CS implies helical Majorana modes (if PHS is also present). Additionally, the edge states may be

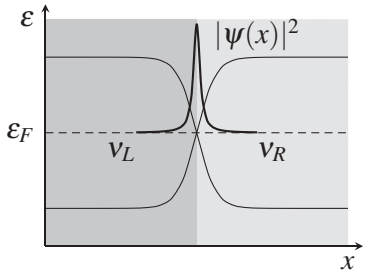

Figure 2.3: A sketch of the bulk-boundary correspondence. If there there is a change in the topological invariant, $\nu_L - \nu_R \neq 0$, there must be a local closing of the gap accompanied by a localized state ψ at the Fermi level ε_F.

conducting, as in the IQH effect, since they will cross the Fermi level which in TSM always lies in the gap.

Edge and bulk dimensions do not always have to differ by one (as the two-dimensional surface of a three-dimensional slab). Exotic states can also be trapped on topological defects (defects that can not be smoothly removed), as exemplified by Majorana zero modes trapped in zero dimensional vortices penetrating a two dimensional topological superconductor. Remarkably, it is possible to extract when such kind of trappings are possible from the periodic table (Schnyder *et al.*, 2008; Stanescu, 2017): a topological defect of dimension r, in a host system of some symmetry class, can support zero modes if the intersection of the corresponding row with column $d = r + 1$ is non-zero.

In the context of TSM, the bulk-boundary correspondence was first used by Halperin (Halperin, 1982) to describe the *chiral edge states* of the IQH effect and was later formalized by many authors (see for example (Volovik, 2003)). Its mathematical foundation can be traced back to the *Atiyah-Singer index theorem* (Atiyah and Singer, 1968; Nakahara, 2003). Roughly speaking, this theorem relates an index describing the topology of a manifold $\mathcal{M}$ to the number of zero energy solutions of differential operators acting on the boundary sub-manifold $\partial\mathcal{M}$. The number of solutions equals precisely the number of edge modes.

The bulk-boundary correspondence will be used frequently in this thesis to understand the formation of Majorana zero modes on domain walls and at edges of one-dimensional topological superconductors.

2.6 Limitations and outlook

To close this chapter, a discussion of some limitations of the previously described framework is in order.

Perhaps the most obvious objection is that it only treats single particle Hamiltonians describing non-interacting fermion systems or, in the case of superconductivity, systems within a mean field approximation. Electrons in real materials are subjected to interactions of various kinds and strengths and for the theoretical models in the periodic table to accurately describe realistic systems, the topological description must remain valid even in the presence of interactions. One way to resolve this problem is to rely on the principle of adiabatic continuity, presented in the introduction. One then assumes that the gapped ground state of the non-interacting system is adiabatically connected to the interacting ground state in a process which at all times maintain the gap. In this way, the classification is maintained, even with interactions. Another approach, discussed in Ch. 4, is to instead use a field theory description of TSM, which allows for very powerful statements regarding the effects of interactions.

There is also the possibility that interactions alter the classification. This feature was demonstrated by Fidkowski and Kitaev (2010) who showed that a $\mathbb{Z}$ invariant becomes $\mathbb{Z}_8$-valued when interaction terms are added to a topological Hamiltonian. A more well-known example is the FQH effect, which is not adiabatically connected to any non interacting state and instead relies crucially on the presence of strong interactions. The FQH states lies completely out of the classification presented in this thesis.

Generally, the influence of decoherence, thermal fluctuations or other external perturbations are assumed to be negligible due to the presence of the gap. But one may imagine systems where a *density matrix formulation*, rather than a pure state description, of TSM would be appropriate. Research in this direction is indeed ongoing (see for instance Budich and Diehl (2015)) and will hopefully shed some light on how the TSM classification can be extended to more complicated and realistic systems where the influence of the environment can not be ignored. Related to this discussion of external perturbations are non-equilibrium topological states that form because of an external driving. The most prominent example of such systems are topological Floquet insulators (Kitagawa *et al.*, 2010; Cayssol *et al.*, 2013; Roy and Harper, 2017), where the ordinary crystal space periodicity (Bloch periodicity) is supplemented by periodicity in time (Floquet periodicity).

One may also ask whether the combination of unitary and antiunitary symmetries allows for more classes in the periodic table? The answer to this question is affirmative. For instance, it has been shown that imposing additional point group crystal symmetries can result in splitting some of the classes into

more topologically distinct sub-classes (Watanabe *et al.*, 2016). The crystal symmetry has to be present only on average, so the crystal symmetry protected states are not destroyed by moderate disorder.

The last few years have witnessed an increased activity in understanding *gapless* topological states of matter. Such states are by definition not covered by the framework discussed in this thesis since they do not have any energy gap. Still topology may play a big role as demonstrated by the proposal and discovery of the *Weyl semimetal* (Herring, 1937; Wan *et al.*, 2011; Xu *et al.*, 2015). The main feature of this system is the presence of robust band touching points, known as Weyl nodes, in a three-dimensional BZ. These nodes act as magnetic monopoles in momentum space and are characterized by a chiral $\mathbb{Z}$ charge resulting in exotic boundary modes known as *Fermi arc states*. Most interestingly, the Weyl semimetal constitutes a direct experimental platform for exploring the *chiral magnetic effect* (Nielsen and Ninomiya, 1981) which is a condensed matter realization of the *chiral anomaly* in quantum field theory (Adler, 1969; Bell and Jackiw, 1969).

Despite the great success in the theoretical understanding of TSM, the experimental realization of many proposals have turned out to be challenging. Still, a major incentive for the theoretical community is the possibility to use the exotic edge states associated with non-trivial bulk topology as building blocks of topological quantum computers (Freedman *et al.*, 2003; Nayak *et al.*, 2008; Stanescu, 2017). Other possible applications include new spintronics devices, energetically effective computer components where the absence of scattering processes, originating from topological protection, substantially reduces dissipation.

3. Majorana zero modes in one-dimensional wires

A MAIN DIRECTION OF RESEARCH in the field of topological quantum matter is the hunt for *Majorana zero modes*. These modes are zero energy states bound to topological defects or edges in topological superconductors and are presently considered as a promising route towards realizing topological quantum computations (Kitaev, 2003; Freedman *et al.*, 2003; Nayak *et al.*, 2008).

This chapter begins with a general introduction to Majorana zero modes, followed by a description of one of their most promising properties, non-Abelian statistics. The introduction is succeeded by a quite extensive discussion, with focus on topological aspects, of two important models that exhibit Majorana zero modes. Moreover, the chapter also contains a description on how to calculate experimentally observable quantities related to Majorana zero modes through the scattering formalism and also the status of current experimental research. The chapter concludes by summarizing the results of PAPERS I-III.

3.1 Introduction to Majorana zero modes

The Dirac equation (Dirac, 1928) describes spin-$\frac{1}{2}$ fermions, most notably the electron and the positron, which are electrically charged. The solution describing those particles is complex and the electron and positron components, ψ and ψ_c respectively, are related through the operation of charge conjugation $\psi_c = \mathcal{C}\psi$.

Ettore Majorana[1] noted that, with a certain choice of Dirac matrices[2], the Dirac equation admits real solutions in the sense that $\psi = \psi_c$ (Majorana, 1937). Such a solution, now known as a *Majorana fermion*, is therefore charge neutral and also its own antiparticle. Majorana further speculated that the known

[1] The fate of Majorana is unknown since he disappeared mysteriously on a boat trip from Palermo to Naples in March 1938.

[2] In fact, this possibility was found already in 1928 by Eddington (Eddington, 1928), but with no interpretation of particles being their own antiparticles.

charge neutral fermions, neutrinos and neutrons, might be described by such real solutions. Although the neutron is now known to not be a Majorana fermion (it is a three-quark complex: a baryon), there is still a possibility that the neutrino is (Avignone *et al.*, 2008).

In condensed matter physics, the basic fermion particles are electrons, which are Dirac fermions. However, it turns out that Majorana fermions can appear as *emerging quasiparticles* in certain types of many-body systems. The notion of a quasiparticle is well established, as exemplified by the well-known *phonons*, *magnons* or *plasmons*[1], which are ubiquitous in the description of traditional condensed matter, and condensed matter physics treats quasiparticles on the same level as elementary particles, with no distinction between their levels of "realness".

Within the second quantisation formalism, suitable for describing many-body systems, it is always possible to divide fermion creation, $c_j^\dagger$, and annihilation, c_j, operators into two real operators[2], labelled A and B, according to

$$\left.\begin{aligned} c_j &= (\gamma_{Aj} + i\gamma_{Bj})/2 \\ c_j^\dagger &= (\gamma_{Aj} - i\gamma_{Bj})/2 \end{aligned}\right\} \Leftrightarrow \begin{cases} \gamma_{Aj} = c_j + c_j^\dagger, \\ \gamma_{Bj} = ic_j^\dagger - ic_j. \end{cases} \tag{3.1}$$

From the canonical fermion anti-commutation relations $\{c_i^\dagger, c_j\} = \delta_{ij}$, it follows that the Majorana operators must satisfy

$$\gamma_{A(B)j} = \gamma_{A(B)j}^\dagger, \qquad \{\gamma_{Ai}, \gamma_{Bj}\} = 2\delta_{AB}\delta_{ij}. \tag{3.2}$$

The self-conjugate property of these operators implies that a quasiparticle created by such an operator is its own antiparticle, and that adding it to or removing it from the many body quantum state has the same effect. In this way the γ-operators actually describe Majorana fermions.

So far, this re-writing is just a unitary transformation, yielding another representation of the electron fermion degrees of freedom, where each electron now is represented by two Majorana fermions. In most cases, this transformation is not very useful, since instead of an electron, one just has two bound Majorana fermions instead. Nevertheless, it is interesting to ask whether there are systems where the two Majorana fermions constituting one electron are spatially separated and can be manipulated and observed independently.

Indeed, the right-hand side of Eq. (3.1) suggests that a natural hunting ground for Majorana fermions are weakly interacting superconductors in which the quasiparticle excitations are superpositions of electrons and holes (known

[1] The condensed matter electron is also a quasiparticle, since its mass is renormalized by interactions.

[2] Compare with a complex number divided into two real numbers.

as *Bogoliubov particles* or *Bogoliubons*) whose electrical charge is only conserved modulo $2e$ due to the presence of the Cooper pair condensate[1]. Within the description of such superconductors, the Bogoliubov-de Gennes (BdG) formalism, there is a built-in redundancy or ambiguity known as *particle-hole symmetry* (PHS) relating quasiparticles with positive and negative excitation energies. As a consequence of PHS, there is a general analogy between Bogoliubov quasiparticles and Majorana fermions (Senthil and Fisher, 2000; Chamon *et al.*, 2010; Elliott and Franz, 2015). In this sense, with all the existing experimental support of the BdG formalism, the existence of emergent Majorana fermions in superconductors is well established.

There is, however, a much more fascinating phenomenon that can occur. Bogoliubov quasiparticles can be bound to topological defects such as vortices, edges or domain walls (Caroli *et al.*, 1964; Read and Green, 2000). The PHS requires that such bound states must come in pairs, with the additional possibility of an unpaired $\varepsilon = 0$ state[2]. The composition of the quasiparticle state and the defect is called a *Majorana zero mode* (MZM), a *Majorana bound state* (MBS) or a *Majorana*, and the host superconductor is referred to as a *topological superconductor*. The MZMs are very interesting because of their unusual exchange statistics and are in fact *non-Abelian anyons*. It is therefore important to distinguish between the special MZMs and the general Majorana fermion interpretation of Bogoliubov quasiparticles[3].

To understand which type of superconductors that can host MZMs, consider the operator creating a quasiparticle in an ordinary s-wave superconductor. It would be of the kind $b = uc^\dagger_\uparrow + vc_\downarrow$ where u and v are the electron and hole amplitudes and the c-operators create or destroy electrons and holes with some prescribed spin-projection. The existence of a zero energy charge neutral quasiparticle requires both equal electron and hole amplitudes, $v = u^*$, but also equal spin-projections. That indicates that something different from an ordinary opposite-spin s-wave pairing is needed.

Instead, by considering p-wave superconductors, in which there is an underlying topology restricting the energy spectrum, there are possibilities for MZMs to appear (Read and Green, 2000; Kitaev, 2001). A p-wave superconductor is in fact a topological state of matter, but there is no consensus on the existence of any material hosting such a state (see for instance Kallin (2012)). Instead, much recent research has been devoted to experimentally

[1] If Coulomb interactions are too strong, the equivalence of charge $+e$ and $-e$ excitations breaks down and the BdG-description is not accurate.

[2] The spectrum of the full superconductor must host an even number of such states, but the point is that they can be spatially separated.

[3] Note also that MZMs are not quasiparticles, since they do not have their own dynamics, as they are bound to the defects.

engineer topological superconductors in laboratories by combining already present building blocks such as semiconductors, *s*-wave superconductors, ferromagnets, external magnetic fields, and topological insulators. In certain parameter regimes, these hybrid devices are expected to host MZMs (see Alicea (2012) for a broad overview).

At this point it is suitable to discuss and demonstrate why having isolated MZMs would be so interesting. Apart from being a signature of topological superconductivity, a distinct phase of matter, the MZMs exhibit *non-Abelian statistics* which opens up new ways of performing quantum computations.

3.2 Demonstration of non-Abelian statistics

It is commonly taught in introductory quantum mechanics that the wave function of a system of bosons or fermions has to be symmetric or anti-symmetric respectively upon exchange of any two particles. One can view this sign as the wave function acquiring a phase of 0 or π from the exchange process.

This property turns out to break down in spatial dimensions $d \leq 2$ (Leinaas and Myrheim, 1977). In one dimension, the concept of bosons and fermions is not even meaningful, since particles can not be exchanged when confined to a line. This feature leads to incredibly rich physics, for instance the Luttinger liquid (Haldane, 1981).

In two dimensions, it is possible for the wave function to pick up *any* phase, resulting in what is known as *anyonic statistics* (Wilczek, 1982)[1]. Particles having this peculiar property are referred to as *anyons*. Anyons typically come in two broad classes. They can either be *abelian* and particle exchange results in a $U(1)$ phase factor, or the exchange results in a completely new state; the phase factor is replaced by a $U(N)$ matrix and the anyons are called *non-abelian*.

A straightforward way of understanding the latter case in more detail, that also puts MZMs directly onto the stage, is to consider a system of four spatially separated MZMs on a two-dimensional plane[2] (Read and Green, 2000; Ivanov, 2001; Akhmerov *et al.*, 2015). Two fermion creation operators may then be constructed according to

$$c_1^\dagger = \frac{1}{2}(\gamma_1 + i\gamma_2), \quad c_2^\dagger = \frac{1}{2}(\gamma_3 + i\gamma_4) \tag{3.3}$$

[1] The usage of the word "statistics" is somewhat misleading since it has nothing to do with statistics in the usual mathematical sense, but it is the conventional nomenclature. Using "topological phase interaction" might be more appropriate.

[2] One may for example consider four vortices in a planar *p*-wave superconductor.

together with their respective annihilation operators. The MZMs are zero energy states in the middle of the superconducting gap and it will be assumed that any other energy scale involved with the movement of MZMs is much smaller than that gap; an *adiabatic* assumption. The MZMs then form a ground state with four-fold degeneracy[1], since all single particle fermionic states can be either occupied or empty with no difference in energy. The four basis states of the ground state space are

$$|00\rangle \quad |11\rangle \quad |10\rangle \quad |01\rangle, \tag{3.4}$$

where the three latter states are constructed by acting with the fermionic creation operators on the empty vacuum state $|00\rangle$, through the relations $c_i|00\rangle$ with $i = 1,2$. For instance, $|11\rangle = c_1^\dagger c_2^\dagger |00\rangle$.

At this point, it is crucial to note that there never can be any single occupation of a Majorana state since there is no way of constructing a sensible number operator as $\gamma_j^\dagger \gamma_j = \gamma_j \gamma_j \equiv 1$. The only meaningful occupation is the original fermionic one.

Operators that exchange two MZMs, labelled by m and n, can be derived on quite general premises (see for instance Alicea (2012) or Akhmerov *et al.* (2015)). Requiring fermion parity conservation, locality (in the sense that only the two exchanged Majorana operators should be involved) and unitarity yields the operator

$$B_{mn} = \frac{1}{\sqrt{2}}(1 \pm \gamma_m \gamma_n), \tag{3.5}$$

where the two signs correspond to a clock- or anti-clockwise exchange. For the remainder of this section, only the clock-wise exchange operator will be used. The exchange operator acts on the MZMs according to

$$\begin{aligned} B_{mn}\gamma_m B_{mn}^\dagger &= -\gamma_n \\ B_{mn}\gamma_n B_{mn}^\dagger &= +\gamma_m, \end{aligned} \tag{3.6}$$

which can be checked by using the canonical anti-commutation relations. Starting from the state $|00\rangle$ and exchanging Majorana number 1 and 3 results in

$$B_{13}|00\rangle = \frac{1}{\sqrt{2}}(1+\gamma_1\gamma_3)|00\rangle = \frac{1}{\sqrt{2}}(1+c_1^\dagger c_2^\dagger)|00\rangle = \frac{1}{\sqrt{2}}(|00\rangle + |11\rangle). \tag{3.7}$$

This is a quite profound result, since the exchange creates a new quantum state, a superposition of the basis states. This is fundamentally different from just picking up an overall phase as for fermions or bosons. It should also be clear

[1] Using "de-Gennes-eracy" might be appropriate here.

that such an exchange is interesting for constructing qubits, the cornerstone of a potential quantum computer. The reason for that is that the exchange only depends on the topological or global properties of the performed exchange and the details of the exchange are irrelevant. As such, using non-Abelian exchange as quantum gates brings with it a protection from local perturbations since the encoded information is highly non-local.

By performing two sequential exchanges one notices that the order of exchange is important. For instance,

$$B_{12}B_{23} \neq B_{23}B_{12} \Leftrightarrow [B_{12}, B_{23}] \neq 0, \tag{3.8}$$

independently of the starting state. With some further analysis, one can also show that the exchange operators B_{mn} form a representation of a group called the *Braid group*. If the group elements in a group fail to commute like in Eq. (3.8), the corresponding group is said to be non-Abelian. It is in this way MZMs are to be understood as non-Abelian anyons.

In the example just given, the calculation above was performed in two spatial dimensions where the meaning of exchange is quite clear. For the remainder of this chapter, however, the MZMs will be located on the edges of one-dimensional wires. It is then natural to ask if the concept of braiding or exchange is still meaningful. The answer is affirmative. For instance, in Alicea *et al.* (2011) it is reported that non-Abelian exchange can be performed in a setup where edge MZMs are moved around using electronic gates in T-junction networks of one-dimensional wires. The description of such wires will be discussed next.

3.3 The Kitaev chain model

An exactly solvable and conceptually rich model exhibiting unpaired MZMs, proposed by Kitaev, consists of the Hamiltonian (Kitaev, 2001)

$$\mathcal{H} = \sum_{j=1}^{N} \left[-t(c_j^\dagger c_{j+1} + c_{j+1}^\dagger c_j) + \Delta c_j c_{j+1} + \Delta^* c_{j+1}^\dagger c_j^\dagger - \mu(c_j^\dagger c_j - \frac{1}{2}) \right], \tag{3.9}$$

and describes a one-dimensional chain with $N \gg 1$ sites (for simplicity, the lattice constant is set to unity) that can be empty or occupied by spin-less (spin-polarized) fermions, created or annihilated at site j by operators $c_j^\dagger$ and c_j. These operators fulfil the canonical fermionic anti-commutation relations $\{c_i^\dagger, c_j\} = \delta_{ij}$, while all other anti-commutators are zero.

The hopping amplitude between next neighbouring sites is given by t[1], μ

[1]The hopping t can generally be complex. This possibility will be discussed in a later section.

is the chemical potential and $\Delta = |\Delta| e^{i\theta}$ is the superconducting order parameter. In the Hamiltonian, the order parameter is accompanied by two creation or annihilation operators that describe creation or annihilation of electron pairs living on *neighbouring sites*. As will be shown below, this construction introduces superconducting pairing of p-wave type. In the present case of spin-less fermions, ordinary on-site s-wave pairing is not possible because of the Pauli principle: $(c_j)^2 = (c_j^\dagger)^2 = 0$.

It is important to note that the Hamiltonian (3.9), does not commute with the total number operator $N_F = \sum_{j=1}^{N} c_j^\dagger c_j$ and the total number of fermions is not conserved. However, the Hamiltonian does commute with the fermion parity operator $P = (-1)^{N_F}$, so fermion parity, the fermion number modulo 2, is a conserved quantity. The parity of the many body ground state is of crucial importance in understanding this model and will be discussed extensively in Sec. 3.3.1.

To see how unpaired Majorana zero modes appear in Kitaev's model, the fermion operators on each site are re-written in terms of two *real* Majorana operators (Majoranas for short), A and B, defined by

$$\left.\begin{aligned} c_j &= e^{-i\theta/2}(\gamma_{Aj} + i\gamma_{Bj})/2 \\ c_j^\dagger &= e^{+i\theta/2}(\gamma_{Aj} - i\gamma_{Bj})/2 \end{aligned}\right\} \Leftrightarrow \begin{cases} \gamma_{Aj} = e^{+i\theta/2} c_j + e^{-i\theta/2} c_j^\dagger, \\ \gamma_{Bj} = -ie^{+i\theta/2} c_j + ie^{-i\theta/2} c_j^\dagger, \end{cases} \tag{3.10}$$

such that the the superconducting phase θ is effectively removed. In terms of Majorana operators, the Hamiltonian (3.9) becomes

$$\mathcal{H} = \frac{i}{2} \sum_{j=1}^{N} \left[-\mu \gamma_{Aj} \gamma_{Bj} + (|\Delta| + t) \gamma_{Bj} \gamma_{Aj+1} + (|\Delta| - t) \gamma_{Aj} \gamma_{Bj+1} \right]. \tag{3.11}$$

In this Majorana basis, the interesting behaviour of the model is revealed in two special parameter limits.

(a) The "trivial" limit: $|\Delta| = t = 0$ and $\mu < 0$. With this choice, the Hamiltonian becomes

$$\mathcal{H} = \frac{i|\mu|}{2} \sum_{j=1}^{N} \gamma_{Aj} \gamma_{Bj} = |\mu| \sum_{j=1}^{N} \left[c_j^\dagger c_j - \frac{1}{2} \right]. \tag{3.12}$$

Here, Majorana operators from the same site (see Fig. 3.1a) are paired and form a unique and empty (and therefore insulating) ground state. As argued by Kitaev, and as will be clear below, the insulating behaviour is in fact present for the whole parameter range $|\mu| > 2t$. This can be intuitively understood by the following argument. The region $\mu < -2t$

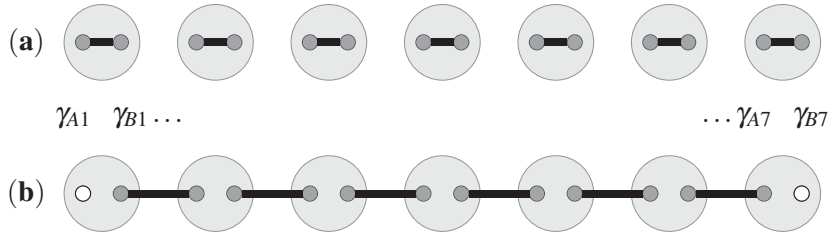

Figure 3.1: Two types of Majorana operator pairings in a chain with seven electronic sites. In **(a)**, Majorana operators are paired on the same site, while in **(b)**, the pairing occurs between neighbouring sites, leaving two unpaired Majorana operators, γ_{A1} and γ_{B7}, at the edges.

is where no particles at all are present in the energy band (the exact description of the energy bands is given in Sec. 3.3.1) so the chosen regime is definitely an insulator since the superconducting pairing (happening at the Fermi-level) occurs between empty levels. The region $\mu > 2t$ corresponds to a completely full band, which by a particle-hole transformation is equivalent to the former parameter region.

(b) The "topological" limit: $|\Delta| = t$ and $\mu = 0$. Now instead

$$\mathcal{H} = it\sum_{j=1}^{N-1}\gamma_{Bj}\gamma_{Aj+1} = 2t\sum_{j=1}^{N-1}\left[\tilde{c}_j^\dagger\tilde{c}_j - \frac{1}{2}\right], \tag{3.13}$$

where in the second equality, a new set of fermion operators $\tilde{c}_j = \frac{1}{2}(\gamma_{Bj} + i\gamma_{Aj+1})$ has been defined. With this parameter choice, Majorana operators couple between *neighbouring* sites (see Fig. 3.1b).

Remarkably, the expression (3.13) does not include the two operators γ_{A1} and γ_{BN}. These can be combined into a single fermionic operator $f = \frac{1}{2}(\gamma_{A1} + i\gamma_{BN})$, which has zero energy (being absent from the Hamiltonian) and is extremely non-local in the sense that it resides on the two edges of the system. Due to the zero energy of this fermion mode, there are two degenerate ground states differing in fermionic parity.

The situation of having a non-local fermionic state, or equivalently two separately located MZMs, extends to the parameter range $|\mu| < 2t$. The MZMs are then not simply given by γ_{A1} and γ_{BN} but instead some linear combination of additional Majorana operators. The corresponding wave functions decay exponentially $e^{-x/\xi}$, where L is the wire length and x is the distance from the edge, into the wire bulk on a length scale given by the superconducting coherence length ξ. Furthermore, the overlap of

the edge wavefunctions results in an exponential splitting $e^{-L/\xi}$ between the two degenerate ground states, effectively giving the edge states finite energy. This is usually referred to as *gapping out* the states. Still, if the wire is sufficiently long, the overlap is negligible and the states remain at zero energy.

In summary, the behaviour of these two special limits extends to two separate regions in parameter space (see Fig. 2.1b). One of the regions, the topological phase, has exponentially localized MZMs on the edges, while the other trivial phase has not. As will now be shown, these features follow from an underlying topological structure.

3.3.1 Topological structure and invariants

In order to unveil the topological properties of the Hamiltonian (3.9) it is most convenient to impose periodic boundary conditions, which allows a momentum space representation. Doing so, it is useful to introduce $\Psi_k^\dagger = (c_k^\dagger, c_{-k})$ so that the Hamiltonian can be written as $\mathcal{H} = \frac{1}{2}\sum_k \Psi_k^\dagger h(k) \Psi_k$ with $h(k)$ given as

$$\begin{aligned} h(k) = {} & 2|t|\sin(k)\sin(\phi)\mathbb{1} + \big(-\mu - 2|t|\cos(k)\cos(\phi)\big)\tau_z \\ & - 2\Re(\Delta)\sin(k)\tau_y + 2\Im(\Delta)\sin(k)\tau_x, \end{aligned} \tag{3.14}$$

where the possibility of a complex $t = |t|e^{i\phi}$ has been added. The Pauli-matrices τ_i act in particle-hole space, and $\Re$ and $\Im$ denote the real and imaginary parts respectively. The energy bands are given by[1]

$$\varepsilon_\pm(k) = 2|t|\sin(k)\sin(\phi) \pm \Big[\big(\mu + 2|t|\cos(k)\cos(\phi)\big)^2 + 4|\Delta|^2\sin^2(k)\Big]^{1/2}. \tag{3.15}$$

A most notable feature of the band structure is that the effective band gap, $\varepsilon_+(k) - \varepsilon_-(k)$, depends on k and that the gap closes when $\mu = \pm 2t$. This closing can only happen at $k = 0$ or $k = \pi$ (recall that $\pm\pi$ refers to the same point in the BZ)[2]. As will be clear soon, these two gap closing points constitute topological phase transitions between two topologically distinct phases of matter.

The BdG Hamiltonian (3.14) has in general only a single symmetry[3], PHS,

[1] This is most easily derived by using the identity $h(k)^2 = \mathbb{1}\varepsilon(k)^2$, valid for any Hamiltonian expressed as a linear combination of Pauli matrices.

[2] In the limit of a very large system, both these points belong to the BZ but for finite lattice systems, the boundary conditions and the even/oddness of the number of sites must be treated carefully.

[3] If t is taken to be real, the model actually has an additional symmetry, as described in the following sections.

which in the chosen basis reads $\mathcal{P} = \tau_x \mathcal{K}$. It sets the constraint

$$\tau_x h^T(k) \tau_x = -h(-k). \tag{3.16}$$

Since $\mathcal{P}^2 = \mathbb{1}$, the one-dimensional Kitaev chain model generally belongs to symmetry class $\mathcal{D}$ and therefore has a $\mathbb{Z}_2$-invariant distinguishing two topological regimes. This invariant will now be explicitly constructed in various ways.

Ground state parity

The physical motivation for finding an invariant can be thought of in the following way (Akhmerov *et al.*, 2015). The PHS of a generic BdG-Hamiltonian requires the energy eigenstates to come in pairs: given an energy eigenstate $|\psi\rangle$ with energy ε, there must be another eigenstate $|\tilde{\psi}\rangle = \mathcal{P}|\psi\rangle$ with energy $-\varepsilon$. It follows that the energy spectrum of a general BdG-Hamiltonian is always mirror symmetric around $\varepsilon = 0$.

Next, one may imagine a process that deforms two arbitrary BdG - Hamiltonians into each other. By calculating the energy spectrum for all steps in the deformation process it may happen that some energy levels cross at $\varepsilon = 0$. In general, such an energy crossing is related to some symmetry and some conserved quantity (von Neumann and Wigner, 1929). It turns out that as long as there is an energy gap around $\varepsilon = 0$, a generic BdG Hamiltonian actually has a conserved quantity which is the *ground state fermion parity*. A superconductor does not conserve the particle number due to the pairing terms, but provided the superconductor is isolated, it conserves the even- or oddness of the particle number, which is precisely the fermionic parity.

The parity is not a single particle property but instead one of the many body state. To relate the energy crossings to the parity it must be remembered that the BdG-doubling trick to extract the single particle spectrum is artificial and that the two $\pm\varepsilon$ states actually refer to a *single* Bogoliubov quasiparticle state. One interpretation of the doubling is therefore that occupying a quasiparticle in the state with $-\varepsilon$ is the same as emptying the one with $+\varepsilon$.

If a zero energy crossing occurs during the deformation, one energy state changes sign and it becomes energetically favourable to add or remove a single quasiparticle. Therefore, the ground state parity will change at zero energy crossings, and are therefore called *fermion parity switches*.

It is therefore natural to use the *ground state parity* as a topological invariant since it can not change unless some state crosses zero energy, meaning that the gap closes. There is a mathematical quantity appropriate to describe this change of parity, known as the *Pfaffian*, which can be introduced with the following heuristic argument (see also App. A for a detailed discussion).

Since the energy eigenvalues of the Hamiltonian $\mathcal{H}$ come in $\pm\varepsilon_n$ pairs, the product of them, the determinant, can be written $\det(\mathcal{H}) = \prod_n(-\varepsilon_n^2)$ and is zero when the gap closes and some energy crosses zero. The Pfaffian can be viewed as the square root of the determinant: $\mathrm{Pf}(H) = \pm i\prod_n \varepsilon_n$, with a consistent choice of the overall sign, and exists for any even-dimensional anti-symmetric matrix: $A^T = -A$. Due to PHS, one may always find a basis where the necessarily even-dimensional BdG-Hamiltonian is anti-symmetric.

At a zero energy crossing, there is a single state that changes sign which in turn forces a sign change of the Pfaffian. The sign of the Pfaffian is therefore a natural candidate for a superconducting topological invariant.

The class $\mathcal{D}$ Pfaffian $\mathbb{Z}_2$ invariant

Consider the translationally invariant Kitaev chain model (3.14) with periodic boundary conditions. The chain is assumed to contain a sufficiently large number of sites so that k can be treated as a continuous variable.

In this case, as discussed in App. A, the ground state parity and the topological invariant is given by

$$\nu = \mathrm{sgn}\{\mathrm{Pf}\left(\tilde{A}(0)\right)\}\mathrm{sgn}\{\mathrm{Pf}\left(\tilde{A}(\pi)\right)\}, \tag{3.17}$$

where $\tilde{A}(k)$ is the BdG-Hamiltonian in the Majorana representation. Up to an overall constant factor, it is given by

$$\tilde{A}(k) = \begin{pmatrix} 0 & \mu + 2t\cos(k) - 2i|\Delta|\sin(k) \\ -\mu - 2t\cos(k) - 2i|\Delta|\sin(k) & 0 \end{pmatrix}. \tag{3.18}$$

If follows that $\mathrm{Pf}\{\tilde{A}(k)\} = \mu + 2t\cos(k) - 2i|\Delta|\sin(k)$ resulting in

$$\nu = \mathrm{sgn}(\mu + 2t)\mathrm{sgn}(\mu - 2t) = \pm 1. \tag{3.19}$$

This final result is in agreement with the intuition that the parameters allowing the gap to close, $\mu = \pm 2t$, should yield an ill-defined invariant. It is important to note though, that the formula (3.19) requires the system to be gapped at all points in the BZ, implying $|\Delta| \neq 0$ (see Eq. (3.15)). It remains to connect the value of ν to the presence of MZMs in the corresponding open system. To this end, note that MZMs were present for the case $\mu = 0 < t = |\Delta|$ which yields $\nu = -1$. Since the topological behaviour, and by the bulk boundary correspondence the presence of MZMs, cannot change unless the gap closes, one can conclude that edge MZMs will always be present as long as $\nu = -1$.

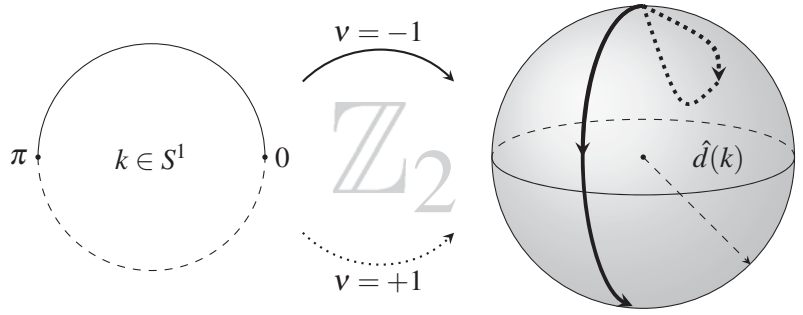

Figure 3.2: Two classes of allowed trajectories of the vector $\hat{d}(k)$ when sweeping the BZ. The black curve runs from pole to pole resulting in a non-trivial phase. The dotted curve, on the other hand, runs from one pole back to the same, resulting in a trivial phase. These types of trajectories can not be deformed into each other without closing the gap.

The class $\mathcal{D}$ geometric invariant

There is a more visual or geometric way of determining the $\mathbb{Z}_2$-invariant (Alicea, 2012). Consider Eq. (3.14) written as $h(k) = \vec{d}(k) \cdot \vec{\tau}$, where $\vec{\tau}$ is the vector of particle-hole Pauli matrices. The basis spinors satisfy $(\Psi^\dagger_{-k})^T = \tau_x \Psi_{-k}$ so that the vector $\vec{d}(k)$ must obey $d_{x,y}(k) = -d_{x,y}(-k)$ and $d_z(k) = d_z(-k)$. Thus, it suffices to study the properties of $\vec{d}(k)$ on half the BZ ($0 \leq k \leq \pi$) since the behaviour in the other half follows directly from these constraints.

Suppose now that the Hamiltonian is gapped in the whole BZ. This imposes the constraint $|\vec{d}(k)| \neq 0$ for all k and a unit vector $\hat{d}(k)$ can be defined. This unit vector now provides a map from half of the BZ to the unit sphere, depicted in Fig. 3.2.

As k runs from 0 to π, $\hat{d}(k)$ starts from either the north or south pole, and ends up back at the same pole or at the opposite one depending on the sign of $-\mu - 2t$. Explicitly, $\hat{d}(0) = \text{sgn}(-2t - \mu)\hat{z}$ and $\hat{d}(\pi) = \text{sgn}(2t - \mu)\hat{z}$ so that the product $\nu = \text{sgn}(\mu + 2t)\text{sgn}(\mu - 2t) = \pm 1$ defines a $\mathbb{Z}_2$-invariant which only can change when the bulk gap closes resulting in $\hat{d}(k)$ being ill-defined for some k. The sign corresponding to a specific pole on the sphere depends on the chosen basis, but the product is invariant under any such choice.

Class $\mathcal{BDI}$ winding invariant

It is also useful to study the topological invariant in a somewhat different setting. Consider a situation where Δ is real, or has a constant phase which can globally be put to zero. Generally, this requires a real hopping parameter t.

With this additional constraint, one may choose $\vec{d}(k)$, defined in the pre-

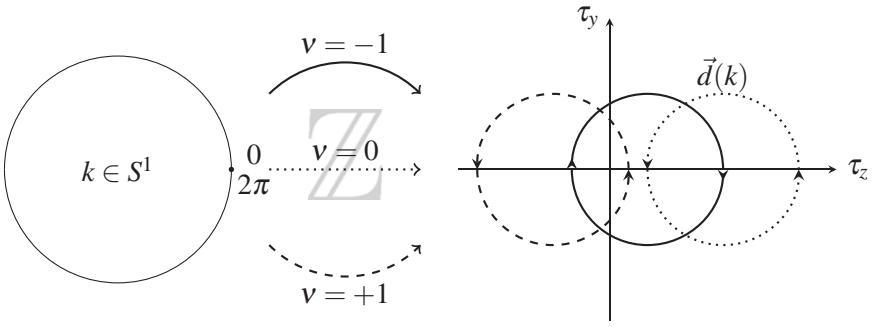

Figure 3.3: Winding around the origin of the vector $\vec{d}(k)$ as k goes from 0 to 2π. The dashed curve winds once in the positive direction: $\nu = +1$, the filled curve winds negatively: $\nu = -1$ and the dotted curve does not wind around the origin: $\nu = 0$. The winding number is ill-defined for a curve touching the origin.

vious section, to be two-dimensional. Without loss of generality, let $\vec{d}(k) = (0, -2\Delta\sin(k), -\mu - 2t\cos(k))^T$. The gap is still given by $|\vec{d}(k)|$. Consider now $\vec{d}(k)$ in the two dimensional $\tau_z - \tau_y$ plane. Taking a non-zero Δ and keeping μ and t fixed, there exists a topological $\mathbb{Z}$-valued *winding number* ν measuring the number of revolutions $\vec{d}(k)$ makes around the origin as k runs from 0 to 2π (see Fig. 3.3). The winding number is given by

$$\nu = \frac{1}{2\pi i}\int_0^{2\pi} dk\, \partial_k \log\left[d_z(k) + i d_y(k)\right] = \Theta(2t - |\mu|)\mathrm{sgn}(\Delta), \tag{3.20}$$

where Θ is the Heaviside step function. The origin of this winding number invariant can be understood from Tab. 2.2. Due to the constraint on Δ to be real, the Hamiltonian has an additional TRS, in the chosen basis equal to $\mathcal{T} = \mathcal{K}$, $\mathcal{T}^2 = +1$. This changes the symmetry classification from class $\mathcal{D}$ to class $\mathcal{BDI}$ which changes $\mathbb{Z}_2$ to $\mathbb{Z}$. Out of the set of integers, only the subset $\{+1, -1, 0\}$ is realised in the Kitaev chain. From Eq. (3.20), it is clear that the winding number distinguishes between chains with opposite sign of the order parameter, and may think of a system where one half of a wire has a fixed zero superconducting phase, while the other half has its phase shifted by π, effectively yielding a negative value of Δ. The bulk winding number is then different in these halves which forces the energy gap to close at the boundary between the halves. Due to the bulk-boundary correspondence, it follows that MZMs must appear on this interface. Systems with this feature are investigated in PAPER I.

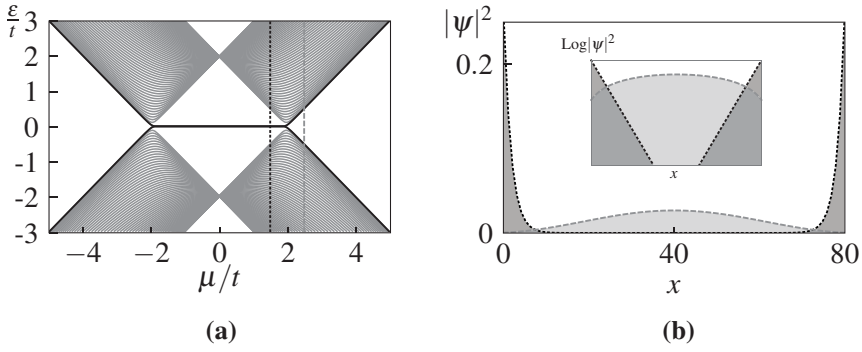

Figure 3.4: (a) The energy spectrum of the Kitaev chain as the chemical potential μ is varied. The superconducting gap $\Delta = 1$ and the number of sites $N = 80$. The bulk states are depicted in gray, while the lowest energy states are black. The black dotted and gray dashed lines denote two parameter choices corresponding to the trivial and non-trivial phase respectively. The energy gap closes at $\mu = \pm 2t$. **(b)** Lowest energy states of the Kitaev chain for the two line cuts in (**a**). Inset: the low energy states on a logarithmic scale, indicating the exponential nature of the non-trivial edge states.

3.3.2 Exact diagonalisation

Before ending the discussion on the Kitaev chain model, it is enlightening to solve the model numerically (see Sec. 2.2). The Hamiltonian is represented by a $2N \times 2N$ matrix H where N is the number of sites in the chain and the factor of 2 comes from the particle-hole degrees of freedom. A useful set of basis states is $\{|i\rangle\}_i$, unit-vectors of length $2N$ where non-zero entries on even and odd positions correspond to occupied holes and particles respectively. Explicitly, an open chain with 6 sites would in this basis be represented by

$$H_{6\times 6} = \begin{bmatrix} H_{\text{on}} & H_{\text{off}} & 0 & 0 & 0 & 0 \\ H_{\text{off}}^{\dagger} & H_{on} & H_{\text{off}} & 0 & 0 & 0 \\ 0 & H_{\text{off}}^{\dagger} & H_{\text{on}} & H_{\text{off}} & 0 & 0 \\ 0 & 0 & H_{\text{off}}^{\dagger} & H_{\text{on}} & H_{\text{off}} & 0 \\ 0 & 0 & 0 & H_{\text{off}}^{\dagger} & H_{\text{on}} & H_{\text{off}} \\ 0 & 0 & 0 & 0 & H_{\text{off}}^{\dagger} & H_{\text{on}} \end{bmatrix}, \tag{3.21}$$

where the 2×2 matrices $H_{\text{on}} = -\mu\tau_z$ and $H_{\text{off}} = -t\tau_z - i\Re(\Delta)\tau_y + i\Im(\Delta)\tau_x$ represent the on-site and off-site contributions respectively. The hopping t has been choosen real. The Hamiltonian matrix can be straightforwardly diagonalized on a computer, and the obtained eigenvectors are the particle/hole occupations along the wire, and the eigenvalues are the single particle energies. The great advantage of this approach is that site dependent parameters

can easily be implemented by modifying $H_{\text{on/off}}$ for any site. Periodic boundary conditions can be implemented by adding H_{off} and $H_{\text{off}}^{\dagger}$ on matrix entries $(6,1)$ and $(1,6)$ respectively.

In Fig. 3.4, the spectrum and the probability distribution for the lowest energy state are depicted for an open Kitaev chain with $N = 80$ sites. Clearly, the spectrum contains exponentially localized zero energy modes in the topological regime $\mu < 2t$, while in the trivial phase $\mu > 2t$ no such states exist. The transition between the phases is accompanied by a closing of the gap, occurring at $\mu = \pm 2t$.

3.4 Topological superconducting wires

While the Kitaev chain model (3.9) is without doubt conceptually important, it is still a toy model, and one may ask whether there are real physical systems that can realize MZMs. Systems with *intrinsic* p-wave superconductivity seems to be rare in nature and it is also not clear how MZMs in these systems would be detected and manipulated (Kallin, 2012; Stanescu, 2017). Instead, the by far most appealing approach to realize MZMs is to engineer *synthetic* topological superconductors by combining already existing building blocks such as topological insulators, ordinary s-wave superconductors and ferromagnets. Such ideas were first proposed by Fu and Kane (Fu and Kane, 2008, 2009), who showed that topological superconductivity and MZMs could be achieved by combining topological insulator edges with an ordinary s-wave superconductor. Subsequently, it was realized that the experimentally unwieldy topological insulators could be replaced by simpler and more accessible materials such as semiconductors or magnets.

For the realization of the Kitaev chain model, there are two dominant directions of current research. The first concerns magnetic impurity chains on top of superconducting slabs (Choy *et al.*, 2011; Nadj-Perge *et al.*, 2013, 2014; Pientka *et al.*, 2014a), while the second consists of superconducting nanowires with strong spin orbit coupling in external magnetic fields (Lutchyn *et al.*, 2010; Oreg *et al.*, 2010). In this thesis, only the second setup will be considered and is analyzed in some detail as follows.

3.4.1 Motivation

To realize the Kitaev chain model (3.9), there are two basic requirements that must be fulfilled: *i)* The electrons must be *effectively spinless*, in the sense that half of the spin degrees of freedom are "frozen out" and *ii)* superconducting p-wave pairing. One could argue that Zeeman spin-polarization by a magnetic field and placing the chemical potential between the polarized bands would be

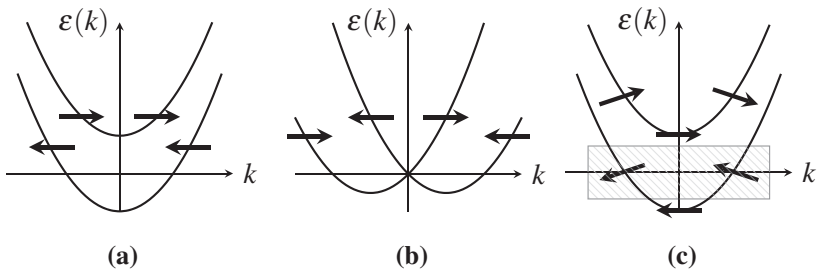

Figure 3.5: Sketch of energy spectra for a 1D wire with parabolic dispersion and spin-polarizations indicated by black arrows. (**a**) A magnetic field spin-polarizes the two bands. (**b**) Rashba spin-orbit coupling splits the two spin degenerate bands into two branches. (**c**) The combination of perpendicular Rashba spin-orbit coupling and magnetic field partially spin-polarizes the bands. If the chemical potential is placed in between the bands, indicated by the dashed rectangle, the proximity effect can induce p-wave superconductivity into the wire.

enough to achieve a spinless regime (see Fig. 3.5a). Unfortunately, it would be difficult to induce superconducting pairing by the *the superconducting proximity effect* from an ordinary s-wave superconductor, since that pairing is possible only between electrons with opposite spins.

A more clever idea is to instead use Rashba spin-orbit coupling to achieve what is known as *spin-momentum locking*, where an electron's spin-polarization is strongly tied to its direction of motion. As shown in Fig. 3.5b, the spin-orbit coupling effectively splits two degenerate spin-bands into two branches where the spin is polarized along a direction perpendicular to the direction of the wire. If a magnetic field, perpendicular to this polarization, is applied, the two bands become separated in energy and with a chemical potential placed between the bands (the dashed region in Fig. 3.5c), half of the spin-degrees of freedom are in-active. The crucial point is now that the spins close to the Fermi level (where the superconducting pairing occurs) are *almost* parallel and induced p-wave pairing is thereby possible. By adjusting the magnetic field strength appropriately, this pairing can be isolated, resulting in an effective topological p-wave superconductor. This explicit mapping will be shown next.

3.4.2 Hamiltonian and mapping onto the Kitaev chain model

The starting point is to consider a single 1D semi-conducting nanowire lying in the x-y plane. The wire has Rashba spin-orbit coupling strength α_R and proximity induced s-wave pairing Δ and is exposed to an external magnetic field $\vec{B}$. The magnetic field can be parametrized with the polar angle

θ measured from the z-axis and the azimuthal angle ϕ measured from the x-axis. Assuming the wire to be thin, so that only a single channel is occupied, this system can be described by a BdG Hamiltonian acting on basis spinors $\psi(w) = (u_\uparrow(w), u_\downarrow(w), v_\uparrow(w), v_\downarrow(w))^T$, where w is the coordinate along the wire, u and v represents electron and hole components and $\uparrow,\downarrow$ refers to the spin-projection along the z-axis. The Hamiltonian reads

$$\mathcal{H}_{\text{BdG}}(p_w) = \begin{pmatrix} h(p_w) & h_\Delta \\ h_\Delta^\dagger & -h^T(-p_w) \end{pmatrix}, \tag{3.22a}$$

$$h(p_w) = \frac{p_w^2}{2m^*} - \mu - \alpha_R p_w(\sigma_y \cos\varphi - \sigma_x \sin\varphi) + \vec{h}\cdot\vec{\sigma}, \tag{3.22b}$$

$$h_\Delta = |\Delta| e^{i\phi_s}(i\sigma_y). \tag{3.22c}$$

In these expressions, $\vec{p}_w = p_w(\cos\varphi, \sin\varphi)$ is the planar momentum operator parametrized by φ, the angle between the wire and the positive x-axis. The effective electron mass is denoted by m^* and μ is the chemical potential. The spin-orbit coupling is assumed to arise from some electrical field pointing in the $\hat{z}$ direction, and favours spin-alignment along some vector, referred to as the spin-orbit vector, in the x-y plane. Furthermore, $\vec{h} \equiv \frac{1}{2} g \mu_B \vec{B}$ is the Zeeman field with g the effective g-factor in the wire, μ_B the Bohr magneton, and $\vec{B}$ is again the external magnetic field. The proximity induced superconducting gap is decomposed as $|\Delta| e^{i\phi_s}$ with the phase factor inherited directly from the underlying s-wave superconductor. The set of Pauli-matrices $\vec{\sigma} = \{\sigma_x, \sigma_y, \sigma_z\}$ act in spin space.

It has been shown (Lutchyn *et al.*, 2010; Oreg *et al.*, 2010; Halperin *et al.*, 2012) that the Hamiltonian (3.22) can be mapped onto the spinless p-wave SC model (3.9). The topological regime of the model occurs when two conditions on the Zeeman field $\vec{h}$ are met (Osca *et al.*, 2014; Rex and Sudbø, 2014):

1. The full field must satisfy $|\vec{h}| > h_c \equiv \sqrt{|\Delta|^2 + \mu^2}$. In addition, if the Hamiltonian (3.22) is put on a lattice, which limits the spectrum, there is an additional upper critical field $\tilde{h}_c \equiv \sqrt{|\Delta|^2 + (\mu - 4t)^2}$, where $t \equiv \frac{\hbar^2}{2m^* a}$ is the hopping parameter and a is the lattice constant. In that case, full field must also satisfy $|\vec{h}| < \tilde{h}_c$ (see below for a derivation of this statement).

2. The projection $\vec{h}_\alpha$ of the Zeeman field onto the direction of the spin-orbit vector must obey $|\vec{h}_\alpha| < |\Delta|$ meaning that there is an upper bound on the component of the Zeeman field pointing in the spin-orbit direction.

The mapping onto the effective p-wave superconductor can be performed as follows. For simplicity, the magnetic field is chosen to be perpendicular to

the wire $\vec{h} = h\hat{z}$ and hence $\vec{h}_\alpha = 0$. In this case, one may construct the following eigen-spinors of the normal state Hamiltonian (3.22b) as

$$|u_+(p_w)\rangle = \begin{pmatrix} e^{-i\varphi}\cos\frac{\theta_p}{2} \\ -i\sin\frac{\theta_p}{2} \end{pmatrix}, \; |u_-(p_w)\rangle = \begin{pmatrix} -e^{-i\varphi}\sin\frac{\theta_p}{2} \\ -i\cos\frac{\theta_p}{2} \end{pmatrix}, \tag{3.23}$$

where $\tan\theta_p = |\alpha p_w/h|$. From the underlying PHS, which in the chosen basis reads $\mathcal{P} = \tau_x\mathcal{K}$, the corresponding hole spinors read

$$|v_+(p_w)\rangle = \begin{pmatrix} -e^{i\varphi}\cos\frac{\theta_p}{2} \\ i\sin\frac{\theta_p}{2} \end{pmatrix}, \; |v_-(p_w)\rangle = \begin{pmatrix} e^{i\varphi}\sin\frac{\theta_p}{2} \\ i\cos\frac{\theta_p}{2} \end{pmatrix}. \tag{3.24}$$

The electron and hole eigen-energies are given by $\pm E_\pm(p_w) = \frac{p_w^2}{2m^*} - \mu \pm \sqrt{\alpha_R^2 p_w^2 + h^2}$. In the strong magnetic field regime, $h \gg \alpha_R$, the spins of a single band are almost parallel, and if μ lies in the gap, one can project the full Hamiltonian onto the lower bands $|u_-(p_w)\rangle$ and $|v_-(p_w)\rangle$. This projection results in the effective spin-less p-wave Hamiltonian (Alicea *et al.*, 2011; Halperin *et al.*, 2012)

$$\mathcal{H}_p = \begin{pmatrix} \frac{p_w^2}{2m_{\text{eff}}} - \mu_{\text{eff}} & -ip_w|\Delta_p|e^{i\phi_p} \\ +ip_w|\Delta_p|e^{-i\phi_p} & -\frac{p_w^2}{2m_{\text{eff}}} + \mu_{\text{eff}} \end{pmatrix}, \tag{3.25}$$

where the effective parameters are $\mu_{\text{eff}} = \mu + h$, $\frac{1}{m_{\text{eff}}} = \frac{1}{m^*}(1 - m^*\alpha_R^2/h)$, $|\Delta_p| = |\alpha_R\Delta/h|$. Most interestingly, in this basis, the effective p-wave phase parameter is given by

$$\phi_p = \phi_s + \varphi, \tag{3.26}$$

where ϕ_s is the bulk s-wave order parameter and $\varphi = \arccos(\hat{x}\cdot\hat{w})$, the angle of the wire with respect to the positive x-axis. For a single uniform wire, this extra geometrical phase contribution is not important since it can be removed by choosing appropriate phase factors for the spinors in (3.23) and (3.24). However, in systems where phase differences are important, and in particular for Josephson junctions, the extra phase shift has observable consequences. This property is important in PAPER II and PAPER III.

3.4.3 Topological phases and invariants

Since there exists a continuous map from the semiconducting wire model (3.22) and the Kitaev chain model (3.9), the appropriate symmetry classes for the model are $\mathcal{D}$ and $\mathcal{BDI}$ with $\mathbb{Z}_2$ and $\mathbb{Z}$ topological invariants respectively.

In this section, these invariants are explicitly constructed, with the Hamiltonian (3.22) as the starting point. However, to ensure the existence of a well-defined k-space topology, the wire is put on a lattice with N sites. The tight-binding Hamiltonian reads

$$\begin{aligned}\mathcal{H} = &\sum_{i=1}^{N} \psi_i^\dagger \Big[(-\mu - 2t)\tau^z\sigma^0 + h\tau^z\sigma^z + \Re(\Delta)\tau^y\sigma^y - \Im(\Delta\tau^x\sigma^y) \Big] \psi_i \\ &+ \sum_{i=1}^{N-1} \psi_i^\dagger \Big[-t\tau^z\sigma^0 - \frac{i\alpha_R}{2}\tau^z\sigma^y \Big] \psi_{i+1} + h.c., \end{aligned} \tag{3.27}$$

where $t = 1/2m^*$ is the hopping parameter with the lattice constant set to unity. The τ-matrices act in particle-hole space. In the expression (3.27), the wire and the magnetic field are again assumed to lie in the x- and z-directions respectively. By imposing periodic boundary conditions, one obtains the bulk Hamiltonian

$$\begin{aligned} h(k) = \Big[&(-2t\cos(k) + 2t - \mu)\tau^z\sigma^0 + h\tau^z\sigma^z \\ &- i\alpha_R\tau^z\sigma^y\sin(k) + \Re(\Delta)\tau^y\sigma^y - \Im(\Delta)\tau^x\sigma^y \Big]. \end{aligned} \tag{3.28}$$

The class $\mathcal{D}$ $\mathbb{Z}_2$ invariant can be straightforwardly derived by the method outlined in App. A. Up to an overall constant factor, the bulk Hamiltonian in the Majorana basis reads

$$\tilde{A}(k) = \begin{pmatrix} 0 & -\rho & \lambda & -\nu \\ \rho & 0 & \nu & \xi \\ -\lambda & -\nu & 0 & \rho \\ \nu & -\xi & -\rho & 0 \end{pmatrix}, \tag{3.29}$$

with elements $\rho = 2\Im\Delta$, $\lambda = 2h + 2(-\mu + 2t) - 2t\cos(k)$, $\nu = 2\Re\Delta + \alpha\sin(k)$ and $\xi = -2h + 2(-\mu + 2t) - 4t\cos(k)$. The invariant is then given by

$$\begin{aligned} \nu &= \mathrm{sgn}\{\mathrm{Pf}\left(\tilde{A}(0)\right)\}\mathrm{sgn}\{\mathrm{Pf}\left(\tilde{A}(\pi)\right)\} \\ &= \mathrm{sgn}(h^2 - |\Delta|^2 - \mu^2)\cdot\mathrm{sgn}(h^2 - |\Delta|^2 - (4t-\mu)^2), \end{aligned} \tag{3.30}$$

where $\nu = -1$ and $\nu = +1$ characterize the topological and trivial phases respectively. Equation (3.30) holds as longs as the spectrum is gapped, requiring a finite α_R. There are two critical magnetic fields

$$h_{c1} = \sqrt{|\Delta|^2 + \mu^2}, \quad \text{and} \quad h_{c2} = \sqrt{|\Delta|^2 + (4t-\mu)^2}, \tag{3.31}$$

where the gap closes. For $h_{c1} < h < h_{c2}$, the wire is in the topological regime. The class $\mathcal{D}$ phase diagram is depicted in Fig. 3.6a.

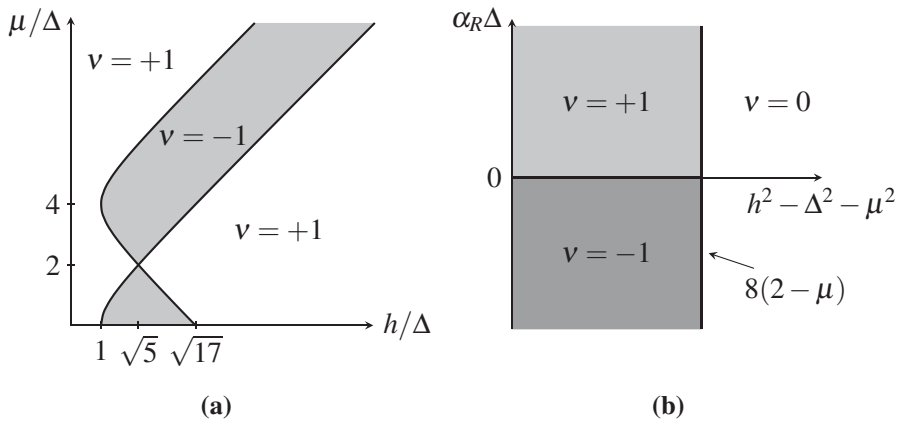

Figure 3.6: Phase diagrams for the model 3.27 in classes (**a**) $\mathcal{D}$ and (**b**) $\mathcal{BDI}$. The hopping parameter $t = 1$ defines the energy scale.

Imposing an additional TRS through the operator $\mathcal{T} = \tau^0\sigma^0\mathcal{K}$, $\mathcal{T}^2 = +1$, the system belongs to class $\mathcal{BDI}$ which has a $\mathbb{Z}$ valued winding invariant. This invariant is conveniently derived by the method of Tewari and Sau (2012). The starting point is the Hamiltonian (3.28) written as

$$h(k) = \hat{h}_0(k)\tau_z + i\hat{\Delta}\tau_y, \tag{3.32}$$

where a hat denotes a matrix in spin-space. With the unitary transformation $U = \exp(-i\frac{\pi}{4}\tau_y)$ the Hamiltonian has the off-diagonal chiral structure

$$h(k) \to Uh(k)U^\dagger = \begin{pmatrix} 0 & \hat{A}(k) \\ \hat{A}^T(-k) & 0 \end{pmatrix}, \tag{3.33}$$

with the matrix $A(k) = \hat{h}_0(k) + \hat{\Delta}$. It follows that

$$\det h(k) = \det\left(Uh(k)U^\dagger\right) = \det A(k) \det A^T(-k), \tag{3.34}$$

so that $\det A(k)$ vanishes if and only if $\det h(k)$ does, which in turn requires a zero eigenvalue, or equivalently a closing of the gap. Explicitly,

$$\det A(k) = (-2t\cos(k) - \mu - 2t)^2 - h^2 + \Delta^2 - \alpha_R^2\sin^2(k) - 2i\alpha_R\Delta\sin(k). \tag{3.35}$$

Consider now the phase of $\det A(k)$ through the variable

$$z(k) \equiv e^{i\theta(k)} \equiv \det A(k)/|\det A(k)|, \tag{3.36}$$

which is well-defined as long as the system remains gapped. One can then define a topological winding number ν, which measures the number of revolutions this phase winds around the origin in the complex plane as k runs through

the BZ. This number can be obtained from the integral

$$\nu = \frac{1}{\pi i}\int_{k=0}^{k=\pi} \frac{dz(k)}{z(k)}, \tag{3.37}$$

where $A(k) = A^*(-k)$ has been used to reduce the integral to half of the BZ. A non-zero winding is only possible if $\theta(k)$ crosses the real axis at points on opposite sides of the origin. Additionally, the sign of the product $\alpha_R\Delta$ will determine the direction of the winding. With these observations, the $\mathcal{BDI}$ invariant for the nanowire can be determined to

$$\begin{aligned}\nu = \operatorname{sgn}(\alpha_R\Delta)\cdot\Theta(8t(2t-\mu)-(h^2-\Delta^2-\mu^2))\\ \cdot\Theta(h^2-\Delta^2-\mu^2),\end{aligned} \tag{3.38}$$

which yields three different phases $\nu = \pm 1, 0$ (see Fig. 3.6b). In Eq. (3.38), Θ denotes the Heaviside step function. The trivial winding, $\nu = 0$ can be identified with the trivial phase in class $\mathcal{D}$. As usual, the system is required to be gapped at all points in the BZ for the invariant to be valid.

3.4.4 Discussion

Regarding the experimental realization of the nanowire setup, it is far from obvious how parameters should be tuned to drive the wire into the topological regime. There are several subtle issues regarding the interplay between competing mechanisms that complicate the picture considerably (Alicea, 2012; Stanescu, 2017).

For example, the proximity coupling in the wire must not be too large, since a large inflow of particles from the underlying superconductor can push the Fermi level above the induced Zeeman gap and spoil the spinless regime. Similarly, a large external field yields a larger freedom to place the chemical potential, but the same time, it suppresses the induced superconductivity.

Another crucial issue is to assure that the nanowire is at least close to being one-dimensional meaning that only one or a few subbands can be occupied. For disordered wires, the detection of how many transverse channels that are occupied is a complicated task and the influence of more than one channel may affect the topological properties. Generally, as long as there is an *odd* number of occupied bands and the wire width does not exceed the coherence length, the wire can support edge MZMs (see Alicea (2012) and references therein).

To summarize, the nanowire model (3.22) is simple in theory, but the experimental realization of such a wire is far from trivial. Consequently, these complications result in experiments that are hard to evaluate properly. Before discussing the experimental detection of MZMs in nanowires, it is useful to introduce some additional calculational tools.

3.5 Scattering theory of topological superconductors

Scattering theory is based on solving a quantum mechanical scattering problem (see Datta (1997) or Nazarov and Blanter (2009) for a general introduction). It consists of finding the linear relation between two sets of incoming and outgoing wave amplitudes, $n = 1, 2, \ldots, N$ (see Fig. 3.7) according to

$$\psi_n^{\text{out}}(\varepsilon) = \sum_{m=1}^{N} S_{nm}(\varepsilon)\psi_m^{\text{in}}(\varepsilon). \tag{3.39}$$

The scattering is assumed to be elastic, so the energy ε is conserved and incoming and outgoing states are at the same energy. To preserve probabilities, $\sum_n |\psi_n^{\text{out}}|^2 = \sum_n |\psi_n^{\text{in}}|^2$ and it follows that the matrix with coefficients S_{nm}, called the *scattering matrix* $S(\varepsilon)$, belongs to the unitary group $U(N)$:

$$S^{-1}(\varepsilon) = S^{\dagger}(\varepsilon). \tag{3.40}$$

The scattering matrix can be obtained from the Hamiltonian $\mathcal{H}$ through the Mahaux-Weidenmüller relation (Mahaux and Weidenmüller, 1969; Dittes, 2000; Fulga *et al.*, 2012)

$$S(\varepsilon) = \mathbb{1} + 2\pi i W^{\dagger}(\mathcal{H} - \varepsilon - i\pi W W^{\dagger})^{-1} W, \tag{3.41}$$

which is essentially a projection of the Green's function $(\varepsilon - \mathcal{H})^{-1}$ onto the scattering states (see Dittes (2000) for details). The $M \times N$ matrix W, where M is the size of the matrix representing $\mathcal{H}$, is called the coupling matrix. This matrix contains the coupling elements between the basis states of $\mathcal{H}$ and the scattering states. The elements of the matrix $-i\pi W W^{\dagger}$ can be viewed as the lead self-energies, which modify the bare energies and life-times for the particles in the system when scattering channels are attached. W is assumed to

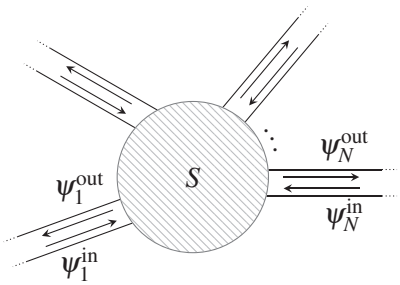

Figure 3.7: The scattering matrix, S, of a physical system, relates two sets of incoming and outgoing wave amplitudes $\psi_n^{\text{in/out}}$, where $n = 1, 2, \ldots, N$ labels the scattering channels.

commute with both the particle-hole and the time-reversal symmetry operators.

Generally, the symmetry relations obeyed by $\mathcal{H}$ are carried over to the scattering matrix. For the choices of $\mathcal{P} = \tau_x\mathcal{K}$ and $\mathcal{T} = \mathcal{K}$, $S(\varepsilon)$ has to obey the relations (Fulga *et al.*, 2012; Beenakker, 2015)

$$S(\varepsilon) = \mathcal{P}S(-\varepsilon)\mathcal{P}^{-1} = \tau_x S^*(-\varepsilon)\tau_x, \qquad \text{in classes } \mathcal{D} \text{ and } \mathcal{BDI} \tag{3.42a}$$

$$S(\varepsilon) = \mathcal{T}S(\varepsilon)\mathcal{T}^{-1} = S^T(\varepsilon), \qquad \text{in class } \mathcal{BDI} \text{ only.} \tag{3.42b}$$

In superconducting systems, the scattering matrix must account for Andreev scattering (see Fig. 3.8), which is a process where electron-like quasiparticles (electrons for short) at $+\varepsilon$ are converted into hole-like quasiparticles (holes for short) at $-\varepsilon$ (Andreev, 1964; Blonder *et al.*, 1982; Nazarov and Blanter, 2009). In the scattering formalism, electrical charge is not conserved in Andreev scattering but the missing charge of $2e$ is instead assumed to be accounted for by the creation or absorption of Cooper pairs in the superconducting condensate[1]. With Andreev scattering taken into account, the dimension of the scattering matrix is necessarily even because of PHS.

From Eq. (3.41), it is clear that it should be possible to relate the topological properties of $\mathcal{H}$ to those of $S(\varepsilon)$. Such a relation would be extremely useful, since abstract topological invariants can be converted into experimentally accessible quantities. Moreover, it makes it possible to calculate topological invariants without access to the full spectrum of the Hamiltonian. Instead, only properties of the system at the Fermi energy, $\varepsilon = \varepsilon_F = 0$, are needed. Indeed, it was shown in Fulga *et al.* (2012) that the topological invariants of $\mathcal{H}$ can generally be expressed in terms of $S(0)$, leading to an alternative topological classification in terms of scattering matrices.

Limiting the discussion again to one-dimensional superconductors in classes $\mathcal{D}$ and $\mathcal{BDI}$, the invariants can be expressed as

$$\nu = \det S(0) = \pm 1, \qquad \text{in class } \mathcal{D} \tag{3.43a}$$

$$\nu = \frac{1}{2}\mathrm{Tr}\left(\tau_x S(0)\right) = 0, \pm 1, \pm 2 \ldots \qquad \text{in class } \mathcal{BDI}. \tag{3.43b}$$

To motivate these expressions, it is useful consider a simple setup where a superconducting wire is connected in one end to a normal metal lead (see Fig. 3.8). The wire is considered long enough so the transmission through it can be neglected and the scattering consists only of reflection. For this reason, the scattering matrix is denoted with r rather than S in the following discussion. The normal metal lead is terminated at the non-connecting end with a

[1] The total charge in any closed system is necessarily conserved: in the BdG formalism this requires a self-consistent calculation of the order parameter.

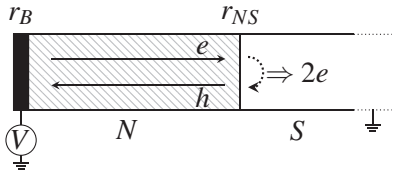

Figure 3.8: A superconducting wire (S) attached to a normal metal lead (N). Andreev scattering is the process in which an electron-like quasiparticle (e) is converted into a hole-like quasiparticle (h) or vice versa. The lead has a voltage difference V with respect to the grounded superconductor resulting in a current flow I. The conductance $G = dI/dV$ can be determined from the reflection matrix r_{NS} whose properties act as signature of topological superconductivity and MZMs at the NS interface.

barrier characterized by the $2N \times 2N$ unitary reflection matrix

$$r_{\mathrm{B}} = \begin{pmatrix} \tilde{r}_{ee} & 0 \\ 0 & \tilde{r}_{ee}^{*} \end{pmatrix}, \tag{3.44}$$

written in block-form in the particle-hole basis. Since only the Fermi energy properties are of importance here, the condition $\varepsilon = 0$ is implicitly assumed throughout the remainder of this section. Moreover, scattering against the barrier does not mix electrons or holes, resulting in the block diagonal structure. In the expression (3.44), $\tilde{r}_{hh} = \tilde{r}_{ee}^{*}$ by PHS.

Scattering from the lead onto the normal-superconducting (NS) interface is characterized by the unitary reflection matrix

$$r_{\mathrm{NS}} = \begin{pmatrix} r_{ee} & r_{eh} \\ r_{eh}^{*} & r_{ee}^{*} \end{pmatrix}, \tag{3.45}$$

where the complex coefficients r_{eh} and $r_{he} = r_{eh}^{*}$ describe Andreev reflection. The condition for a zero energy bound state at the NS interface, a MZM, is given by the resonance condition (Beenakker, 1991; Fulga *et al.*, 2011)

$$\det(1 - r_{\mathrm{B}} r_{\mathrm{NS}}) = 0. \tag{3.46}$$

Thus, the number of bound states equals the number of independent solutions to this equation, which in turn is given by the number of $+1$ eigenvalues of the matrix $r_{\mathrm{B}} r_{\mathrm{NS}}$. To determine the existence of such eigenvalues, it is convenient to perform a unitary transformation

$$r = U r_{\mathrm{NS}} U^{\dagger}, \quad U = \frac{1}{\sqrt{2}} \begin{pmatrix} 1 & 1 \\ -i & i \end{pmatrix}, \tag{3.47}$$

Symmetry class	$\mathcal{D}$	$\mathcal{BDI}$
Topological classification	$\mathbb{Z}_2$	$\mathbb{Z}$
Topological invariant ν	$\det S(0) = \pm 1$	$\frac{1}{2}\mathrm{Tr}\,(\tau_x S(0)) = 0, \pm 1, \ldots$
Number of edge MZMs	$\frac{1}{2}(1-\nu)$	$\lvert\nu\rvert$

Table 3.1: Scattering matrix classification of 1D superconducting wires in classes $\mathcal{D}$ and $\mathcal{BDI}$. $S(0)$ refers to the scattering matrix at the Fermi energy $\varepsilon_F = 0$. The basis of scattering states is chosen such that $\mathcal{P} = \tau_x\mathcal{K}$ and $\mathcal{T} = \mathcal{K}$.

so that the new reflection matrix satisfies $r = r^*$ and the matrix $O_N \equiv U r_\mathrm{B} U^\dagger$ is orthogonal. The number of bound states is then given by the number of $+1$ eigenvalues, denoted by N_0, of the orthogonal matrix $O_N r$. Due to the orthogonality condition, the other $2N - N_0$ eigenvalues must either equal -1 or come in complex conjugate pairs $e^{\pm i\phi}$. Hence, $\det(O_N r) = \det O_N \det r = \det r_\mathrm{NS} = (-1)^{N_0}$, since $\det O_N = \det r_\mathrm{B} = \det \tilde{r}_{ee} \det \tilde{r}^*_{ee} = +1$ due to unitarity. Thus, if $\det r_\mathrm{NS} = -1$, there must be a MZM at NS interface. In this sense, the determinant of the scattering matrix, which in this case only dealt with reflection, measures the even-oddness or the parity of the number of bound states at the interface. This is completely analogous to the class $\mathcal{D}$ $\mathbb{Z}_2$ invariant from Sec. 3.3. In this way $\det r_{NS}$ is a topological index as it does not change unless the gap closes, meaning that some eigenvalue passes through zero.

In the presence of TRS through an operator $\mathcal{T}^2 = +1$, the system belongs to class $\mathcal{BDI}$. By Eq. (3.42), the product $\tau_x r_\mathrm{NS}$ satisfies $(\tau_x r_\mathrm{NS})^2 = \mathbb{1}$ and consequently, its eigenvalues are restricted to ± 1. As long as there is a gap, none of the eigenvalues can change sign, and the sum of the eigenvalues is constant. The trace operation therefore distinguishes between sub-classes of scattering matrices and $\nu = \frac{1}{2}\mathrm{Tr}\,(\tau_x r_\mathrm{NS}) = 0, \pm 1, \pm 2, \ldots$ can be used as an invariant. The number of edge MZMs is, through the bulk-boundary correspondence, given by $|\nu|$ (see Akhmerov *et al.* (2011); Fulga *et al.* (2011); Beenakker (2015) for details).

The results of this discussion are summarized in Tab. 3.1. In the following sections, the scattering theory will be used as the main tool to derive experimental signatures of topological superconductivity and MZMs.

3.6 Experimental Signatures of Majorana Zero Modes

In order to probe MZMs in topological superconductors and to utilize their properties for quantum computations, there are three broad categories of experimental signatures that must be demonstrated (Stanescu, 2017): *i*) The existence and robustness of a zero energy state bound to a topological defect in a superconductor, *ii*) the non-local nature of this state, and *iii*) the demonstration of its non-Abelian statistics. This section will mainly focus on the first of these categories while the other two will only be commented upon briefly.

3.6.1 Tunnelling spectroscopy and zero bias peak quantization

One of the key difficulties in the detection of MZMs is due to their charge neutrality and lack of magnetic moment, and consequently they neither couple *directly* to external electrical nor magnetic fields. However, charged electrons tunnelling into a topological superconductor *do in fact couple* to MZMs because of Andreev reflection.

An incoming electron at the Fermi energy can reflect back as a hole, and because of the equal electron and hole properties of a MZM, the zero energy Andreev reflection is on perfect resonance and has unit probability (Law *et al.*, 2009).

A conceptually simple and direct method to probe the zero energy properties of an edge MZM in a topological superconductor is therefore a measurement of the (charge) tunnelling conductance $G = dI/dV$. By considering the tunnelling experiment setup, depicted in Fig. 3.9a, several authors (Law *et al.*, 2009; Flensberg, 2010; Liu *et al.*, 2012; Fidkowski *et al.*, 2012) have predicted a quantized zero bias peak in the tunnelling conductance (see Fig. 3.9b). Since Andreev reflection is a highly spin-dependent phenomena, spin tunnelling spectroscopy can also be utilized as a tool for the detection of MZMs (He *et al.*, 2014).

In this section, the basic theoretical ideas of charge tunnelling spectroscopy of MZMs will be analyzed from a few different perspectives.

Tunnelling Hamiltonian approach

A simple phenomenological model that captures the essential physics of a normal metal lead coupled to the left edge of a one-dimensional superconductor has the Hamiltonian

$$\mathcal{H}_c = t_c \sum_{\sigma=\uparrow/\downarrow} \left[c_\sigma^\dagger d_\sigma + d_\sigma^\dagger c_\sigma \right], \tag{3.48}$$

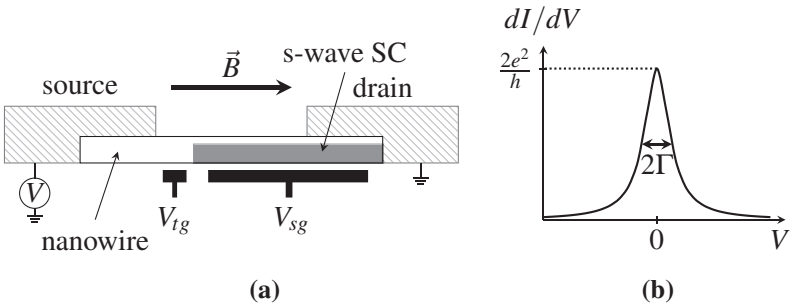

Figure 3.9: (a) Experimental schematics of a tunnelling experiment probing the topological superconductor model (3.22). A semiconducting nanowire is turned into a superconductor by close proximity to an *s*-wave superconductor. The topological regime is achieved by controlling the chemical potential through the supergate V_{sg} and an external magnetic field $\vec{B}$. Two metal leads, source and drain, are connected to the two edges of the superconductor and a current I is driven through the wire. A measurement of the resulting voltage V across the leads yields the conductance dI/dV. The source lead-wire coupling can be tuned by the tunnelling gate V_{tg}.
(b) Quantization of the the tunnelling conductance dI/dV at zero voltage bias $V = 0$. The width of the peak 2Γ, where Γ is related to the tunnelling strength, is non-universal but the peak hight of $2e^2/h$ is, protected by PHS.

where t_c characterizes the strength of the lead-superconductor coupling, $c^\dagger_\sigma$ (c_σ) creates (annihilates) an electron with spin projection σ in the lead and $d^\dagger_\sigma$ and d_σ are the corresponding edge operators of the superconductor. If the superconductor is topological, the wire hosts edge MZMs, and by projecting onto the zero energy subspace, one can write

$$d_\sigma = a^*_\sigma \gamma_L + i b^*_\sigma \gamma_R, \tag{3.49}$$

where $\gamma_{L/R}$ are the MZMs associated with the left and right edges of the wire respectively (see Sec. 3.3) and a_σ and b_σ are the electron and hole amplitudes of the MZMs. In terms of these modes, the tunnelling Hamiltonian becomes

$$\mathcal{H}_c = t_c \sum_{\sigma=\uparrow/\downarrow} \left[\gamma_L (a_\sigma c_\sigma - a^*_\sigma c^\dagger_\sigma) - i\gamma_R (b_\sigma c_\sigma - b^*_\sigma c^\dagger_\sigma)\right]. \tag{3.50}$$

Crucially, if the wire is long enough and the right MZM is localized far away from the lead, one can set $b_\sigma = 0$ and the Hamiltonian instead reads

$$\mathcal{H}_c = t_c \sum_{\sigma=\uparrow/\downarrow} \gamma_L (a_\sigma c_\sigma - a^*_\sigma c^\dagger_\sigma) = g\gamma_L [\psi_1 - \psi^*_1], \tag{3.51}$$

in terms of a new set of electrons $\psi_1 = (a_\uparrow c_\uparrow + a_\downarrow c_\downarrow)/(|a_\uparrow|^2 + |a_\downarrow|^2)$, $\psi_2 = (-a^*_\downarrow c_\uparrow + a^*_\uparrow c_\downarrow)/(|a_\uparrow|^2 + |a_\downarrow|^2)$, and a new coupling $g = t_c(|a_\uparrow|^2 + |a_\downarrow|^2)$. In

this expression, it is clear that the left edge MZM only couples to ψ_1 while ψ_2 is completely disconnected from the wire in the zero energy limit. One can view the two new electrons as having opposite spin-polarization along a direction set by the internal structure of the topological superconductor. In this aspect, the coupling to the topological superconductor is highly spin-selective. MZMs therefore manifest the phenomenon of *selective equal-spin Andreev reflection* (SESAR) (He *et al.*, 2014): an incoming zero energy ψ_1 electron is with unit probability reflected back as a hole with the *same* spin and a Cooper pair with charge $2e$ is transferred into the superconductor. In contrast, a ψ_2 electron will with unit probability be normal reflected and does not contribute to the transport. It is useful to keep in mind that since only one spin species of lead electrons interact with the topological superconductor, the corresponding scattering problem is effectively spinless.

Consider now the setup depicted in Fig. 3.9a. In the trivial regime, ordinary Andreev reflections dominate the subgap charge transport and the zero bias conductance is non-universal: $0 \leq G(0) \leq 4e^2/h$ (Blonder *et al.*, 1982; Takane and Ebisawa, 1992) (see also the derivation below). Tuning the superconductor into the topological regime, for instance by increasing the magnetic field B (see Eq. (3.31)), introduces edge MZMs and SESAR which quantizes the zero bias conductance to $2e^2/h$ (see Fig. 3.9b). The robustness of such a peak is a strong signature of MZMs and topological superconductivity.

Scattering approach

These arguments can be supported by a scattering calculation. Within the formalism presented in Sec. 3.5, one can show directly how PHS of the scattering matrix directly leads to a zero-bias conductance quantization when a spinless normal metal lead is connected to a topological superconductor with edge MZMs (Béri *et al.*, 2009; Law *et al.*, 2009; Fulga *et al.*, 2011; Bagrets and Altland, 2012).

For a single lead connected to a large topological superconductor (such that charging effects are negligible), and for energies much smaller than the gap, $\varepsilon \ll |\Delta|$, the scattering matrix is a reflection matrix, $r(\varepsilon)$, relating outgoing and incoming states through

$$\Psi_{\text{out}}(\varepsilon) = r(\varepsilon)\Psi_{\text{in}}(\varepsilon), \tag{3.52}$$

where $\Psi_{\text{in/out}}(\varepsilon)$ are vectors containing the amplitudes of scattering states at energy ε with incoming and outgoing momenta respectively.

In the particle-hole basis, the reflection matrix is most conveniently divided into sub-blocks

$$r(\varepsilon) = \begin{pmatrix} r_{ee}(\varepsilon) & r_{eh}(\varepsilon) \\ r_{he}(\varepsilon) & r_{hh}(\varepsilon), \end{pmatrix} \tag{3.53}$$

where r_{ee} is the reflection amplitude for an incoming electron, r_{hh} is the reflection amplitude for an incoming hole and r_{eh} and r_{he} are Andreev reflection amplitudes which converts incoming electrons to outgoing holes and vice versa.

The tunnelling conductance for zero temperature and small bias voltages V is dominated by Andreev processes and is given by (Blonder *et al.*, 1982; Takane and Ebisawa, 1992)

$$G(V) = \frac{2e^2}{h} \mathrm{Tr}\, r_{eh}(V) r_{eh}^{\dagger}(V), \tag{3.54}$$

where it is assumed that there is no single particle transmission into the superconductor. The trace is taken over the channels in the lead.

Considering now a single spin-less channel lead attached to a topological superconductor (remember that only one spin species is active in the setup), so that the reflection matrix blocks are scalars.

Secondly, the reflection matrix is unitary due to probability flux conservation and PHS enforces the zero energy constraint $\tau_x r(0) \tau_x = r^*(0)$. These two restrictions allow only two possibilities for the reflection matrix entries: either $|r_{ee}(0)| = 1$, $|r_{eh}(0)| = 0$ or $|r_{ee}(0)| = 0$, $|r_{eh}(0)| = 1$ (Akhmerov *et al.*, 2015). The latter possibility corresponds to $\det r(0) = -1$ and the topological phase. It then follows directly from Eq. (3.54) that the zero bias conductance is quantized to $2e^2/h$ in the topological phase. It has further been shown that this result is stable against certain types of interactions (Fidkowski *et al.*, 2012).

MZMs as Andreev bound states

To gain further insight into the physical mechanisms behind the quantized zero bias peak, it is also useful to analyze Andreev reflection onto a one-dimensional superconductor, where the topological properties are captured by the p-wave nature of the order parameter.

Because of this pairing symmetry, the zero energy Andreev reflection processes $e \to h$ and $h \to e$ are phase shifted by π, in addition to the usual phase shift from the order parameter (Nazarov and Blanter, 2009). This additional phase shift occurs because incoming electrons and outgoing holes (the $e \to h$ process) with Fermi momentum p_F experience an effective gap $\Delta_p \sim +|\Delta_p| p_F$, while incoming holes and outgoing electrons (the $h \to e$ process) have momentum $-p_F$ and experience a gap with the opposite sign $\Delta_p \sim -|\Delta_p| p_F$ (Pientka *et al.*, 2014b). In this way, for $\varepsilon = 0$, a p-wave superconductor, and also d-wave superconductors (Tanaka and Kashiwaya, 1995), is analogous to an optical phase-conjugating mirror (Beenakker, 2012), in which incoming and outgoing particles interfere constructively.

Through this mechanism, a normal lead connected to a topological superconductor becomes completely transparent for states at $\varepsilon = 0$, since any net phase accumulated by an electron-hole-electron or a hole-electron-hole orbit close to the interface becomes zero and multiple paths interfere constructively. In this way, an edge MZM will "leak out" from a topological superconductor into the connected lead and form a resonant Andreev bound state (Nazarov and Blanter, 2009).

This argument can be supported by a simple calculation adapted from Beenakker (2012). Consider first a single scattering channel from a normal lead onto an ordinary one-dimensional *s*-wave superconductor (see Fig.3.8). For low energies $\varepsilon \ll |\Delta|$, the transport is dominated by Andreev reflection and the zero bias conductance is given by (compare with Eq.(3.54))

$$G = \frac{2e^2}{h} R_{\mathrm{A}} \equiv \frac{2e^2}{h} r_{eh}^* r_{eh}, \tag{3.55}$$

where r_{eh} is the amplitude of the process in which an injected lead electron comes back as a hole. The corresponding probability is R_A. The scattering channel is characterized by the electron transmission and reflection amplitudes t and r respectively which satisfy $|t|^2 + |r|^2 = 1$. Due to PHS, the corresponding hole amplitudes are t^* and r^*.

For zero energy scattering, the acquired phase shifts of Andreev reflected electrons and holes are given by (Andreev, 1964; Nazarov and Blanter, 2009; Beenakker, 2012)

$$e^{i\chi_e} = e^{i\chi_h} = e^{-i \arccos \varepsilon/|\Delta|} = \frac{1}{i}, \tag{3.56}$$

and for an electron reaching the superconductor, the probability of Andreev reflection is unity. The full amplitude of an injected electron to reflect back as a hole is given by the sum of scattering events of all orders:

$$\begin{aligned} r_{eh} &= t^* \frac{1}{i} t + t^* \frac{1}{i} r \frac{1}{i} r^* \frac{1}{i} t + t^* \frac{1}{i} \left(r \frac{1}{i} r^* \frac{1}{i} \right)^2 t + \ldots \\ &= t^* \frac{1}{i} \left(1 - r \frac{1}{i} r^* \frac{1}{i} \right)^{-1} t. \end{aligned} \tag{3.57}$$

Here, the first term describes the second order process in which an incoming electron travels through the lead, Andreev reflects, and the resulting hole travels back into the lead. The second term describes the fourth order process where three Andreev reflections occur before a hole is reflected back into the lead, and so on. The total probability becomes

$$R_{\mathrm{A}} = r_{eh}^* r_{eh} = \frac{|t^2||t^2|}{1 + |r|^2} = \frac{T^2}{2 - T^2}, \tag{3.58}$$

where $T = |t^2|$ and $R = |r|^2$ are the transmission and reflection probabilities of the scattering channel, and the relation $T^2 + R^2 = 1$ has been used. By Eq. (3.55), the conductance is obtained as

$$G = \frac{2e^2}{h}\frac{T^2}{2-T^2} \approx \begin{cases} \frac{2e^2}{h} & \text{for} \quad T \approx 1 \\ \frac{2e^2}{h}\frac{T^2}{2} & \text{for} \quad T \ll 1. \end{cases} \tag{3.59}$$

To account for the spin-flip process in s-wave Andreev reflection, this expression must be multiplied by 2. It is clear from Eq. (3.59) that for s-wave Andreev scattering, the conductance is highly dependent on the transmission of the scattering channel and is non-universal: $0 \leq G \leq 4e^2/h$.

The above calculation can be contrasted with that of a topological p-wave superconductor. As discussed above, the zero energy Andreev reflection phase factors differ by a sign for electrons and holes:

$$e^{i\chi_e} = e^{i\chi_h + i\pi} = -e^{i\chi_h} = \frac{1}{i}. \tag{3.60}$$

Again, the Andreev reflection amplitudes are obtained by summing processes of all orders, but the seemingly innocent phase shift alters the amplitude drastically:

$$\begin{aligned} R_{\mathrm{A}} = r_{eh} &= t^*\frac{1}{i}t + t^*\frac{1}{i}rir^*\frac{1}{i}t + t^*\frac{1}{i}\left(rir^*\frac{1}{i}\right)^2 t + \ldots \\ &= t^*\frac{1}{i}\left(1 - rir^*\frac{1}{i}\right)^{-1} t, \end{aligned} \tag{3.61}$$

and the probability becomes unity

$$r_{eh}^* r_{eh} = \frac{|t^2||t^2|}{1-|r|^2} = \frac{T^2}{T^2} = 1. \tag{3.62}$$

For the p-wave superconductor, the zero energy conductance therefore reads

$$G = \frac{2e^2}{h}, \tag{3.63}$$

independently of T. The conductance channel is therefore completely transparent due to interference of normal and Andreev scattering. Any accumulated phase shifts are completely cancelled and the zero energy bound state, the MZM, is robust and universal.

Experimental status

While conceptually simple, to resolve the quantized zero bias peak has turned out to be a challenging experimental task. Initial tunnelling experiments with the setup in Fig. 3.9a reported a zero bias peak in the conductance (Mourik *et al.*, 2012; Deng *et al.*, 2012; Das *et al.*, 2012), but the robust quantization feature of the peak was missing and several alternative explanations for such peaks were readily proposed (Bagrets and Altland, 2012; Liu *et al.*, 2012). In particular, temperature effects can have a negative influence on the zero bias peak quantization (Pientka *et al.*, 2012, 2014b). If the temperature, T, reaches the characteristic broadening Γ, the width of the peak becomes temperature dependent and consequently the peak hight is reduced by a factor or order Γ/T. Finite temperature can also induce inelastic quasiparticle scattering processes which decreases the life time of the zero energy resonance and reduces the peak hight.

A recent experiemental paper, describing a significantly improved experimental setup, has reported robust zero bias peak quantization (Zhang *et al.*, 2017). This observation is an important mile-stone in MZM physics and paves the way for future non-Abelian braiding experiments.

3.6.2 The 4π-Josephson effect

An alternative route towards the detection of MZMs is the 4π-Josephson effect. Already Kitaev (2001) pointed out that the Majorana operators in Eq. (3.10) are 4π-periodic in the superconducting order parameter which results in an unusual version of the Josephson effect. By connecting two topological superconducting wires in a Josephson junction setup (see Fig. 3.10a), a measurement of the Josephson current would contain a topological contribution which is 4π-periodic in the phase difference of the order parameter (Kwon *et al.*, 2004; Fu and Kane, 2009) and provides a signature of topological superconducitivity and MZMs.

Effective Hamiltonian approach

The 4π-periodicity of the current can readily be derived by the approach in Alicea (2012). The starting point is to consider two copies, labelled L and R, of the Kitaev chain (3.9). These two chains are coupled with strength Γ in a Josephson junction setup by the Hamiltonian

$$\mathcal{H}_\Gamma = -\Gamma(c_L^\dagger c_R + c_R^\dagger c_L), \tag{3.64}$$

which describes single electron hopping from the right edge of chain L to the left edge of chain R. The topological regime is characterized by edge MZMs

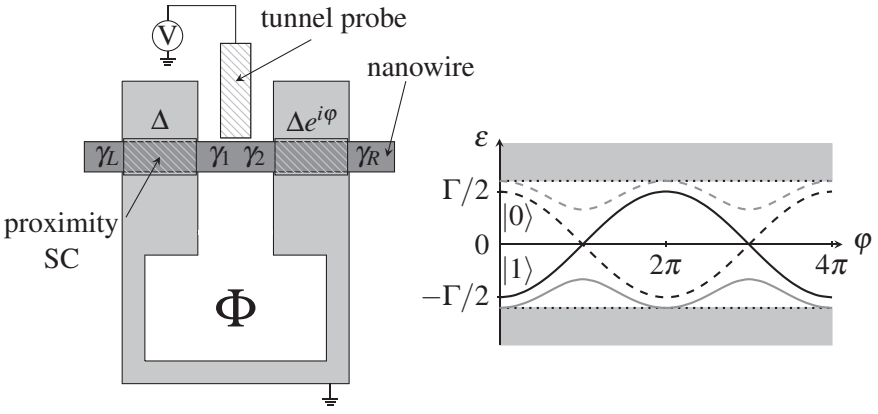

Figure 3.10: **(a)** Experimental schematics of a Josephson junction formed by two segments of proximitized nanowire. A tunnel probe at bias voltage V measures the subgap spectrum in the junction as a function of the phase difference $\varphi = 2\pi\Phi/\Phi_0$ across the junction, where Φ is the magnetic flux and $\Phi_0 = h/2e$ is the superconducting flux quantum. The topological phase is characterized by the presence of MZMs, γ_L,γ_1,γ_2,γ_R, which alter the subgap spectrum and contributes with a 4π-periodic component in the Josephson current. **(b)** Subgap spectrum of the Josephson junction as a function of the phase difference φ. In the topological regime, the two bound states $|0\rangle$, $|1\rangle$ (black lines) and subsequently the ground state, are 4π-periodic due to fermion parity conservation. The trivial regime bound states (gray lines) are 2π-periodic. Note that the full spectrum is 2π-periodic for all phase differences φ.

and those residing in the junction region, γ_1 and γ_2, hybridize and form an ordinary fermion with an energy that depends on the phase-difference of the junction. To see this, the edge electron operators c_L and c_R are first expressed in terms of Majorana operators according to Eq. (3.10) and choosing a phase convention, for instance $\Delta_L = |\Delta|$, $\Delta_R = |\Delta|e^{i\varphi}$. By discarding the negligible overlap with the outer MZMs, one can project (3.64) onto the zero energy subspace, which yields an effective subgap Hamiltonian

$$\mathcal{H}_{\text{eff}} = -\frac{\Gamma}{2}\cos(\frac{\varphi}{2})i\gamma_1\gamma_2 = -\Gamma\cos(\frac{\varphi}{2})(n_0 - 1/2). \tag{3.65}$$

Here, φ is again the phase difference across the junction and n_0 is the number operator, with eigenstates $|0\rangle$,$|1\rangle$, of the fermion state in the junction region (see Fig. 3.10b).

Importantly, since $\mathcal{H}_{\text{eff}}$ commutes with n_0, this occupation number is conserved. If the system is initialized in a state with $n_0 = \tilde{n}_0$ the corresponding

Josephson current reads

$$I = \frac{2e}{\hbar}\frac{d\langle \mathcal{H}_{\text{eff}}\rangle}{d\varphi} = \frac{e\Gamma}{2\hbar}\sin(\frac{\varphi}{2})(2\tilde{n}_0 - 1). \tag{3.66}$$

This expression for the tunnelling current reveals a fractional and 4π Josephson effect. Fractional, in the sense that it expresses single electron tunnelling, "half" of a Cooper pair, across the junction, and also a 4π-periodicity in φ. These features are in stark contrast to the conventional Josephson effect, where only Cooper pair tunnelling can mediate a current in the subgap regime and a 2π-periodicity in φ.

The topological formation of the single electron state n_0 in the junction opens up for the possibility of single electron tunnelling, but the origin of the 4π-periodicity is more complicated. Its origin can be traced to the observation that the Kitaev Hamiltonian (3.9) is 2π-periodic in the superconducting phase, as for any superconductor, but the many body ground state of the Josephson junction system is not.

Suppose that $\varphi = 0$ and $\tilde{n}_0 = 1$, such that the Hamiltonian (3.65) is in the ground state with energy $-\Gamma/2$ (see Fig. 3.10b). Crucially, since both the fermion occupancy of n_0 and the global fermion parity are conserved, tuning φ to 2π yields an excited state with energy $+\Gamma/2$. Because of the outer edge MZMs, γ_L and γ_R, there is always a degeneracy between odd and even parity ground states, but since fermion occupancy at the junction region is conserved, the ground state parity can not switch. The system can decay back into the ground state only if the fermionic state corresponding to the unpaired outer MZM can tunnel into the junction region but this mechanism is strongly suppressed if the wires are long compared to the coherence length. Tuning φ further from 2π to 4π results in the system returning to the ground state again which results in a 4π-periodicity. This periodicity is inherited by the current, according to Eq. (3.66).

An important feature of the subgap spectrum is the double degeneracy through the formation of two uncoupled MZMs at the crossing $\varphi = \pi$. If this crossing would turn into an anti-crossing, the spectrum would revert into the ordinary 2π-periodicity and the system would be trivial. As discussed above, the crossing is however protected by fermion parity conservation and is a strong signature of topological superconductivity. This feature is discussed in PAPER I.

SNS scattering approach

The 4π-periodicity of the subgap spectrum and the current can also be derived within the scattering formalism, (see Fig. 3.11), where two p-wave superconductors (S) are connected by a piece of a normal metal (N). A useful basis for

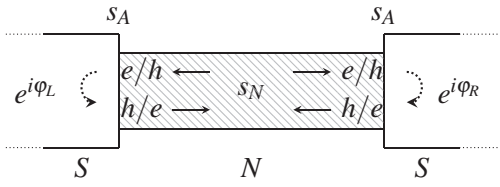

Figure 3.11: Scattering approach to the 4π-Josephson effect. The normal region (N) is modelled by a scattering matrix s_N which describes transmission in which electron and holes do not mix. Andreev reflection onto the outer superconductors is described by s_A. The Andreev reflected particles acquire phases that depend both on the superconducting phase difference, $\varphi_L - \varphi_R \equiv \varphi$ and the p-wave nature of the pairing.

scattering states is $\Psi_{\text{in/out}} = (\Psi^e, \Psi^h)^T_{\text{in/out}} = (\psi^e_L, \psi^e_R, \psi^h_L, \psi^h_R)^T_{\text{in/out}}$, from which it follows that scattering in the normal (N) region is described by

$$\Psi_{\text{out}}(\varepsilon) = s_N(\varepsilon)\Psi_{\text{in}}(\varepsilon). \tag{3.67}$$

This scattering matrix does not mix electrons and holes and it is therefore block-diagonal in particle-hole space:

$$s_N(\varepsilon) = \begin{pmatrix} s(\varepsilon) & 0 \\ 0 & s^*(-\varepsilon) \end{pmatrix}, \tag{3.68}$$

where the electron-electron scattering is described by the transmission, t, t', and reflection r, r' amplitudes according to

$$s = \begin{pmatrix} r & t' \\ t & r' \end{pmatrix}. \tag{3.69}$$

The scattering matrix relating hole states is given by $s^*(-\varepsilon)$ due to PHS. If the outer superconductors are in the topological p-wave phase, Andreev scattering processes at the normal-superconductor interfaces are described by

$$\Psi_{\text{in}} = s_A(\varepsilon)\Psi_{\text{out}}, \tag{3.70}$$

with

$$s_A(\varepsilon) = \begin{pmatrix} 0 & s_{eh} \\ s_{he} & 0 \end{pmatrix}, \quad s_{eh} = \begin{pmatrix} e^{i\tilde{\chi}_L} & 0 \\ 0 & e^{i\tilde{\chi}_R} \end{pmatrix}, \quad s_{he} = \begin{pmatrix} e^{i\chi_L} & 0 \\ 0 & e^{i\chi_R} \end{pmatrix}. \tag{3.71}$$

The accumulated phases in the Andreev reflections are

$$\tilde{\chi}_L = +\varphi_L - \arccos(\varepsilon/|\Delta_p|) \tag{3.72a}$$
$$\tilde{\chi}_R = +\varphi_R - \arccos(\varepsilon/|\Delta_p|) + \pi \tag{3.72b}$$
$$\chi_L = -\varphi_L - \arccos(\varepsilon/|\Delta_p|) + \pi \tag{3.72c}$$
$$\chi_R = -\varphi_R - \arccos(\varepsilon/|\Delta_p|). \tag{3.72d}$$

In these expressions, the extra terms of π come from the p-wave nature of the pairing. The $\arccos(\varepsilon/|\Delta_p|)$ term is the usual phase matching factor in the subgap regime $\varepsilon \ll |\Delta_p|$ (Andreev, 1964; Beenakker, 1991; Haim *et al.*, 2015). The matrix $s_A(\varepsilon)$ is unitary if the superconductors are assumed large enough, such that single particle transmission through them is completely suppressed.

Electrons and holes scattering in the normal region of the junction can form Andreev bound states (ABS) due to constructive interference of periodic scattering paths. With Eq. (3.67) and Eq. (3.70), the consistency condition for such ABS reads (Beenakker, 1991)

$$s_A(\varepsilon)s_N(\varepsilon)\Psi_{\text{in}} = \Psi_{\text{in}}. \tag{3.73}$$

which has non-trivial solutions if and only if

$$\det[1 - s^*(-\varepsilon)s_{he}(\varepsilon)s(\varepsilon)s_{he}(\varepsilon)] = 0. \tag{3.74}$$

To continue with analytical calculations, it is assumed that the energy dependence of the scattering matrix can be neglected, which holds in the short junction limit $L \ll \xi$, where L is the length of the normal region and ξ is the superconducting coherence length. The only remaining energy dependence comes from $\arccos(\varepsilon/|\Delta_p|)$ in the phase factors. A straightforward calculation results in the two energy solutions to Eq. (3.74)

$$\varepsilon_\pm = \pm|\Delta_p|\sqrt{T}\cos(\frac{\varphi}{2}), \tag{3.75}$$

where $T = |t|^2$ is the transmission probability through the normal region and $\varphi = \varphi_L - \varphi_R$ is the phase difference across the junction. It follows that regardless of the transmission (as long as it is finite), there must be two zero energy ABS if $\varphi = \pi$. The corresponding Josephson current is 4π-periodic and is given by (Kwon *et al.*, 2004)

$$I = \frac{2e}{\hbar}\sum_\pm \frac{\partial\varepsilon_\pm}{\partial\varphi}\tanh[\frac{\beta\varepsilon_\pm}{2}] = \frac{2e|\Delta_p|\sqrt{T}}{\hbar}\sin(\frac{\varphi}{2}), \tag{3.76}$$

as the inverse temperature $\beta \to \infty$. If the factors of π in Eq. (3.72b) and Eq. (3.72c) are neglected, the setup describes instead a Josephson junction with s-wave superconductors. A similar calculation then yields the ordinary spin-degenerate bound state and Josephson current equations (Haberkorn *et al.*, 1978):

$$\varepsilon_\pm = \pm|\Delta_s|[1 - T\sin^2(\varphi/2)]^{1/2}, \quad I = \frac{e|\Delta_s|}{2\hbar}\frac{T\sin(\varphi)}{[1 - T\sin^2(\varphi/2)]^{1/2}}. \tag{3.77}$$

Experimental status

The experimental observation of the 4π-Josephson effect would be a strong signature of topological superconductivity and MZMs. Similar to the tunnelling experiments outlined in Sec. 3.6.1, there are many subtle complications in the detection of a 4π periodic Josephson current.

First of all, the anomalous current must be disentangled from a potentially larger ordinary 2π-periodic contribution, which sets a lower bound on the required current resolution (see Alicea (2012) for details).

Secondly, the small but finite overlap to the outer edge MZMs provides a tunnelling mechanism in which the fermionic occupation of the junction is ruined. To avoid this problem, variation of the phase difference must be fast compared to a time scale set by the energy overlap. On the other hand, the variation can not be so fast that it is comparable to the inverse bulk gap, since that could induce quasiparticle excitations between the subgap states which also spoils the 4π periodicity and yields an ordinary 2π periodic current. Quasiparticle excitations from thermal fluctuations could also provide a third mechanism that restores the 2π-periodicity.

A related predicted signature of MZMs in a Josephson junction setup is the doubling of Shapiro steps. A conventional Josephson junction subjected to both an AC voltage, with frequency ω, and a DC voltage V, develops steps in the current-voltage characteristics, so-called *Shapiro steps*, whenever $2eV = nh\omega$, where $n = 0, 1, 2, \ldots$ is satisfied (Shapiro, 1963). In the presence of Majorana mediated single electron tunnelling, the resonance condition is expected be modified to $eV = nh\omega$, resulting in the disappearance of every other Shapiro step (Kwon *et al.*, 2004). One such missing Shapiro step was reported in Rokhinson *et al.* (2012).

Signatures consistent with a 4π-periodic Josephson effect and single electron tunnelling in an *InAs* nanowire junction setup were also recently reported by Laroche *et al.* (2017).

3.6.3 Non-locality and non-Abelian statistics

There are several proposals to demonstrate the non-local nature of the MZMs, that is, two spatially separated MZMs constitute a single Dirac fermion. For instance, in Nilsson *et al.* (2008), it is reported that *Majorana mediated crossed Andreev reflection* in a one-dimensional wire could be used for this purpose. This phenomenon occurs when an injected electron at one end of the wire, is accompanied by the emission of a hole at the other end. The net effect of this process is the splitting of a single Cooper pair over the two halves of the wire. The cross correlation of the lead current fluctuations is maximally correlated in the presence of MZMs and can be used as their detection.

The task of demonstrating non-Abelian statistics, which the most remarkable feature of MZMs, is a difficult experimental challenge. Not only must the other two categories of experiments be well established, but the demonstration requires also both the implementation of controlled fusing and braiding of MZMs as well as readout of the highly non-local encoded information. Moreover, the difficulties of scalability might also be highly nontrivial. So far, no experiments on non-locality and braiding statistics have been performed.

3.7 Outlook

Majorana's vision of a fermion being its own antiparticle is well established within condensed matter physics through the notion of superconducting Bogoliubov quasiparticles (see Chamon *et al.* (2010) for a thorough analysis). In addition, the existence of their tantalizing relative, the topological MZM, has through recent experiments strong support (Zhang *et al.*, 2017; Laroche *et al.*, 2017). Nonetheless, to demonstrate the most remarkable property of the MZMs, their non-Abelian statistics, remains a difficult experimental challenge, but hopefully such experiments will take place within a few years.

Ideally, the experimental pursuit of MZMs points the way towards the realization of even more exotic quasiparticles, such as *parafermions* (see for instance Alicea and Fendley (2016)), and will also be first platform for demonstrating topological quantum computation. Although it might not be possible at all to construct a scalable topological quantum computer, the new generation of Majorana quantum devices is a small but important step towards finding that out.

3.8 Paper I: Topological aspects of π phase winding junctions in superconducting wires

3.8.1 Motivation

As discussed towards the end of Sec. 3.3.1, the reality constraint of the superconducting order parameter in the Kitaev chain model introduces a winding number invariant and the model belongs to symmetry class $\mathcal{BDI}$. This invariant distinguishes between chains with different signs of the order parameter, and two connected chains with a phase difference of π are therefore necessarily separated by a local closing of the gap and the presence of MZMs. This observation motivated a study of two types of such π-shifted Josephson junctions. On the one hand, one can imagine the order parameter to be real and changing sign, or on the other hand having the amplitude fixed and a "winding" of the phase from 0 to π. These types of junctions are quite distinct and the properties of their sub-gap spectrum in comparison with trivial Josephson junctions could be imagined as a probe of topological superconductivity.

3.8.2 Main results

There are three main results in the paper. First, it contains an explicit mapping between the low energy Kitaev chain and the well-known SSH model (see Su *et al.* (1979), Takayama *et al.* (1980), and the references in PAPER I). Secondly, the paper contains a detailed analysis on the conditions for MZMs in one-dimensional Josephson junctions, and a description of the bound state spectrum in a π phase winding junction. In such a junction, the underlying TRS protecting the zero energy states that exist in a π-junction with a real order parameter is broken. It is shown that although no zero energy states can be expected on general grounds, it is possible to tune states to arbitrarily low energies by shrinking the junction length. This feature is shown to not exist in a trivial Josephson junction. Furthermore, the paper contains some speculations on how the results might be used as a bulk (in contrast to edge) probe of topological superconductivity in an experimental setup. Finally, the paper also contains an effective topological field theory which captures the behaviour of movable phase winding junctions.

3.9 Paper II: Extended Majorana zero modes in a topological superconducting - normal T-junction

3.9.1 Motivation

While the experimental implications of the results in PAPER I were not very concrete, the results provided good understanding of the conditions for bound state formation in topological Josephson junctions. In addition, PAPER I dealt only with toy models, and is of interest to use the more experimentally relevant model of the semiconducting wire to analyze topological Josephson junctions. These considerations led to the idea of a three armed Josephson junction, a T-junction, with experimentally relevant parameters as a platform for topological superconductivity and MZMs.

3.9.2 Main results

The first important result of the paper is a general scattering description of the T-junction with the methods discussed in Sec. 3.5 and Sec. 3.6.2. This description provides an analytical method to determine the condition for MZMs in the junction, solely in terms of symmetries. The paper also contains a tight-binding numerical simulation of the T-junction which agrees with the analytical results. The main observation, supported by both analytical and numerical calculations, is that MZMs can be very delocalized in the T-junction, and are spatially distributed over quite long distances, in contrast to being exponentially localized, as ordinary edge MZMs. It is also shown how one can tune the spatial distribution of the junction MZMs with the superconducting phases. Finally, it is shown that all the results above in principle can be experimentally probed with tunnelling spectroscopy.

3.10 Paper III: Geometric Josephson effects in chiral topological nanowires

3.10.1 Motivation

In a recent publication (Kvorning *et al.*, 2017), it was proposed that the geometric curvature in a two-dimensional chiral superconductor can give rise to a spontaneous creation of magnetic fields and electrical currents, the so-called *geo-Meissner* and *geo-Josephson effects*. From Eq. (3.26) and the following discussion, it should be clear that the Josephson current can have a geometric contribution also in one dimension. These two observations led to the proposal of geometric effects in nanowire topological Josephson junctions.

3.10.2 Main results

The main result of the paper is the demonstration of a geometric contribution to the phase of the effective p-wave phase, deep in the topological limit of the nanowire model outlined in Sec. 3.4.2. This geometric contribution is argued to manifest itself in various Josephson junction setups. Moreover, the phase dependence in arbitrarily shaped planar nanowires is shown to give rise to an explicit relation between the wire curvature and the superconducting current density. The origin of these effects is argued to be the directional dependence of the Rashba spin-orbit coupling.

4. Effective field theories for topological states of matter

IN THE SAME WAY Landau-Ginzburg theory describes symmetry breaking phases of matter, topological field theory is the appropriate low energy effective description of topological quantum matter. Such a description is useful not only for the non-interacting TSM discussed in Ch. 2 but also topologically ordered systems such as *spin liquids* or fractional quantum Hall states.

The first part of this chapter gives a very brief introduction to the archetypical TSM, the integer quantum Hall effect which belongs to class $\mathcal{A}$ in two dimensions. The topic of quantum Hall physics is vast, and in this thesis only the key principles have been summarized for brevity. The interested reader is referred to the excellent lecture notes by Tong (2016) for further reading. In addition to the quantum Hall system, the related two-dimensional *Chern insulators* and the $\mathbb{Z}_2$ *time-reversal symmetric topological insulators*, in classes $\mathcal{A}$ and $\mathcal{AII}$ are also discussed.

In the second part, these systems are discussed from a quantum field theory point of view. The concepts of effective response actions and topological field theories are introduced.

4.1 The classical Hall effect

To describe the *classical* Hall effect (Hall, 1879), consider a two-dimensional electron gas immersed in a strong perpendicular magnetic field B. The transport characteristics of the electrons is described by the *conductivity tensor* σ, defined by

$$j_i = \sum_j \sigma_{ij} E_j, \quad i,j \in \{x,y\}, \tag{4.1}$$

which relates the electronic current densities j_i to the electric field components E_j. The related *resistivity tensor* is defined as $\rho \equiv \sigma^{-1}$. The question is how to predict and measure the dependence of σ (or ρ) on the magnetic field.

The typical experimental setup to probe the system is that of a *Hall bar*. The two-dimensional electron gas is formed in a semiconducting hetereostructure (for details, see for instance Datta (1997)) with L and W denoting the

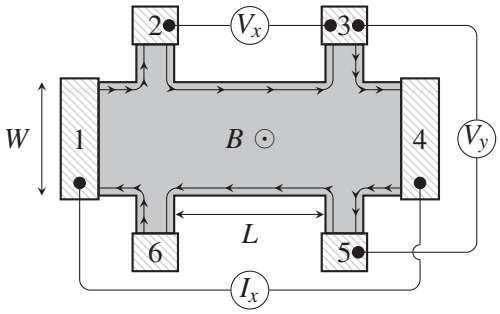

Figure 4.1: Schematics of a Hall bar setup. A current is driven between leads 1 and 4, and the transverse and longitudinal voltages V_y and V_x are measured as the magnetic field B is varied. The quantum Hall regime is characterized by unidirectional (chiral) edge states and a Hall conductance $\sigma_H \equiv I_x/V_y$ quantized in units of e^2/h.

device length and width respectively (see Fig. 4.1). Moreover, the electron gas is connected to six leads which enable measurements of all the components of σ. The way the Hall bar is usually probed is to drive a current $I_x = j_x W$ in the x-direction while measuring the resulting *longitudinal* and *Hall* (or transverse) voltages $V_x = V_2 - V_3 = V_6 - V_5$ and $V_y = V_3 - V_5 = V_2 - V_6$ respectively. Here, V_i denotes the electric potential in lead i and there is no applied current density in the transverse direction $I_y = j_y L = 0$. The classical *Hall effect* is the phenomenon that an applied current in the x-direction generates a voltage in the perpendicular y-direction. From the measurements one may with Eq. (4.1) extract the components of σ or ρ. The *Hall conductance* is defined as

$$G_H = \frac{I_x}{V_y} = \frac{j_x W}{E_y W} = \frac{j_x}{E_y} = \sigma_{xy} \equiv \sigma_H. \tag{4.2}$$

It is a consequence of the two-dimensional nature of the problem that the Hall conductance (resistance), which is what is measured in an experiment, is independent of the sample geometry and therefore equals the conductivity (resistivity) which is a microscopic property of the sample. This identification does not hold for the longitudinal quantitites.

To calculate σ, one may use the simple *Drude model* (Ashcroft and Mermin, 1976; Tong, 2016) with the result

$$\sigma = \frac{\sigma_0}{1+\omega_c^2\tau^2}\begin{pmatrix} 1 & -\omega_c\tau \\ \omega_c\tau & 1 \end{pmatrix}, \tag{4.3}$$

where $\sigma_0 \equiv ne^2\tau/m$ is the *Drude conductivity*, n is the electron density, m is the effective electron mass, $\omega_c = eB/m$ is the *cyclotron frequency* and τ is the

average scattering time. Inverting the conductivity tensor yields the classical predictions[1]

$$\rho_{xx} = \frac{m}{ne^2\tau} \quad \text{and} \quad \rho_H \equiv \rho_{xy} = \frac{B}{ne}. \tag{4.4}$$

It is then clear that a Hall measurement gives important information about the sample, in particular the electron density n. The longitudinal resistivity is seen to vanish for an infinitely pure sample, $\tau \to \infty$. It is worthwhile to note that since σ is a tensor, it is perfectly possible to have $\sigma_{xx} = \rho_{xx} = 0$ simultaneously in the presence of a magnetic field. This observation suggests that the distinction between insulating and conducting behaviour is not entirely clear for a Hall system.

4.2 The integer quantum Hall effect

The *integer quantum Hall effect* (IQH effect) occurs when the Hall measurement is performed in the quantum regime, where the characteristic quantum energy exceeds the thermal broadening: $\hbar\omega_c \gg k_B T$. In 1980, Klaus von Klitzing and co-workers measured the Hall and longitudinal resistances (von Klitzing *et al.*, 1980) in this limit, with a result similar to that in Fig. 4.2.

The most striking feature of the measurement data is the formation of plateaux of constant $R_{xy} \equiv \rho_{xy}$ for extended ranges of the magnetic field and abrupt transitions between neighbouring plateaux accompanied by spikes in the longitudinal resistance R_{xx}. On these plateaux, the Hall resistance takes values $\rho_{xy} = \frac{1}{\nu}\frac{h}{e^2}$ where ν is a positive integer, up to nearly one part in a billion. Further analysis shows that each plateau occurs when the magnetic field takes values $B = \Phi_0 n/\nu$, where n is the electron density and $\Phi_0 \equiv h/e$ is the *magnetic flux quantum*.

The precise quantization of the Hall resistance[2] has, remarkably, been observed to be completely independent of any microscopic details of the used devices, indicating the universality of the phenomenon, known as the integer quantum Hall effect. Clearly, these results are incompatible with the classical predictions (4.4), and a quantum mechanical treatment is needed.

[1] A simple way of obtaining the same result for $\rho_{xy} = \rho_H$ is to consider a stationary electron gas, $\vec{j} = 0$, with charge density ne in a perpendicular field $\vec{B} = B_z\hat{z}$. By assuming translational invariance, one can Lorentz boost to a new frame with velocity v, and obtain new components of the electromagnetic field $E'_y = -vB_z$ and $j'_x = -nev$. The Hall conductance becomes $\sigma_H = j'_x/E'_y = ne/B$.

[2] Note that both the conductance and the resistance are quantized. As a rule of thumb, the conductance is mostly referred to from the theory point of view, while the resistance is the quantity most common in experimental discussions.

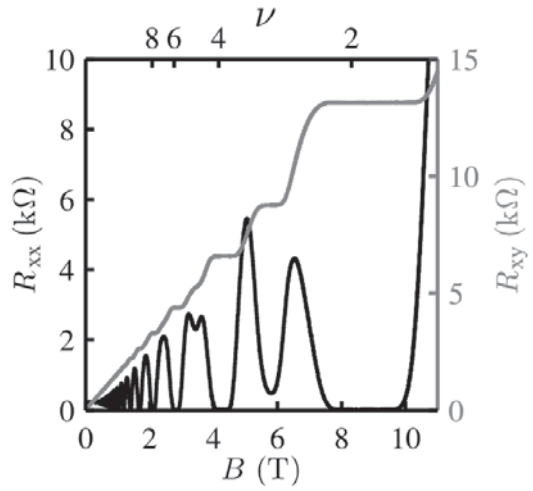

Figure 4.2: Quantum Hall measurement data at temperature 1.9 K. The Hall resistance R_{xy} (in grey) forms plateaux with values $\frac{h}{\nu e^2}$ with $\nu \in \mathbb{Z}$, accompanied with vanishing longitudinal resistance R_{xx} (in black). Figure reproduced from Suddards *et al.* (2012).

4.2.1 Quantum mechanical treatment: Landau levels

Assuming that electron interactions can be neglected, a quantum mechanical treatment of planar electrons in a perpendicular magnetic field leads to the formation of flat *Landau levels* (Landau, 1930) (see Fig. 4.3a). These levels have quantized energies $\varepsilon_p = \hbar\omega_c(p+1/2)$, where $p = 0, 1, 2\ldots$ and similar to the classical treatment, the characteristic energy scale is the cyclotron frequency $\hbar\omega_c = \hbar eB/m$.

In a finite system, each Landau level has a huge degeneracy, which for periodic boundary conditions (equivalent to imagining the sample is a torus) equals the number of flux quanta threading the sample $\mathcal{N}_\Phi = eBA/h = \Phi/\Phi_0$, where A is the sample area. One may then define the *filling factor* $\nu \equiv N/\mathcal{N}_\Phi$ where N is the total number of electrons, which reflects the number of filled Landau levels. Moreover, the density of electrons, $n = N/A$, can be expressed entirely in terms of ν according to $n = \nu/2\pi l_B^2$, where the *magnetic length* $l_B \equiv \sqrt{\hbar/eB}$ is the characteristic length scale for magnetic quantum phenomena.

Equating the classical result $\rho_{xy} = B/ne$ with the observed $\rho_{xy} = h/\nu e^2$ one can see that the electron density needed to to get the resistance of plateau number ν is $n = B\nu/\Phi_0$ which is *exactly* the density to fill ν Landau levels. This density is consistent with the magnetic fields on the plateaux. In fact, a supporting calculation shows that the Hall resistance of a single filled Landau

levels is precisely $\rho_{xy} = h/e^2$. Consequently, when ν Landau levels are filled, the Hall resistance equals $\rho_{xy} = h/\nu e^2$.

One therefore concludes that each plateaux corresponds to an integer number of filled Landau levels. Furthermore, when such an integer number of levels is filled, there is a gap of $\hbar\omega_c$ to the next level, making the system insulating and the longitudinal resistance vanishes. On the other hand, such reasoning does not at all explain why the Hall resistance would be quantized for a finite range of different filling factors close to those corresponding to filled Landau levels. A partially filled Landau level would also have plenty of empty charge carrying states which would allow for non-zero values of ρ_{xx} in the presence of small electrical fields. The solution to this problem is the presence of disorder.

4.2.2 The role of disorder

Based on degenerate perturbation theory, adding disorder to the Hall system will generally lift the degeneracy of the Landau levels (see Fig. 4.3a). The disorder potential, $V_d(x,y)$, is assumed to be small compared to the Landau level difference, $V_d(x,y) \ll \hbar\omega_c$, so that perturbation theory indeed valid and the disorder does not wash out the Landau levels. Another effect of disorder is to localize the quantum states. A small band of states in the middle of each Landau level will be extended but the surrounding states are localized because of the disorder potential. Therefore, while the Landau levels are broadened there is still a *mobility gap*, a gap between localized and extended states. As long as the chemical potential lies in the mobility gap, the Hall conductance can not change when the filling factor is varied (either by changing B or n), since the electronic states being filled are localized and cannot conduct any current. The Hall conductance will therefore remain constant over a wide range of magnetic fields which explains the plateaux formation.

In addition, several calculations (see for instance Prange (1981)) have established that to all orders in perturbation theory, the loss of current by the localized states in a Landau level is exactly compensated by the mobile states carrying a compensating excess current, and the Hall conductance remains e^2/h per Landau level[1]. It is interesting to note that the formation of quantized Hall conductance plateaux crucially relies on the presence of random disorder in the samples; precision from dirt.

[1] As elegantly formulated by Laughlin (1988): *"...it is as though the remaining delocalized states understood that one of their comrades had been killed and were pulling harder to make up for its loss."*

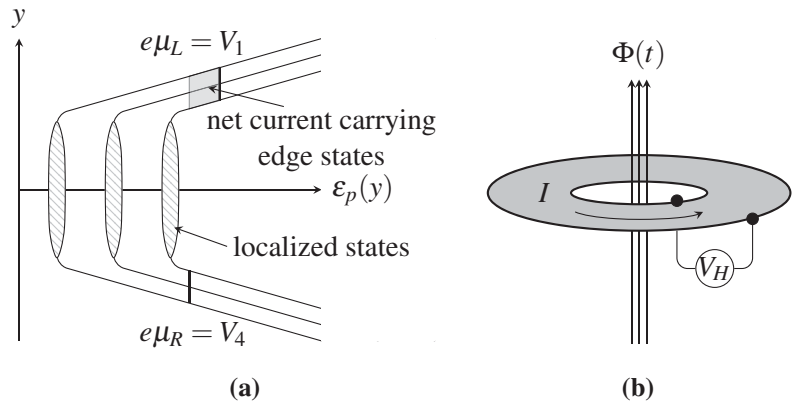

Figure 4.3: **(a)** The Landau level energy spectrum of planar electrons in the presence of a perpendicular magnetic field and confining electrostatic potential. In the presence of disorder, the Landau levels are broadened into localized states which do not carry any current, but are responsible for the resistance plateaux in Fig. 4.2. The net current in the quantum Hall device is carried by chiral edge states maintained at a potential difference $V = e(\mu_L - \mu_R)$ between the edges. Figure adapted from Datta (1997). **(b)** Corbino disc geometry in the Laughlin gauge argument. An adiabatically threaded flux $\Phi(t)$ generates an azimuthal current I. The ratio I/V_H is the Hall conductance and equals the number of electrons radially transferred when Φ is tuned from zero to Φ_0.

4.2.3 Edge states

The importance of edge states in the IQH effect was first pointed out by Halperin (1982) who showed that in the presence of a boundary, implemented by some confining electrostatic potential $U(y)$, the net current in the sample is mediated along the edges of the sample (see Fig. 4.1). In this picture, it is clear that the edge states are *chiral* which means that they travel in a clockwise manner[1] (see Fig. 4.1). The direction is set by the derivative of the confining potential $U(y)$ according to $v(n,k) = \frac{1}{eB}\frac{\partial U(y)}{\partial y}$ (see Fig. 4.3a), which clearly have different signs on opposing edges.

Crucially, the states carrying current in one direction are spatially separated from those carrying current in the other direction. For an electron to backscatter, which is the source of any longitudinal resistance, it would have to scatter from one side of the sample to the other. However, this process is strongly suppressed if the Fermi energy lies in the mobility gap. In addition to the exponentially small overlap of opposing edge wavefunctions, there are no current carrying states in the bulk. Only when the Fermi energy lies on a bulk

[1]The direction is set by the magnetic field. Swapping the magnetic field direction reverses the orbits of of the edge states.

Landau level, there exists a continuum of states in the transverse direction and the edge states can backscatter, leading to a finite longitudinal resistance.

Therefore, if there is an applied potential difference $V_1 - V_4 = e(\mu_L - \mu_R)$ between lead 1 and lead 4, the upper edge of the sample (with edge states carrying current in the positive x-direction) is in equilibrium with lead 1, $V_1 = V_2 = V_3$, and all upper edge states below the chemical potential μ_L are filled (see Fig. 4.3a). Similar reasoning holds for the lower edge with chemical potential $e\mu_R = V_4 = V_5 = V_6$. For M occupied edge states, the net current is therefore $I_x = M\frac{e^2}{h}V_y$, where $V_y = V_x$. This argument can be supported with a short scattering calculation.

4.2.4 Quantization of the Hall conductance I: scattering approach

Given the existence of chiral edge states immune to back-scattering described above, the prediction of a zero longitudinal resistance and a quantized Hall resistance can be readily derived within a scattering approach (Büttiker, 1988; Datta, 1997). Consider the multi-terminal Landauer-Büttiker formula in the zero temperature limit

$$I_p = \frac{e^2}{h}\sum_q T_{pq}(\varepsilon_F)\,[V_p - V_q]\,. \tag{4.5}$$

This formula relates the currents and potentials in scattering channel p through the transmission matrix T_{pq}, containing the probabilities for electrons to scatter from channel q to channel p. All scattering is assumed to take place close to the Fermi energy ε_F. With the assumptions above, one can write the full transmission matrix as

$$T = M\begin{pmatrix} 0 & 0 & 0 & 0 & 0 & 1 \\ 1 & 0 & 0 & 0 & 0 & 0 \\ 0 & 1 & 0 & 0 & 0 & 0 \\ 0 & 0 & 1 & 0 & 0 & 0 \\ 0 & 0 & 0 & 1 & 0 & 0 \\ 0 & 0 & 0 & 0 & 1 & 0 \end{pmatrix}, \tag{4.6}$$

where the matrix elements T_{pq} are non-zero only for neighbouring leads in the counter-clockwise direction (see Fig. 4.1) due to the presence of M robust chiral edge states. Next, terminal 4 is assumed to be grounded, $V_4 = 0$, and due to the assumption of absence of back-scattering, one may also take $V_2 = V_3 = V_1$ and $V_5 = V_6 = 0$. Since electrons on the the upper and lower edges are in equilibrium with terminals 1 and 4 respectively, using Eq. (4.5) $I_1 = -I_4 =$

$\frac{Me^2}{h}V_1$ and consequently

$$R_L \equiv \frac{V_2 - V_3}{I_1} = \frac{V_6 - V_5}{I_1} = 0, \tag{4.7a}$$

$$R_H \equiv \frac{V_2 - V_6}{I_1} = \frac{V_3 - V_5}{I_1} = \frac{1}{M}\frac{h}{e^2}. \tag{4.7b}$$

In this picture, the quantization of the Hall conductance or resistance holds because it simply measures the number of populated, perfectly conducting edge channels (as long as currents and voltages are small in comparison to the mobility gap) in units of the conductance quantum. Certainly, this number is an integer.

The outlined calculation depends crucially on the assumption that any edge back-scattering can be neglected. In addition, it also assumed that electron interactions could be neglected and a single particle description is accurate. To fully appreciate the robustness and universality of the conductance quantization, even in the presence of interactions and disorder, one needs to think about the IQH in a slightly different way.

4.2.5 Quantization of the Hall conductance II: Gauge invariance approach

The independence of the Hall conductance quantization on microscopic details, indicates that it should be the result of some underlying fundamental principle. A powerful argument supporting this idea was first given by Laughlin (1981) and later refined by Halperin (1982) and Niu *et al.* (1985). The argument is based on two principles: *i)* $U(1)$ gauge invariance or the conservation of electrical charge, and *ii)* the existence of a *mobility gap*: an energy gap between *current carrying* electron states. In this section, a version of Laughlin's argument will be presented, closely following Karlhede *et al.* (1993).

Since the IQH effect is independent of the sample geometry, the electrons in the Hall bar can instead be imagined to move in an annular geometry, usually referred to as a *Corbino disc* (see Fig. 4.3b). Through the hole of the annulus, one may imagine the threading of a thin magnetic flux Φ and there is a weakly coupled voltmeter measuring the potential difference V_H between the two edges. Consider now the adiabatic threading of a single flux quantum Φ_0 through the hole[1]. This procedure will induce a tangential current $I = \partial E/\partial\Phi$, where E is the total energy of the system, around the annulus. One can now imagine two distinct types of quantum states in the system, those that surround the hole, and those that do not. The non-surrounding states will

[1] This threading corresponds to driving a current between two terminals in the rectangular Hall bar.

be unaffected by the magnetic flux, but the surrounding states will experience an Aharonov-Bohm phase $\oint \vec{A} \cdot d\vec{l} = 2\pi\Phi/\Phi_0$ (Aharonov and Bohm, 1959). Hence, the treading of an integer multiple of flux quanta can neither affect the Hamiltonian nor its spectrum. The only possible change of the system is the repopulation of the energy levels, a phenomenon often referred to as *spectral flow*.

In simplest case of free particles in the absence of disorder, one can readily verify that the adiabatic threading of a single flux quantum produces a radial shift in the single-particle wave functions. In this case, all wave functions after the threading has shifted to its radial neighbour. The net result is that for p filled Landau levels, exactly p electrons are transported from one edge to the other. The energy change due to this procedure is by definition $\Delta E = epV_H$ and the current becomes

$$I = \frac{\Delta E}{\Delta\Phi} = \frac{epV_H}{h/e} = p\frac{e^2}{h}V_H. \tag{4.8}$$

Accordingly, the Hall conductance is found to be quantized

$$\sigma_H \equiv \frac{I}{V_H} = p\frac{e^2}{h}. \tag{4.9}$$

The real power of the argument lies however in the following. Regardless of the disorder potential and interactions there must exist at least two extended states per Landau level: one chiral state close to each of the annular edges. When threading the flux, the localized states will not undergo spectral flow, but the inner state starts to shift outwards into the disordered region. Due to charge conservation, the net effect must be that one state also must come out of this region and a single charge is pushed through out to the outer edge, and the argument still holds.

4.2.6 The Hall conductance as a topological invariant

The first connection between the quantized Hall conductance and topology was obtained for non-interacting electrons in a periodic potential and a uniform magnetic field (Thouless *et al.*, 1982). The periodic potential leads to the formation of Bloch bands (see Sec. 2.2) which remain a good description for rational values of the magnetic flux in units of Φ_0. It was shown that each of the Bloch bands carry an integer contribution to the Hall conductance given by the *(first) Chern number*[1] of the mapping between the *magnetic Brillouin*

[1] In the context of Bloch theory, the Chern numbers are sometimes called TKNN integers after their discoverers.

zone[1] and the space of Bloch Hamiltonians. These numbers are topological, in the sense that they cannot change under continuous deformations of the system. It is useful to think of the Chern number as a generalization of the Euler characteristic (see Sec. 2.1) to more abstract manifolds than surfaces in Euclidian space. The Chern number will be discussed in more detail in the next section, but for now it suffices to say that the total Hall conductance of the prescribed system can be shown to be the sum of all Chern numbers of the occupied Bloch bands in units of e^2/h.

The identification of the Hall conductance as a topological invariant turned out to be far more general than that given by the single-particle approach. Later work by Niu *et al.* (1985) and Avron and Seiler (1985), established that the Hall conductance remains a topological invariant, even in the presence of random disorder and interactions. By using the Kubo formula (Kubo, 1957; Tong, 2016) they showed that the bulk Hall conductance is given by

$$\sigma_H = \frac{e^2}{h}\int_0^{2\pi} d\phi_x \int_0^{2\pi} d\phi_y \frac{1}{2\pi i}\left(\langle\frac{\partial\Psi_0}{\partial\phi_x}|\frac{\partial\Psi_0}{\partial\phi_y}\rangle - \langle\frac{\partial\Psi_0}{\partial\phi_y}|\frac{\partial\Psi_0}{\partial\phi_x}\rangle\right), \tag{4.10}$$

which is e^2/h times the Chern number of the mapping between the "flux torus" of all possible boundary conditions (labelled by the phases ϕ_x and ϕ_x, which can be interpreted as magnetic fluxes threaded through the holes of the torus of the sample) to the space of normalized many body ground states $|\Psi_0\rangle$ with arbitrary phase. The important question lies in why one should average over the different boundary conditions, which is crucial to the quantization. As argued in Niu *et al.* (1985), there are several reasons that justify this procedure. First, since the sample is considered to be large, the boundary conditions, which are anyway an artificial construct, must not affect the physics, so one might as well average over all possibilities. Secondly, under the assumption that there are no long range correlations between electrons in the ground state, it can be shown that $\partial\sigma_H/\partial\phi_j$ vanishes in the thermodynamic limit, regardless of many-body interactions and disorder. Hence, the physical Hall conductance should equal its average which is quantized for topological reasons.

Generally, the topological quantization of the Hall conductance occurs because of electromagnetic gauge invariance (charge conservation) and an energy gap between a singly degenerate many body ground state to current carrying states. Relaxing the second requirement slightly and considering possible ground state degeneracies leads to the possibility of a Hall conductance which is a rational fraction of e^2/h. The discovery of the fractional quantum Hall

[1] In the presence of a magnetic field, the concept of a Brillouin zone is still useful under certain modification. Specifically, its size depends on the value of the magnetic flux. See for instance Kohmoto (1985) for details.

effect (Tsui *et al.*, 1982), defined by such a quantization, came therefore as a suprise to the physics community, because of the previously outlined strong arguments for the integer quantization of the Hall conductance. The description of fractional quantum Hall states is a vast subject of its own and goes beyond the general theme in this thesis. The reason for this is that to describe the fractional states, the strong interactions between electrons must be taken into account. The interested reader is referred to (Tong, 2016; Hansson *et al.*, 2017) for further reading.

4.3 Chern insulators

An important step in understanding the general structure of TSM was achieved by Haldane who constructed a simple lattice model with a quantized Hall conductance but in a *net zero magnetic field* (Haldane, 1988). This property is called *the anomalous quantum Hall effect* and the class of models exhibiting such behaviour is called *Chern insulators*. Rather than repeating Haldane's analysis, this section is devoted to a more general approach with insights from more recent research.

The key ingredient to understanding why Chern insulators are possible, given the importance of the magnetic field in the IQH effect, is the breaking of TRS. Such breaking is by no means dependent on the presence of any magnetic field, which was the important step taken by Haldane. This means also that the IQH effect, which can be understood in terms of free electrons, fits into the general framework of topological insulators and superconductors (see Sec. 2.4). Indeed, one may identify both the IQH states and the Chern insulators as two-dimensional systems in class $\mathcal{A}$ which has an associated $\mathbb{Z}$-valued Chern number topological invariant. This invariant will be described and discussed briefly as follows. The mathematically interested reader is referred to (Nakahara, 2003) for a more detailed discussion.

4.3.1 The Berry potential, the Berry field strength and the Chern number

The (first) Chern number of the m-th Bloch band $|u_m(k)\rangle$ of a general two-dimensional band theory is defined as

$$n^{(m)} = \frac{1}{2\pi}\int_{T^2} dk_x dk_y \, \mathcal{F}^{(m)}_{k_x k_y}(k), \quad (k) \equiv (k_x, k_y) \tag{4.11}$$

where $\mathcal{F}^{(m)}_{ij}(k) = \partial_{k_i}\mathcal{A}^{(m)}_j(k) - \partial_{k_j}\mathcal{A}^{(m)}_i(k)$ is the *Berry curvature* corresponding to the *Berry gauge potential* $\mathcal{A}^{(m)}(k)$ (Berry, 1984) with components

$$\mathcal{A}^{(m)}_j(k) = i\,\langle u_m(k)|\,\partial_j\,|u_m(k)\rangle\,, \quad j \in \{k_x, k_y\}. \tag{4.12}$$

There is a freedom to multiply $|u_m(k)\rangle$ with a phase factor $e^{i\phi(k)}$, under which the gauge potential transforms as $\mathcal{A}_j^{(m)}(k) \to \mathcal{A}_j^{(m)}(k) - \partial_{k_j}\phi(k)$. Moreover, since the BZ$= T^2$ is periodic and hence lacks a boundary, one could naively use Stoke's theorem to conclude

$$n^{(m)} = \frac{1}{2\pi}\int_{\partial BZ} d\vec{k}\cdot\mathcal{A}^{(m)}(k) = 0. \tag{4.13}$$

This result does not hold however if there exists some singularity in $\mathcal{A}^{(m)}(k)$. If this is the case, at k_0 say, one can remove this singularity by a local gauge transformation in the region $\mathcal{D}$ containing k_0. The gauge potential is now singular free in both $(T^2-\mathcal{D})$ and $\mathcal{D}$, but on their overlap, the boundary $\partial\mathcal{D}$, the choices of gauge potential must be related by a gauge transformation. Since $\partial(T^2-\mathcal{D}) = -\mathcal{D}$, using Stoke's theorem in this case gives

$$n^{(m)} = \frac{1}{2\pi}\oint_{\partial\mathcal{D}} d\vec{k}\cdot\vec{\partial}_k\phi(k). \tag{4.14}$$

Because $\phi(k)$ is periodic, its integral around $\partial\mathcal{D}$ equals an integer multiple of 2π and hence $n^{(m)}$ is an integer.

It is useful to view the Chern number as an obstruction to a global gauge choice of $\mathcal{A}^{(m)}$, which is nothing but a magnetic monopole in the BZ. While the Chern numbers of the individual bands might change during continuous deformations of the system, as long as the gap to occupied bands is maintained, the *total Chern number* $\sum_{\varepsilon_m<\varepsilon_F} n^{(m)}$ will not, and constitutes an appropriate $\mathbb{Z}$ invariant of class $\mathcal{A}$ in two dimensions (Avron *et al.*, 1983).

By using the Kubo formula (Kubo, 1957; Thouless *et al.*, 1982; Tong, 2016) one can relate the Hall conductance to the topological invariant as

$$\sigma_H = \frac{e^2}{h}\sum_{\varepsilon_m<\varepsilon_F} n^{(m)}, \tag{4.15}$$

manifesting its topological nature. For later use, it is worthwhile to note that $\sum_{\varepsilon_m<\varepsilon_F}\mathcal{F}^{(m)}_{k_xk_y}(k)$ is an odd function of k in the presence of TRS. In that case, the total Chern number of the occupied bands and the Hall conductance vanishes (Bernevig and Hughes, 2013).

4.3.2 Chern number invariant for a two-band system

For the simple case of a two-band model with Hamiltonian $h(k) = \vec{d}(k)\cdot\vec{\sigma}$, the Chern numbers of the associated two bands $|u_\pm(k)\rangle$ can be obtained from the compact formula

$$n^{(\pm)} = \mp\frac{1}{4\pi}\int_{T^2} dk_x dk_y\, \hat{d}\cdot\left(\partial_{k_x}\hat{d}\times\partial_{k_y}\hat{d}\right), \tag{4.16}$$

where $\hat{d} \equiv \vec{d}/|\vec{d}|$ (the k-dependence is suppressed in the following for simplicity). To prove Eq. (4.16), it is convenient to use spherical coordinates $\vec{d} = |d|(\sin\theta\cos\phi, \sin\theta\sin\phi, \cos\theta)$, with which one obtains the (gauge dependent) eigenvectors

$$|u_+\rangle = \begin{pmatrix} \cos\frac{\theta}{2} e^{i\phi} \\ \sin\frac{\theta}{2} \end{pmatrix}, \; |u_-\rangle = \begin{pmatrix} \sin\frac{\theta}{2} e^{i\phi} \\ -\cos\frac{\theta}{2} \end{pmatrix}. \tag{4.17}$$

One may then directly calculate the gauge invariant Berry curvature, which has only one non-vanishing component $\mathcal{F}^{\pm}_{\theta\phi} = \mp\frac{1}{2}\sin\theta$. Up to a constant, $\mathcal{F}^{\pm}_{\theta\phi}$ is nothing but the spherical coordinate Jacobian determinant on S^2:

$$\begin{aligned} \mathcal{F}^{\pm}_{\theta\phi} &= \mp\frac{1}{2} \begin{vmatrix} \sin\theta\cos\phi & \sin\theta\sin\phi & \cos\theta \\ \cos\theta\cos\phi & \cos\theta\sin\phi & -\sin\theta \\ -\sin\theta\sin\phi & \sin\theta\cos\phi & 0 \end{vmatrix} \\ &= \frac{1}{2}\hat{d}\cdot\left(\partial_\theta\hat{d}\times\partial_\phi\hat{d}\right), \end{aligned} \tag{4.18}$$

where in the last equality, the triple product representation of the determinant has been used. Transforming back to cartesian coordinates[1], and inserting the result into Eq. (4.11), one obtains Eq. (4.16).

The expression Eq. (4.16) can be interpreted as the the degree of the map $\phi : T^2 \ni k \mapsto \hat{d}(k) \in S^2$, which measures the number of times the image of T^2 wraps around S^2.

To illustrate the previous discussion with a concrete example, consider the following simple choice (Qi *et al.*, 2006)

$$\vec{d}(k) = (\sin k_x, \sin k_y, m + \cos k_x + \cos k_y), \tag{4.19}$$

where m is some parameter. In the continuum limit: $\sin k \to k$, $\cos k \to 1 - k^2/2$, this Hamiltonian becomes a two-component Dirac Hamiltonian and is therefore sometimes called the *Dirac-model*.

The energies of Eq. (4.19) are given by $\pm|\vec{d}|$ and for general values of m, the system is an insulator with an energy gap $2|\vec{d}|$. On the other hand, for $m = -2$, $m = +2$ or $m = 0$, the gap closes and the bands touch at $k = (0,0)$, $k = (\pi,\pi)$, and $k = (0,\pi)$ and $k = (\pi,0)$ respectively. As long as these points are avoided and the gap is open, one may use Eq. (4.16) and obtain

$$n^{(-)} = \begin{cases} -1 & -2 < m < 0, \\ +1 & 0 < m < 2, \\ 0 & \text{otherwise}, \end{cases} \tag{4.20}$$

[1] Using the antisymmetry of the triple product, one may use the alternative expression $\mathcal{F}^{\pm}_{k_x k_y} = \mp\frac{1}{2|\vec{d}|^3}\vec{d}\cdot\left(\partial_{k_x}\vec{d}\times\partial_{k_y}\vec{d}\right)$.

which by (4.15) verifies the model as a Chern insulator. At the gap closing points $n^{(-)}$ is ill-defined, indicating the topological phase transitions. These points can be viewed as sources of Berry flux, or in other words as magnetic monopoles.

4.4 Time-reversal symmetric topological insulators in two dimensions

In 2005, Kane and Mele showed in two seminal papers (Kane and Mele, 2005a,b) that the presence of TRS can lead to a new type of TSM, topologically distinct from the IQH states and the Chern insulators. The basic idea is to take two copies of Haldane's Chern insulator (Haldane, 1988), one for each spin, but with opposite orientation of the net zero magnetic field. This combination respects TRS since time-reversal reverses both the direction of spin and the magnetic field. The resulting system is a bulk insulator with spin currents travelling in opposite directions on the edges, and is known as a $\mathbb{Z}_2$- or *time-reversal symmetric topological insulator*[1].

In this incarnation, the spin projection σ_z is preserved, but the main insight of Kane and Mele was that one may add TRS preserving couplings (typically spin-orbit coupling terms) between the spin-sectors that breaks spin-rotation symmetry, without affecting the topological properties of the state. Instead, the presence of TRS, described by an operator $\mathcal{T}^2 = -1$, ensures Kramers degeneracy (see Sec.2.3) that protects the state. Instead of separately conserved spin-currents on the edge, there are Kramers pairs of oppositely travelling edge states, which does not correspond to any fixed spin direction. Nonetheless, the presence of such *helical edge states* is the topological signature of the system, which is also sometimes referred to as the *quantum spin Hall effect* (QSH effect). It is important to note though that while similar in name to the IQH state, the QSH state does not in general have a quantized spin conductance. This happens only when spin-rotation symmetry is present, which is generally not the case.

The two-dimensional TRS invariant topological insulator has been generalized to three dimensions (Fu *et al.*, 2007; Moore and Balents, 2007; Hsieh *et al.*, 2008; Roy, 2009) with peculiar surface states consisting of a single two-dimensional massless Dirac fermion, in other words "a quarter of graphene".

[1] Sometimes, this model is simply referred to as a topological insulator. However, in this thesis, that name is used generically for all non-superconducting systems in the periodic table

4.4.1 Class $\mathcal{AII}$ topological invariant in $d = 2$

As described in Sec. 4.3.1, the presence of TRS dictates that the total Chern number of the occupied bands, and by Eq. (4.15), also the Hall conductance must vanish. Instead, as indicated by the periodic table (Tab. 2.2, class $\mathcal{AII}$, $d = 2$) the topological nature of the system is characterized by a $\mathbb{Z}_2$-valued invariant which will be discussed in this section.

For two-dimensional systems with TRS but also with spin-rotation symmetry, one can define *spin Chern numbers* to use as a topological invariant (Sheng *et al.*, 2006). To derive these numbers, the full Bloch Hamiltonian is written in separate spin-blocks as

$$h(k) = \begin{pmatrix} h_\uparrow(k) & 0 \\ 0 & h_\downarrow(k) \end{pmatrix}, \tag{4.21}$$

and the spin Chern numbers $n_\uparrow$ and $n_\downarrow$ are just the Chern numbers for $h_\uparrow(k)$ and $h_\downarrow(k)$ respectively. Since each separate spin sector breaks TRS, the spin Chern numbers are well defined, but their sum must vanish $n_\uparrow + n_\downarrow = 0$. Nonetheless, their average $n_\sigma = (n_\uparrow - n_\downarrow)/2$ can be used to define a $\mathbb{Z}_2$ invariant $\nu \equiv (-1)^{n_\sigma}$.

However, in the absence of spin-rotation symmetry, the spin Chern numbers are not well defined anymore. The idea is that instead of using the spin degree of freedom, one uses the Kramers degeneracy to define separate Chern numbers for the two Kramers sectors of the Hilbert space (Sato and Ando, 2017). Labelling the Bloch eigenstates with Kramers indices according to $|u_n^I(k)\rangle$ and $|u_n^{II}(k)\rangle \equiv e^{i\varphi(k)}\mathcal{T}\,|u_n^I(-k)\rangle$, one may define

$$n_I = \frac{1}{2\pi}\int_{BZ} dk_x dk_y\, \mathcal{F}^{I-}_{k_x k_y}(k_x, k_y), \tag{4.22a}$$

$$n_{II} = \frac{1}{2\pi}\int_{BZ} dk_x dk_y\, \mathcal{F}^{II-}_{k_x k_y}(k_x, k_y), \tag{4.22b}$$

where $\mathcal{F}^{I(II)-}_{k_x k_y}$ are now the total Berry field strengths of the respective total Berry vector potentials $\mathcal{A}^{I(II)-}$ with components

$$\mathcal{A}^{I-}_j(k) = i\sum_{\varepsilon_n<\varepsilon_F} \langle u_n^I(k)|\,\partial_j\,|u_n^I(k)\rangle\,, \tag{4.23a}$$

$$\mathcal{A}^{II-}_j(k) = i\sum_{\varepsilon_n<\varepsilon_F} \langle u_n^{II}(k)|\,\partial_j\,|u_n^{II}(k)\rangle\,, \tag{4.23b}$$

where $j \in \{k_x, k_y\}$. The Kramers Chern numbers are integers, and $n_I + n_{II} = 0$ because of TRS. Since the I, II labels lack any physical meaning, they can be aribrarily exchanged. However, such an exchange reverses the signs of n_I and n_{II} since $n_I \to n_{II} = -n_I$ and $n_{II} \to n_I = -n_{II}$. The Kramers Chern numbers

are therefore not unique, but on the other hand, their *parities* are. By defining the $\mathbb{Z}_2$ index ν

$$\nu \equiv (-1)^{n_I} = (-1)^{n_{II}} = \pm 1, \tag{4.24}$$

one obtains a topological quantity invariant under exchange of Kramers labels. A two-dimensional system with TRS and $\nu = -1$ is topologically distinct from an ordinary insulator which has $\nu = +1$. Similar $\mathbb{Z}_2$ indices can be defined for the generalization of the topological insulator to three (and higher) dimensions (Moore and Balents, 2007). For a discussion on other approaches to the $\mathbb{Z}_2$ invariant, see Kane (2013) and references therein.

4.4.2 $\mathbb{Z}_2$ nature of the edge states

Kramers theorem provides a good explanation of the $\mathbb{Z}_2$ nature of the edge states. If there is only a single Kramers pair on one edge in a rectangular sample, TRS forbids the backscattering of one state into the other since that would break the Kramers pair. In addition, the possibility of back scattering into a Kramers partner on another edge of the sample is exponentially suppressed in the sample size.

With two pairs present, a right-moving state could scatter into a left-moving state that is not it's Kramers partner, a process that will generally gap out these states. Such arguments lead to the general conclusion is that an odd number of states will be stable (and a single Kramers pair must persist if states scatter into each other) and an even number can gap out completely.

One can support this argument with a scattering calculation (Bardarson, 2008; Akhmerov *et al.*, 2015). Consider the problem of N pairs of edge states scattering onto some disordered region on the edge. The vectors of wave amplitudes of scattering states to the left and to the right of the scattering region are related by

$$\begin{pmatrix} \Psi_L^{\text{out}} \\ \Psi_R^{\text{out}} \end{pmatrix} = S \begin{pmatrix} \Psi_L^{\text{in}} \\ \Psi_R^{\text{in}} \end{pmatrix} = \begin{pmatrix} r & t' \\ t & r' \end{pmatrix} \begin{pmatrix} \Psi_L^{\text{in}} \\ \Psi_R^{\text{in}} \end{pmatrix}, \tag{4.25}$$

where the $2N \times 2N$ unitary scattering matrix S (the energy dependence is suppressed for notational ease) has been put on block form, which defines the $N \times N$ reflection and transmission matrices, r, r', t, and t'. In the presence of TRS (including the disorder), the time-reversed states must be related by *the same* scattering matrix and since time-reversal exchanges incoming to outgoing scattering states, one can write

$$\mathcal{T} \begin{pmatrix} \Psi_L^{\text{in}} \\ \Psi_R^{\text{in}} \end{pmatrix} = S\mathcal{T} \begin{pmatrix} \Psi_L^{\text{out}} \\ \Psi_R^{\text{out}} \end{pmatrix}. \tag{4.26}$$

Using the unitarity of S and combining Eq. (4.25) and Eq. (4.26) it follows that

$$S = \mathcal{T} S^\dagger \mathcal{T}^{-1}. \tag{4.27}$$

Now, if $\mathcal{T}^2 = -1$ one can choose $\mathcal{T} = i\sigma_y\mathcal{K}$ and after a basis change of the outgoing modes $S \to i\sigma_y S$, it follows that the scattering matrix can be taken to be antisymmetric[1]

$$S = -S^T. \tag{4.28}$$

It follows further that also the reflection matrices r and r' must be antisymmetric. Note then that for N odd, $\det r = -\det r = 0$ (and similarly for r') and both these matrices must have at least one zero eigenvalue each. Consequently, there must be at least one Kramers pair that is transmitted through the scattering region with unit probability[2]. Hence, one can conclude that for a TRS invariant system with $\mathcal{T}^2 = -1$ and N odd, there must at least one pair of dissipationless propagating edge states. For N even, no such statement can be made and all edge states generally scatter. Thus, there are two distinct possibilities, as indicated by the two-valued $\mathbb{Z}_2$ invariant. One may interpret this result as a manifestation of the bulk-boundary correspondence (see Sec. 2.5).

4.4.3 Experimental evidence for helical edge states

A single Kramers pair of edge states results in an unambiguous signature of six terminal resistance measurements in a QSH bar setup. This setup is very similar to that in Fig. 4.1, with the modification that there are edge states connecting *each neighbouring pair* of leads.

The resistances can be therefore be obtained by slightly modifying the calculation in Sec. 4.2.4. With dissipationless helical modes travelling between each pair of leads, the transmission matrix of the system reads

$$T_{helical} = T + T^T, \tag{4.29}$$

where T is the IQH transmission matrix in Eq. (4.6) with the additional constraint $M = 1$ (assuming a single robust pair of helical modes). By using the Landauer-Büttiker formula in Eq. (4.5) and assuming a single current $I_1 = -I_4 \equiv I_{14}$ from lead 1 to lead 4, where the latter is taken to be grounded, one obtains the resistances

$$R_{23,14} \equiv \frac{V_2 - V_3}{I_{14}} = \frac{h}{2e^2} \tag{4.30a}$$

$$R_{14,14} \equiv \frac{V_1 - V_4}{I_{14}} = \frac{3h}{2e^2}, \tag{4.30b}$$

which are the observed values in the quantum spin Hall regime in HgTe quantum wells (Roth *et al.*, 2009). In addition, these resistances were shown to be

[1] In contrast, for $\mathcal{T}^2 = +1$, S can be taken to be symmetric by choosing $\mathcal{T} = \mathcal{K}$.

[2] Nevertheless, finite temperature allows for in-elastic back-scattering leading to a finite conductivity.

independent of the device geometry, so that the observed values indeed support a QSH effect with helical edge states.

4.5 Effective field theories

The purpose of an effective field theory is to avoid any microscopic description of a physical system and instead describe its physical properties in a course-grained manner. One may think of an effective theory as averaging over the behaviour on microscopic distances and high energies which hopefully will generate a simpler theory at larger distances and lower energies (see the discussion of *emergence* in Sec. 1.1). That such theories are extremely useful to describe TSM is quite evident, since the properties of such systems are almost by definition independent of most microscopic details.

In the following sections, two types of effective field theories will be considered. Theories of the first type are known as *effective response actions*, which encode the response of the system to low energy external perturbations, typically electromagnetic fields. Unconventional *topological response*, a concept that will be clear below, can in fact be viewed as a defining property of topological states of matter. It is important to note that an effective response action does not contain any dynamics, and the input field configuration is instead added by hand, for instance motivated by some experiment.

The second type of effective theories are *topological field theories* which describe the system in terms of emergent *hydrodynamical* fields which are related to matter currents. As the name suggests, a topological field theory encodes topological properties of the system, and in particular the dynamics depend crucially on the topology of the space-time manifold of the system. By coupling the internal fields to external electromagnetic fields, one may upon integration obtain the aforementioned response theories. What is more interesting however is to couple the hydrodynamical fields to quasiparticle currents which will then be endowed with *topological interactions*. Such interactions are result in abelian anyonic statistics and the special case of transmuting bosons into fermions (and vice versa) in two space-dimensions.

In the presence of boundaries on the space-time manifold, topological field theories dictates the presence of exotic edge dynamics, which is in turn constitute a remarkable field theory manifestation of the bulk-boundary correspondence (see Sec. 2.5). By themselves, bulk and the boundary theories can be *anomalous*: they violate some fundamental physical principle, but together they form a consistent physical theory.

4.5.1 Effective response action

The electromagnetic response of the integer quantum Hall states, or equivalently the Chern insulators, can be encoded in an effective response action. The basic idea of such an action is similar to that of a thermodynamic poten-

tial, in the sense that by taking appropriate derivatives, observable quantities are obtained. The effective response action Γ is a functional not only of variables like the temperature and the chemical potential, but also of space-time dependent external fields. In this thesis, the electromagnetic gauge potential $A_\mu(x)$[1] is the field of interest, but one may also think of response to classical gravitational fields or curvature. In the following, the temperature and chemical potential are assumed to be zero.

The appropriate response action for the quantum Hall effect is the *Chern-Simons* action (Chern and Simons, 1974; Dunne, 1999; Zee, 1995)

$$\Gamma[A] = \frac{\nu}{4\pi}\int d^3x\, \varepsilon^{\mu\nu\lambda} A_\mu \partial_\nu A_\lambda, \tag{4.31}$$

where $d^3x = dtdxdy$ is the $2+1$ dimensional space-time measure, ν is some constant to be determined and $\varepsilon^{\mu\nu\lambda}$ is the totally antisymmetric tensor in $D = 2+1$ space-time dimensions[2]. By construction, the field A_μ describes an *additional* electromagnetic perturbation of the ground state. The external magnetic field responsible for the formation of the quantum Hall state is already encoded by $\nu \neq 0$.

To see that this action captures the relevant Hall response, one first must remember that the local current density is the functional derivative of the action with respect to A_μ:

$$\langle j^\mu \rangle \equiv \frac{\delta\Gamma[A]}{\delta A_\mu}|_{A=A^{ex}} = \frac{\nu}{2\pi}\varepsilon^{\mu\nu\lambda}\partial_\nu A^{ex}_\lambda, \tag{4.32}$$

where it is emphasized that the insertion of the external field configuration is performed after functional differentiation. Note also that if ν is assumed to be globally constant, the current is locally conserved $\partial_\mu \langle j^\mu(x)\rangle = 0$.

From this expression, it follows that an applied electric field in the x-direction induces a Hall current in the negative y-direction with Hall conductance $\sigma_H = \nu/2\pi = \nu e^2/h$ with units restored. One may therefore suspect that ν must be an integer to correctly describe the integer quantum Hall effect. In fact, it can be shown that gauge-invariance dictates $\nu \in \mathbb{Z}$ (see for instance Witten (2015)). By taking the time component of (4.32), one notes that a local magnetic flux induces an a change in the local charge density, which also follows from current conservation. One concludes that the action (4.31) indeed encodes the correct electromagnetic response (4.32).

[1] For notational ease, the space time index $(x) \equiv (t,x,y)$ is most often suppressed in this chapter. If several space-time arguments needs to be displayed, these will be labelled according to the rule $(1) \equiv (t_1,x_1,y_1)$ and so on.

[2] The convention used is that greek letter indices represent space-time indices t,x,y and latin letter indices refer to the spatial components x,y.

There is however a serious problem with the Chern-Simons response action. It is not invariant under $U(1)$ gauge transformations $A_\mu \to A_\mu + \partial_\mu \chi$, where χ is some space time function (on the other hand, the response (4.32) is gauge invariant). In the absence of any edges, this is not a problem since integrating by parts, discarding the boundary term and assuming current conservation gives back the original action. In a real sample, there must be edges however, so the gauge non-invariance is clearly a problem. In particular, the presence of chiral edge states (see Sec. 4.2.3) for a quantum Hall system with boundaries, indicates the importance of adding possible edge contributions into the theory. It turns out that the appropriate theory incorporating edge effects is a *topological field theory*, which will give additional important insights to the quantum Hall effect. This is the topic for the following sections.

4.5.2 Topological action

There are in fact a handful of general principles that will simplify the derivation of the topological field theory (Zee, 1995):

(i) The system of interest lives in $D = 2+1$ space-time dimensions.

(ii) The electromagnetic current j^μ is conserved, $\partial_\mu j^\mu = 0$, which in the prescribed space-time dimension $D = 2+1$ implies that it can be written as the curl of some vector field b_λ according to $j^\mu = \frac{1}{2\pi}\varepsilon^{\mu\nu\lambda}\partial_\nu b_\lambda$. The current is clearly invariant under transformations $b_\lambda \to b_\lambda + \partial_\lambda \Lambda$, where Λ is an ordinary space-time function and b_λ is indeed a gauge potential. In addition, because of its relation to the conserved current, b_λ is sometimes referred to as *hydrodynamical*. The normalization of the current is important which will be clear below.

(iii) The theory should be local and capture the long distance and low energy behaviour of the system. Specifically, this means that the Lagrangian density should contain as few terms as possible in a mass (or derivative) expansion of the field variables.

(iv) Because the system has a non-zero Hall conductance, parity and time-reversal symmetries are broken.

With these considerations, the simplest possible gauge invariant[1] Lagrangian density that can be constructed is the Chern-Simons term of mass dimension three

$$\mathcal{L} = -\frac{1}{4\pi\nu} b_\mu \varepsilon^{\mu\nu\lambda}\partial_\nu b_\lambda + \ldots \tag{4.33}$$

[1]Note that $b_\mu b^\mu$ is of mass dimension two, but is not gauge invariant.

where the pre-factor will be clear below and where $(\ldots)$ denotes higher order derivative terms, most notably the Maxwell term $\sim f_{\mu\nu}f^{\mu\nu}$. At long distances and low energies, the dynamics is dominated by this Chern-Simons term, provided $1/\nu \neq 0$. Accordingly, such terms will be neglected in the following discussion.

One may now wonder why $\mathcal{L}$ is written in terms of the gauge potential b_μ, rather than the current j^μ. The reason is that the simplest term that can be constructed with the current alone is $j^\mu j_\mu$ which has mass dimension 4 and is actually the Maxwell term. To get a lower order gauge invariant term, one must use the inverse derivative operator which results in the *non-local* Hopf term $\sim j^\mu \frac{1}{\varepsilon_{\mu\nu\lambda}\partial_\nu} j^\lambda$. The introduction of a gauge potential is simply a way to have a local Lagrangian density and action (Zee, 1995).

To understand why an action containing the Lagrangian density (4.33) is *topological*, first notice that it does not involve the metric tensor and therefore does note depend on the space-time geometry. Consequently, correlation functions will not depend on the metric either, and it turns out that it is only the *topological* properties of space-time that are important. Note also that the Hamiltonian density vanishes and the theory therefore describes only the zero energy properties of the system. Hence, excitations are not treated in the theory. While this might indicate a trivial theory, the quantum state degeneracy, denoted by d, of this zero energy space is a highly non-trivial matter, and turns out to also depend crucially on the space-time topology: $d = |\nu|^{-g}$, where g is the *genus* of the space-time manifold (see Sec. 2.1).

The next step is to couple the gauge field b_μ to the external vector potential A_μ. This is done by the usual minimal coupling $A_\mu j^\mu$ which after an integration by parts and discarding the boundary term yields the Lagrangian density

$$\mathcal{L} = -\frac{1}{4\pi\nu} b_\mu \varepsilon^{\mu\nu\lambda}\partial_\nu b_\lambda - \frac{1}{2\pi}\varepsilon^{\mu\nu\lambda} b_\mu \partial_\nu A_\lambda . \tag{4.34}$$

Upon further integrating out b_μ one obtains again the response action (4.31). On the other hand, coupling b_μ directly to a quasiparticle current j_q^μ reveals other important topological properties of the theory. One may think of j_q^μ as some emergent current of excitations in the system. This current is introduced in the theory by adding the term $j_q^\mu b_\mu$ to the Lagrangian density. The equations of motion for b_μ then becomes

$$\varepsilon^{\mu\nu\lambda}\partial_\nu b_\lambda = -\varepsilon^{\mu\nu\lambda}\partial_\nu A_\lambda - 2\pi j_q^\mu , \tag{4.35}$$

indicating that the field strength of the gauge field b_μ is completely determined by the external sources A_μ and j_q^μ. Hence, b_μ is not a dynamical field and the equations of motions are just constraints. This is however only true for an infinite system, with trivial topology and without boundaries. Introducing

boundaries, or holes in the space-time manifold, will introduce dynamics into the system.

Upon integrating out the field b_μ in the presence of the quasiparticle current one obtains a response action with this source included:

$$\Gamma[A, j_q] = \frac{\nu}{4\pi} \int d^3x \, \varepsilon^{\mu\nu\lambda} A_\mu(x) \partial_\nu A_\lambda(x) \tag{4.36}$$

$$+\pi\nu \int d^3x \, d^3y \, j_q^\mu(x) \left(\frac{1}{\varepsilon^{\mu\nu\lambda}\partial_\lambda} \right) (x-y) \, j_q^\nu(y), \tag{4.37}$$

where the second *Hopf term* describes the statistical or *topological interaction* between the quasiparticles, in the sense that it describes the topological *linking number* of the quasiparticle world-lines. If these quasiparticles are considered electrons or holes, as appropriate in the integer quantum Hall effect, the parameter ν must be an odd integer. In that case, the interaction term induces the fermionic minus sign upon exchange which is one reason for the chosen normalization of b_μ. On the other hand, other values of ν allow for more exotic exchange and this is a simple way of understanding the formation of abelian anyons in the fractional quantum Hall effect: through Eq. (4.35), the b_μ-field attaches flux onto the quasiparticles which upon exchange with each other generates arbitrary statistical phases through the Aharonov-Bohm effect (Aharonov and Bohm, 1959; Wilczek, 1982).

4.5.3 Topological field theory from functional bosonization

At this point, it is reasonable to ask whether there is any systematic way to obtain the topological field theory (4.34) without resorting to educated guesses, and subsequently obtaining the correct response action Eq. (4.31)? The answer to this question is affirmative, and there is even a way of systematically obtaining similar response theories for other types of systems. A general method to do this is known as *functional bosonization* which is outlined below, closely following Chan *et al.* (2013). While the method holds for general space-time dimensions, in the following $D = 2+1$ for transparency.

The starting point is the partition function

$$\mathcal{Z}[A] = \int \mathcal{D}[\bar{\psi}, \psi] \exp(iS[\bar{\psi}, \psi, A]), \tag{4.38}$$

where $S[\bar{\psi}, \psi, A]$ is the fermion action of the system in question. The fermion current j_μ is coupled to the *external* $U(1)$ gauge potential A through the usual source term $A_\mu j^\mu$.

Expectation values or correlation functions of current operators can be obtained from the generating functional $\ln\mathcal{Z}[A]$ through functional differentiation

$$\langle j^{\mu_1}(1)j^{\mu_2}(2)\ldots\rangle = \frac{1}{i}\frac{\delta}{\delta A_{\mu_1}(1)}\frac{1}{i}\frac{\delta}{\delta A_{\mu_2}(2)}\ldots\ln\mathcal{Z}[A]|_{A=A^{ex}}. \tag{4.39}$$

Note that in (4.39), the differentiation is with respect to $\ln\mathcal{Z}[A]$ so that the correlation function is *connected*[1].

The idea of functional bosonization is to exploit the gauge invariance of the action and the functional integral measure under local $U(1)$ gauge transformations. The transformation $A_\mu \to A_\mu + a_\mu$ with $a_\mu = \partial_\mu\chi$ being a pure gauge[2], leaves the partition function invariant and one can write

$$\mathcal{Z}[A] = \int \mathcal{D}[a]_{\text{pure}}\mathcal{Z}[A+a], \tag{4.40}$$

up to a possible normalization. This expression means that one may integrate over all gauge fields a_μ satisfying the pure gauge condition $f_{\mu\nu}(a) \equiv \partial_\mu a_\nu - \partial_\nu a_\mu = 0$ for all pair of indices. The pure gauge constraint can be conveniently implemented in the partition function by inserting the δ functional

$$\prod_x\prod_{\mu=1}^{3}\varepsilon^{\mu\nu\lambda}\delta\{[f_{\nu\lambda}(a(x))]\}. \tag{4.41}$$

Next, the delta functional can be exponentiated by introducing an auxiliary vector field b_μ and one obtains

$$\mathcal{Z}[A] = \int \mathcal{D}[a,b]\mathcal{Z}[A+a]\exp(-\frac{i}{4\pi}\int d^3x\, b_\mu\varepsilon^{\mu\nu\lambda}f_{\nu\lambda}(a)), \tag{4.42}$$

where the normalization $-1/4\pi$ will be clear below. Finally, by shifting $a \to a - A$ one obtains

$$\mathcal{Z}[A] = \int \mathcal{D}[a,b]\mathcal{Z}[a]\exp(-\frac{i}{4\pi}\int d^3x\, b_\mu\varepsilon^{\mu\nu\lambda}(f_{\nu\lambda}(a) - f_{\nu\lambda}(A)). \tag{4.43}$$

From this expression, there is a correspondence between expectation values of j^μ and expectation values of the auxiliary field b_μ, which can be viewed as a bosonisation rule[3]:

$$\langle j^{\mu_1}(1)j^{\mu_2}(2)\ldots\rangle = \langle\frac{1}{2\pi}\varepsilon^{\mu_1\nu_1\lambda_1}\partial_{\nu_1}b_{\lambda_1}(1)\frac{1}{2\pi}\varepsilon^{\mu_2\nu_2\lambda_2}\partial_{\nu_2}b_{\lambda_2}(2)\ldots\rangle. \tag{4.44}$$

[1] For instance, $\langle j^{\mu_1}(1)j^{\mu_2}(2)\rangle = \langle j^{\mu_1}(1)j^{\mu_2}(2)\rangle_0 - \langle j^{\mu_1}(1)\rangle_0\langle\, j^{\mu_2}(2)\rangle_0$, where the subscript 0 refers to the functional average with respect to the full partition function.

[2] This requirement is in fact too restrictive. On non-trivial manifolds, the requirement is that all Wilson loop operators $e^{i\int_\gamma a_\mu dx^\mu}$ should equal the identity operator.

[3] In 1+1 dimensions, the corresponding expression holds as an operator identity, that is without the averaging, within the context of *bosonization*. The outlined procedure can be viewed as a generalization of this procedure, hence the name.

The last step of the bosonization procedure is to evaluate $\mathcal{Z}[a]$. Generally, this procedure can not be done exactly (except in $D = 1+1$ dimensions) but if there is a gap in the system, one may perform a derivative expansion as discussed above. The IQHE system belong to class $\mathcal{A}$, where TRS, PHS and CS are broken (see Sec. 2.3). In that case $\mathcal{Z}[a]$ can be expanded to lowest order as

$$\ln \mathcal{Z}[a] = i\frac{\nu}{4\pi}\int d^3x\, \varepsilon^{\mu\nu\lambda} a_\mu \partial_\nu a_\lambda$$

which is again the Chern-Simons action. The total effective Lagrangian density then reads

$$\mathcal{L} = -\frac{1}{2\pi} b_\mu \varepsilon^{\mu\nu\lambda}\partial_\nu(a_\lambda - A_\lambda) + \frac{\nu}{4\pi}\varepsilon^{\mu\nu\lambda} a_\mu \partial_\nu a_\lambda \tag{4.45}$$

Upon integration of the quadratic a_μ field, one obtains the approximate partition function

$$\mathcal{Z}[A] = \int \mathcal{D}[b] \exp(i\int d^3x \mathcal{L}), \tag{4.46}$$

with a new low energy Lagrangian density

$$\mathcal{L} = -\frac{1}{4\pi\nu} b_\mu \varepsilon^{\mu\nu\lambda}\partial_\nu b_\lambda + \frac{1}{2\pi}\varepsilon^{\mu\nu\lambda} b_\mu \partial_\nu A_\lambda . \tag{4.47}$$

In the absence of boundaries, one may also integrate out b_μ and obtain the action (4.31) again. On the other hand, the action (4.47) provides a way to overcome the difficulties when edges are present.

4.5.4 Theory of the edge

To study edge effects in the IQH system, the quantum Hall state is for concreteness assumed to cover the plane $y < 0$ and therefore has an edge along the x-axis[1]. Under the gauge transformation $\delta A_\mu \equiv A'_\mu - A_\mu = \partial_\mu \chi$, the action picks up the following boundary term

$$\delta\Gamma[A] = \frac{\nu}{4\pi}\int dt dx\, \chi E_x, \tag{4.48}$$

where $E_x = \partial_t A_x - \partial_x A_0$ is the electrical field along the x-direction. This result implies that the edge current is not conserved which is a serious problem with the theory. The solution to this puzzle comes from using an action with the Lagrangian density (4.47). The first thing to notice is that the b_0 component is not dynamical, but instead a Lagrange-multiplier enforcing the bulk constraint

[1] Note however that since there is no metric in this problem, the x-coordinate might equally parametize *any* (appropriately behaved) closed spatial curve in the plane.

$\varepsilon^{ij}\partial_i b_j + \nu\varepsilon^{ij}\partial_i A_j = 0$ with the solution $b_i = -\nu A_i + \partial_i\varphi$, for some scalar field φ. Substituting this solution back into the action and at the same time choosing the overall gauge $b_0 = 0$ results after some tedious but straightforward integrations by parts and rearrangements in the action

$$S[\varphi,A] = \frac{1}{4\pi\nu}\int dtdx\,(\partial_t\varphi - \nu A_0)(\partial_x\varphi - \nu A_x) - \frac{1}{4\pi}\int dtdx\,\varphi E_x + \frac{\nu}{4\pi}\int d^3x\,\varepsilon^{\mu\nu\lambda}A_\mu\partial_\nu A_\lambda, \tag{4.49}$$

where $\varphi(x,t) \equiv \varphi(x,0,t)$ has support only along the boundary $y = 0$. To preserve charge conservation and gauge invariance this field must transform as $\varphi \to \varphi + \nu\chi$ which identifies it as a *phase field*. Note then that the first term is separately invariant under gauge transformations while the terms on the second line have exactly cancelling gauge variations. The combination of the two *anomalous* terms are together gauge-invariant.

To see that φ represents a chiral boson, one can choose the different gauge fixing condition $b_{\tilde{0}} \equiv b_0 - ub_x = 0$, or equivalently add the gauge invariant potential term $-u/4\pi\nu\,(\partial_x\varphi - \nu A_x)^2$ to the Lagrangian density (Wen, 1992). The parameter u can through the resulting equations of motion be interpreted as the velocity of a unidirectional, that is chiral, boson[1] which depends on the details of the edge. Physically, u corresponds to the Hall drift velocity E/B of electrons close to the edge. Note also that the term containing u must be added by hand as some sort of boundary condition, since the topological field theory can not possibly contain any microscopic details on how the edge is formed.

From the action (4.49), one may directly extract the equal time canonical commutation relations (Faddeev and Jackiw, 1988; Jackiw, 1993)[2]

$$[\varphi(x), \partial_{x'}\varphi(x')] = 2\pi i\nu\delta(x - x'), \tag{4.50}$$

which identifies $\frac{1}{2\pi\nu}\partial_x\varphi(x)$ as the canonical momentum conjugate to $\varphi(x)$.

Varying the boundary contribution of the action (4.49) with respect to $-A_0$ and A_x gives respectively the boundary charge $\rho_{\text{edge}} = \frac{1}{2\pi}(\partial_x\varphi - \nu A_x)$ and the boundary current $j_{\text{edge}} = 0$[3]. The equation of motion of φ reads

$$\partial_x(\partial_t\varphi - \nu A_0) = 0, \tag{4.51}$$

Varying the action with respect to A_y gives the bulk current perpendicular to the edge $j_y = -\dot{\rho}_{\text{edge}} = \frac{\nu e^2}{2\pi}E_x$ by use of Eq. (4.51). One can therefore conclude, that while the charge current is not conserved separately on the edge and

[1] In $D = 1+1$, there is no clear distinction between bosons and fermions.

[2] In short, from a Lagrangian density on the form $\mathcal{L} = \frac{1}{2}\xi_i C_{ij}\dot{\xi}_j$, one may directly obtain the commutation relations $[\xi_i, \xi_j] = iC^{-1}_{ij}$.

[3] Note that there is an edge contribution from the last term of the action (4.49).

in the bulk, the total current is and one may write

$$\partial_\mu j^\mu_{\text{bulk}} \neq 0, \tag{4.52a}$$
$$\partial_\mu j^\mu_{\text{edge}} \neq 0, \tag{4.52b}$$
$$\partial_\mu \left(j^\mu_{\text{bulk}} + j^\mu_{\text{edge}} \right) = 0. \tag{4.52c}$$

In the context of quantum Hall physics, this *anomaly cancellation* was first pointed out by Stone (1991), but it is a specific realization of a more general phenomenon discovered by Callan and Harvey (1985). In some sense, it can be viewed as a field theory analogue of the bulk-boundary correspondence (see Sec. 2.5).

Interestingly, charge, thermal, or magnetic dipole responses and their corresponding anomalies provide a definition of topological insulators and superconductors that goes beyond the single-particle picture outlined in Ch. 2, (Ryu *et al.*, 2012; Witten, 2015).

4.5.5 Topological field theory for time-reversal symmetric topological insulators in two dimensions

To construct a field theory for the two dimensional topological insulator described in Sec. 4.4, one can proceed similarly to the IQH treatment, but instead define two conserved spin currents. The topological Lagrangian density reads

$$\mathcal{L} = -\frac{1}{4\pi n_\uparrow} \varepsilon^{\mu\nu\lambda} b_{\uparrow\mu} \partial_\nu b_{\uparrow\lambda} - \frac{1}{4\pi n_\downarrow} \varepsilon^{\mu\nu\lambda} b_{\downarrow\mu} \partial_\nu b_{\downarrow\lambda}, \tag{4.53}$$

and consists of one independent gauge field $b_{\uparrow/\downarrow\mu}$ for each spin direction, corresponding to two separately conserved currents and a $U(1) \times U(1)$ gauge structure. Since the two gauge fields come with opposing signs of their spin Chern numbers, $n_\uparrow + n_\downarrow = 0$, there is no quantum Hall effect, and no chiral edge states. Instead there is one pair of helical edge states which constitute a chiral spin current. However, this construction works only for the special case of spin-conservation, and to capture the more general situation with a single conserved current, one would have to implement some sort of $U(1) \times U(1) \to U(1)$ symmetry breaking. One method of constructing such a model was shown by Chan *et al.* (2013).

4.6 Outlook

The concepts of effective and topological field theories are indispensable tools in the description of TSM. Not only because they are based on fundamental

and strong principles which do not require any microscopic input but also, perhaps more importantly, because they provide a method of going beyond the single particle description. Moreover, field theory unifies the descriptions of TSM and the more complicated topologically ordered systems, and even more interestingly, it bridges the descriptions of condensed matter and high-energy physics.

4.7 Paper IV: Monopole response and a non-local order parameter for the Chern insulator

4.7.1 Motivation

The concept of a local order parameter is not very useful in the description of TSM, since their very definition indicates that local measurements cannot distinguish between such phases of matter. Nonetheless, the concept of *non-local order parameters* could be expected to play a role in distinguishing different topological phases of matter. The goal of this project is to construct and analyze such operators for various topological systems, in particular the two-dimensional integer quantum Hall states and Chern insulators. In the context of quantum Hall physics, the idea of using such operators can be traced back to Girvin and MacDonald (1987) and Read (1989).

One of the ideas in this project is to investigate the behaviour of a certain type of *twist operators*

$$\eta(x_1,x_2,\ldots,x_N) = \exp\left(i \int_{\mathbb{R}^2} d^2x\, \rho(x) \sum_{j=1}^{N} \alpha_j \arg(x-x_j) \right), \tag{4.54}$$

where $\rho(x)$ is the local charge density, α_j are constants and $\arg(x)$ is the argument function, the angle between x and the positive x-axis. The goal is to calculate the ground state expectation value $\langle \eta(x_1,x_2) \rangle$ within a field theory description of a Chern insulator. Based on numerical calculations, it is expected that the long range behaviour of those operators is given by

$$\langle GS|\eta(x_1,x_2)|GS\rangle \sim |x_1-x_2|^{-\alpha} \quad \text{for } \nu = 0, \tag{4.55a}$$

$$\langle GS|\eta(x_1,x_2)|GS\rangle \sim e^{-|x_1-x_2|/\xi} \quad \text{for } \nu = 1, \tag{4.55b}$$

where α and ξ are some microscopic constants. Hence the operator $\eta(x_1,x_2)$ has a distinct behaviour in the two regimes, and can be used as a non-local order parameter.

4.7.2 Preliminary results

The first important insight, which forms the basis of the numerical calculations, is that $\eta(x_1,x_2)$ can be interpreted as the overlap of the Chern insulator ground state before and instantaneously after the insertion of two oppositely oriented flux-tubes of flux $\pm 2\pi$ positioned at x_1 and x_2 respectively. This observation leads directly to calculating the ground state response to such a perturbation. In the trivial $\nu = 0$ phase, the appropriate response action is the dielectric and

diamagnetic Maxwell action

$$\Gamma[A] = \int d^3x \left(\frac{\alpha}{4\pi} E^2 - \frac{\beta}{4\pi} B^2 \right), \tag{4.56}$$

where α and β are constants depending on the microscopic details, and E and B are the electrical and magnetic fields respectively. The expectation value of the charge density, $\langle \rho(x) \rangle$ can be obtained from Eq. (4.39). Through the cumulant expansion, one obtains $\langle \eta(x_1, x_2) \rangle = K|x_1 - x_2|^{-\alpha}$, where K is a constant and α is the dielectric constant. Hence, this calculation confirms Eq. (4.55a).

Attempting to repeat the calculation for the topological phase, there are several new features that need to be taken into consideration. First of all, the appropriate response action is now the sum of the actions (4.31) and (4.56). The second important insight is that the flux insertion depicted above can be viewed as two two-dimensional monopole configurations, which are known to complicate the Chern-Simons theory (Henneaux and Teitelboim, 1986; Pisarski, 1986; Affleck *et al.*, 1989; Diamantini *et al.*, 1993; Grigorio *et al.*, 2011). One of the reasons for the difficulty is that monopole configurations necessarily introduce boundaries into the theory, which in turn indicates that the response theory is not valid anymore, because of the presence of chiral bosons on the boundaries. Hence, the calculation of $\langle \eta(x_1, x_2) \rangle$ must, in some way or another, take these bosons into account. At the time of writing, this is ongoing work.

5. Epilogue

THE THEME OF THIS THESIS is the description of topological states of matter (TSM). In some aspects, this class of matter can be thought of as a simpler version of topologically ordered states of matter, in the sense that it can be understood in terms of free fermions and ordinary band theory rather than through models of complicated strongly correlated and interacting systems. Nevertheless, TSM constitute a remarkable class of matter, whose relatively simple description brings together a wide range of topics in mathematics and physics.

The outline of a general framework of describing TSM was presented in Ch. 2. The main idea was to classify non-interacting, gapped, and free fermion systems in various space dimensions according to their transformation properties under anti-unitary quantum mechanical symmetries. This classification is built on well-known concepts from ordinary band theory and quantum theory, but in combination with more abstract mathematical structures such as *random matrix theory*, *algebraic topology* and *K-theory*. The result of this classification, in addition to putting earlier work from the 1980's in a broader context, is a periodic table reminiscent of Mendelevs periodic table of the elements. Each entry of this table, known as a symmetry class and labelled with the aforementioned properties, is assigned a $\mathbb{Z}_2$, $\mathbb{Z}$ or vanishing group which determines the number of topologically distinct Hamiltonians (or ground states). The classification is quite general since it is based on antiunitary symmetries which are very basic symmetries, expected to persist the presence of disorder and randomness. On the other hand, the introduction of additional unitary symmetries, such as crystal symmetries, has been shown to be just as important and extends the classification further. Ongoing work is also to expand the classification to bosons, interacting systems, non-equilibrium systems, and gapless systems.

Ch. 3 treated topological superconductivity in one-dimensional systems and is the foundation for the enclosed PAPERS I-III. Ettore Majorana's prediction of a self-conjugate fermionic elementary particle has been appreciated in recent years to be realized in condensed matter by ordinary quasiparticles in weakly interacting superconductors. Such Majorana fermions must however not be confused with their more exotic relative: the Majorana zero mode, which is not a fermion but a non-Abelian anyon. Such modes appear as topo-

logical defects in a certain class of superconductors, called topological superconductors which are included in the classification of TSM. Topological superconductors can not be adiabatically transformed into ordinary superconductors without closing the superconducting gap, identifying them as a distinct phase of matter. Moreover, the lack of naturally occurring candidates of topological superconductors has spurred a tremendous effort in designing such systems artificially by combining widely accessible experimental building blocks available from nanotechnology. Presently, the research field of Majorana zero modes is also one of the most pursued experimental routes towards topologically protected quantum computations.

The theme of Ch. 4 was the quantum field theoretical description of TSM. In addition to introducing the archetype TSM, the integer quantum Hall effect, and its more recent descendants, the chapter contained a discussion on how quantum field theory can be used to describe such systems. Specifically, it was argued that effective response actions capture the electromagnetic response of TSM, but to retain electromagnetic gauge invariance, topological field theory naturally enters the description. These field theories were argued to be independent of any microscopical details and accordingly, they capture the very essence of TSM. Most interestingly, topological field theories also connect the bulk and the boundary properties of TSM in a natural way through anomaly-cancellation: the theories of the bulk and the boundary are by themselves anomalous, they violate some fundamental conservation law, but in combination they are consistent. Hence, TSM provide experimental platforms for physical systems that can not appear in isolation. The chapter also discussed briefly the classification of TSM in terms of edge anomalies. Such a classification is not only a complement to the classification of Ch. 2, but contains also additional strong statements regarding TSM with interactions.

To conclude this thesis it certainly appropriate to extend the core principles stated in the introduction with the obvious additional entry:

Topology concerns the notion that in many physical systems, it is the global features, invisible by local measurements, that are important. In particular, there are states of matter that must be distinguished by their topological properties rather than by Landau's symmetry breaking principle. Such topological states of matter can be expected to have emergent robust properties, independent of their microscopic details, which make them suitable for metrology, quantum sensing and quantum computations.

While it is fair to say that concrete and mainstream applications of topological systems are still in the starting grounds, the prediction and verification of TSM is without doubt an additional triumph of theoretical physics. One can expect, on the other hand, that the door to the world of topological quantum matter has only been opened slightly.

A. The Pfaffian and the superconducting ground state parity

THE *Pfaffian* of a $2n \times 2n$ anti-symmetric matrix $A = -A^T$, denoted as $\mathrm{Pf}(A)$, is defined in terms of the totally antisymmetric tensor $\varepsilon_{i_1,i_2,\ldots,i_{2n}}$ as

$$\mathrm{Pf}(A) = \frac{1}{2^n n!} \varepsilon_{i_1,i_2,\ldots,i_{2n}} A_{i_1,i_2} A_{i_3,i_4} \ldots A_{i_{2n-1},i_{2n}}. \tag{A.1}$$

For the simple cases of $n = 1$ and $n = 2$, the Pfaffians are explicitly given by

$$\mathrm{Pf}\begin{pmatrix} 0 & a \\ -a & 0 \end{pmatrix} = a, \tag{A.2}$$

and

$$\mathrm{Pf}\begin{pmatrix} 0 & a_{12} & a_{13} & a_{14} \\ -a_{12} & 0 & a_{23} & a_{24} \\ -a_{13} & -a_{23} & 0 & a_{34} \\ -a_{14} & -a_{24} & -a_{34} & 0 \end{pmatrix} = a_{12}a_{34} + a_{14}a_{23} - a_{13}a_{24}, \tag{A.3}$$

respectively. Given some constant λ and an arbitrary $2n \times 2n$ matrix B, the Pfaffian has the following properties

$$\mathrm{Pf}(A^T) = (-1)^n \mathrm{Pf}(A). \tag{A.4a}$$
$$\mathrm{Pf}(\lambda A) = \lambda^n \mathrm{Pf}(A). \tag{A.4b}$$
$$\mathrm{Pf}(A)^2 = \det(A). \tag{A.4c}$$
$$\mathrm{Pf}(BAB^T) = \det(B)\mathrm{Pf}(A). \tag{A.4d}$$

In some sense, the Pfaffian is the square root of the determinant, and as will be shown next, it can be used to calculate the ground state parity of a one-dimensional superconductor. The discussion closely follows Kitaev (2001). Any BdG-Hamiltonian can be written on a general Majorana form according to

$$\mathcal{H} = \frac{i}{2} \sum_{i,j} \gamma_i^T A_{ij} \gamma_j, \tag{A.5}$$

where, $\gamma_j = (\gamma_{Aj}, \gamma_{Bj})^T$ and the matrix A is even-dimensional, real and anti-symmetric. As such, it has strictly imaginary eigenvalues that come in complex conjugate pairs $\pm i\varepsilon_\lambda$, where $\varepsilon_\lambda \geq 0$. The matrix can always be brought to a *block diagonal form* with a real orthogonal transformation W

$$A_J = WAW^T = \mathrm{diag}_\lambda \begin{pmatrix} 0 & \varepsilon_\lambda \\ -\varepsilon_\lambda & 0 \end{pmatrix}, \tag{A.6}$$

so that Hamiltonian is in its *canonical form*

$$\mathcal{H}_{\mathrm{Canonical}} = \frac{i}{2}\sum_{ij} \tilde{\gamma}_i^T A_{Jij} \tilde{\gamma}_j = \sum_\lambda \varepsilon_\lambda \left[a_\lambda^\dagger a_\lambda - \frac{1}{2} \right], \tag{A.7}$$

where $\tilde{\gamma}_j$ are linear combinations of γ_j and $a_\lambda = \frac{1}{2}(\tilde{\gamma}_{Aj} + i\tilde{\gamma}_{Bj})$, $a_\lambda^\dagger = \frac{1}{2}(\tilde{\gamma}_{Aj} - i\tilde{\gamma}_{Bj})$ is a set of ordinary fermions. In the canonical form, the fermion parity of the ground state, $P_0(\mathcal{H}_{\mathrm{Canonical}})$, is by definition even, since it consists of emptying all a_λ-fermion states. This feature is captured by defining

$$P_0(\mathcal{H}_{\mathrm{Canonical}}) \equiv \mathrm{sgn}\{\mathrm{Pf}(A_J)\} = \mathrm{sgn}\{\prod_\lambda \varepsilon_\lambda\} = +1. \tag{A.8}$$

From Eq. (A.4d), it follows that $\mathrm{Pf}(A_J) = \mathrm{Pf}(WAW^T) = \mathrm{Pf}(A)\det(W)$ and consequently

$$P_0(\mathcal{H}) = \mathrm{sgn}\{\det(W)\} = \mathrm{sgn}\{\mathrm{Pf}(A)\}. \tag{A.9}$$

Assume now that $\mathcal{H}$ is continuously deformed, by changing some parameter, and a single eigenvalue, say ε_μ, crosses zero. Then the μ:th block in A_J would change sign and to restore the canonical form, one must act with the transformation $W_\mu = \mathrm{diag}(0,0,\ldots,\sigma_x,\ldots,0)$ where the Pauli-x matrix acts on block μ only. Since $\det(W_\mu) = -1$ it follows that the ground state parity necessarily changes with such an energy crossing.

Consider now a translationally invariant system, with N sites and n fermionic degrees of freedom per site. One can then index a set of Majorana operators $\gamma_{l\alpha}$ with $m = l,\ldots,N$ and $\alpha = 1,\ldots,2n$. The Hamiltonian can be written as

$$\mathcal{H} = \frac{i}{2}\sum_{l,m}\sum_{\alpha,\beta} A_{\alpha\beta}(l-m)\gamma_{l\alpha}\gamma_{m\beta}. \tag{A.10}$$

Due to the translational invariance $m-l$ should be taken mod N. Moreover, the matrix $A_{\alpha\beta}(l-m)$ can be Fourier transformed into

$$\tilde{A}_{\alpha\beta}(k) = \sum_j e^{ikj} A_{\alpha\beta}(j), \tag{A.11}$$

where the matrix $\tilde{A}(k)$ has the symmetries

$$\tilde{A}^{\dagger}(k) = -\tilde{A}(k) = \tilde{A}^{T}(-k). \tag{A.12}$$

The sets of Bloch momenta are given by

$$\begin{cases} k = 2m\pi/N, & m = 0,1,\ldots,N-1, \quad \text{for PBC} \\ k = (2m+1)\pi/N, & m = 0,1,\ldots,N-1, \quad \text{for APBC} \end{cases} \tag{A.13}$$

where the two cases of periodic or anti-periodic boundary conditions have been distinguished. At this point, it is useful to pay some extra attention to the particle-hole symmetric momenta $k = -k$ which are fulfilled by $k = 0$ and $k = \pi$. The first of these momenta belongs to both sets regardless of N being even or odd, while the point $k = \pi$ only exists for N even and PBC or N odd and APBC.

The Pfaffian of A can now be evaluated in k-space where it is block diagonal:

$$\begin{aligned} \mathrm{Pf}(A) &= \prod_{k} \mathrm{Pf}\left(\tilde{A}(k)\right) = \prod_{k\neq -k} \mathrm{Pf}\left(\tilde{A}(k)\right) \prod_{k=-k} \mathrm{Pf}\left(\tilde{A}(k)\right) \\ &= \prod_{k>0} \mathrm{Pf}\left(\tilde{A}(k)\right) \mathrm{Pf}\left(\tilde{A}(-k)\right) \prod_{k=-k} \mathrm{Pf}\left(\tilde{A}(k)\right) \\ &= \prod_{k>0} \det\left(\tilde{A}(k)\right) \prod_{k=-k} \mathrm{Pf}\left(\tilde{A}(k)\right), \end{aligned} \tag{A.14}$$

where in the final step, Eq. (A.4a) and Eq. (A.4c) have been used. Since $\det\left(\tilde{A}(k)\right) = i^{-2n}\det\left(i\tilde{A}(k)\right) = i^{-2n}\prod_n \varepsilon_n = i^{-2n}\prod_{n>0} -\varepsilon_n^2 = (-1)^n(-1)^n\prod_n \varepsilon_n^2 > 0$, it follows that

$$\mathrm{sgn}\{\mathrm{Pf}(A)\} = \prod_{k=-k} \mathrm{sgn}\{\mathrm{Pf}\left(\tilde{A}(k)\right)\}. \tag{A.15}$$

Consequently, in k-space, the ground state parity is highly sensitive to the boundary conditions and whether there is an even or odd number of sites:

$$P_0(\mathcal{H}) = \begin{cases} \mathrm{sgn}\{\mathrm{Pf}\left(\tilde{A}(0)\right)\}\mathrm{sgn}\{\mathrm{Pf}\left(\tilde{A}(\pi)\right)\} & \text{for } N \text{ even and PBC} \\ \mathrm{sgn}\{\mathrm{Pf}\left(\tilde{A}(0)\right)\} & \text{for } N \text{ odd and PBC} \\ +1, & \text{for } N \text{ even and APBC} \\ \mathrm{sgn}\{\mathrm{Pf}\left(\tilde{A}(\pi)\right)\} & \text{for } N \text{ odd and APBC.} \end{cases} \tag{A.16}$$

The ground state parity alone is therefore not enough to distinguish between the two phases of the Kitaev chain model. Instead the invariant can elegantly be defined as

$$\nu = P_0^{pbc}(\mathcal{H})P_0^{apbc}(\mathcal{H}) = \mathrm{sgn}\{\mathrm{Pf}\left(\tilde{A}(0)\right)\}\mathrm{sgn}\{\mathrm{Pf}\left(\tilde{A}(\pi)\right)\}, \tag{A.17}$$

where the presence of MZMs of the open system is always indicated by $\nu = -1$, regardless of the even-oddness of N or the boundary conditions.

One interesting aspect of the expression (A.17) is that it can be interpreted as closing the chain into a ring, and comparing the ground state parities when zero flux $\Phi = 0$, and a superconducting flux quantum $\Phi = h/2e = \pi$ (in units where $\hbar = h/2\pi = e = 1$) respectively are threaded through the ring. If the parities are different, corresponding to an odd number of fermion parity switches, another flux quantum must be threaded through the ring for the system to come back to the ground state. This property is closely related to the 4π-Josephson effect.

Acknowledgments

TO WRITE A THESIS AND COMPLETE A PHD DEGREE is an endeavour certainly not completed in isolation. I therefore want thank those that have helped me make this achievement possible.

First and foremost, I want to express my deepest gratitude to my main supervisor *Eddy Ardonne*. Not only for accepting me as a PhD student, but in particular for his professional expertise, enthusiasm, cheerfulness, and never-ending encouragement. I am also extremely grateful for the freedom he has given me to pursue research of my own liking and for all his proofreading and feedback on papers, theses, seminars and job applications, especially during the last couple of hectic weeks.

I am also extremely grateful for having had *Hans Hansson* as my co-supervisor. His constant support, open door policy, feedback and guidance in a wide variety of matters has been invaluable during my studies. I have also very much enjoyed our many lunch discussions, especially those about words and language.

Besides my supervisors, I want to thank *Jan Budich*, *Thomas Kvorning*, *AtMa Chan*, and *Shinsei Ryu* for additional fruitful research collaboration. Thomas deserves an extra big thanks for being a very nice travel partner, but especially for the hard work on our joint project during the last weeks before completing this thesis.

During the past years, I have had the pleasure to pursue my degree in an amazing environment with fantastic colleagues who will be deeply missed. In particular, I want to thank *Mikael Fremling* for his fantastic guidance during my first days as a PhD student, *Babak Majidzadeh Garjani* for all the nice gym sessions together and our discussions about life, physics and mathematics, my dear present room mates *Iman Mahyaeh* and *Axel Gagge* for their friendliness and for their valuable input on my projects, and *Ole Andersson* for patiently and pedagogically answering all my questions on geometry and topology and also for his proofreading of this thesis.

Many thanks also go to *Supriya Krishnamurthy* and *Fawad Hassan* for all the listening, all the car rides and for your continuous encouragement, *Emil Bergholtz*, *Jonas Kjäll* and *Jonas Larsson* for all guidance and support during my job applications, *Sören Holst* for fruitful and inspiring collaboration on the mechanics courses, and *Flore Kunst* and *Yaron Kedem* for pleasant travels.

During the early stage of my PhD studies, I had the great fortune to spend one week at the physics department at Lund University. This visit was hosted by *Hongqi Xu*, *Martin Leijnse*, *Chunlin Yu*, and *Simon Abay Gebrehiwot*, to whom I want to express my sincerest thanks.

I am also thankful for the many discussions with my fellow condensed matter Chalmerist *Pontus Laurell*, and for his kind invitations to both the University of Texas in Austin and to his home.

During my PhD studies, I have had the fortune of attending various conferences and schools. This has partly been possible due to two generous travelling stipends from *Knut och Alice Wallenbergs stiftelse* and *Fonden för främjandet av fysikalisk forskning* which are gratefully acknowledged.

There are also many people, not explicitly related to my doctoral studies, but since they have been part of my life during the past years, still they have been extremely instrumental to the completion of this thesis.

I want to thank *Viktoria Larsson*, the outstanding coach of the Albanova gym, for teaching me the fine art of powerlifting. The training sessions with her and the other members of the gym has been a true highlight during my studies.

My dear Stockholm and Göteborg friends: especially *Erik Lindstedt*, my partner in science, for all our discussions about life as a PhD student, *Eric Björklund* for all the food, fun, and beer, *Viktor Andersson* for all the coffee and nice sessions of Dota2-watching, *Christer Lidén* and *Riina Turunen* for all your support and wonderful dinners, and *Joel Rundberg* and *Ebba Strömberg* for all the good times together as friends and fellow parents during the last couple of years of my studies.

I also want to express my sincerest gratitude to my brother *David Spånslätt*, my parents *Jan* and *Caroline Spånslätt*, and my parents-in-law *Olof* and *Anna Rugarn* for all their care, support and encouragement. *Olof* is further gratefully acknowledged for the thorough proofreading of this thesis.

Last, but definitely not least, I want to thank my wonderful family: *Elin Rugarn*, my amazing wife and best friend, for her understanding, encouragement, endurance, love and care, and my children *Edith* and *Sam Rugarn* for being the joy of my life. It is my hope that one day you will also pursue and fulfill your dreams, whatever they may be.

Christian Spånslätt,
Stockholm, April 23, 2018

Bibliography

Adler, S. L. (1969), Phys. Rev. **177**, 2426.

Affleck, I., J. Harvey, L. Palla, and G. Semenoff (1989), Nuclear Physics B **328** (3), 575.

Aharonov, Y., and D. Bohm (1959), Phys. Rev. **115**, 485.

Akhmerov, A. R., J. P. Dahlhaus, F. Hassler, M. Wimmer, and C. W. J. Beenakker (2011), Phys. Rev. Lett. **106**, 057001.

Akhmerov, A. R., J. Sau, B. van Heck, R. Skolasinski, and S. Rubbert (2015), "Topology in condensed matter: Tying quantum knots," .

Alicea, J. (2012), Rep. Prog. Phys. **75** (7), 076501.

Alicea, J., and P. Fendley (2016), Annual Review of Condensed Matter Physics **7** (1), 119.

Alicea, J., Y. Oreg, G. Refael, F. von Oppen, and M. P. A. Fisher (2011), Nature Physics **7**, 412 EP .

Altland, A., and B. Simons (2010), *Condensed matter field theory*, 2nd ed. (Cambridge University Press).

Altland, A., and M. R. Zirnbauer (1997), Phys. Rev. B **55**, 1142.

Andreev, A. (1964), Sov. Phys. JETP **19** (5), 1490.

Ashcroft, N., and N. Mermin (1976), *Solid State Physics*, 1st ed. (Brooks Cole).

Atiyah, M. F., and I. M. Singer (1968), Annals of Mathematics **87** (3), 484.

Avignone, F. T., S. R. Elliott, and J. Engel (2008), Rev. Mod. Phys. **80**, 481.

Avron, J. E., and R. Seiler (1985), Phys. Rev. Lett. **54**, 259.

Avron, J. E., R. Seiler, and B. Simon (1983), Phys. Rev. Lett. **51**, 51.

Bagrets, D., and A. Altland (2012), Phys. Rev. Lett. **109**, 227005.

Bardarson, J. H. (2008), J. Phys. A **41** (40), 405203.

Bardeen, J., and W. H. Brattain (1948), Phys. Rev. **74**, 230.

Beenakker, C. W. J. (1991), Phys. Rev. Lett. **67**, 3836.

Beenakker, C. W. J. (2012), in *Quantum Mesoscopic Phenomena and Mesoscopic Devices in Microelectronics*, edited by I. Kulik and R. Ellialtioglu (Springer Netherlands).

Beenakker, C. W. J. (2015), Rev. Mod. Phys. **87**, 1037.

Bell, J. S., and R. Jackiw (1969), Il Nuovo Cimento A **60** (1), 47.

Béri, B., J. N. Kupferschmidt, C. W. J. Beenakker, and P. W. Brouwer (2009), Phys. Rev. B **79**, 024517.

Bernevig, B. A., and T. L. Hughes (2013), *Topological insulators and topological superconductors*, 1st ed. (Princeton University Press).

Bernevig, B. A., T. L. Hughes, and S.-C. Zhang (2006), Science **314** (5806), 1757.

Berry, M. V. (1984), Proc. Roy. Soc. of London A **392** (1802), 45.

Blonder, G. E., M. Tinkham, and T. M. Klapwijk (1982), Phys. Rev. B **25**, 4515.

Bott, R. (1959), Annals of Mathematics , 313.

Budich, J. C., and S. Diehl (2015), Phys. Rev. B **91**, 165140.

Büttiker, M. (1988), Phys. Rev. B **38**, 9375.

Callan, C., and J. Harvey (1985), Nuclear Physics B **250** (1), 427 .

Caroli, C., P. D. Gennes, and J. Matricon (1964), Phys. Lett. **9** (4), 307 .

Cartan, E. (1926), Bull. Soc. Math. France **54**, 214.

Cayssol, J., B. Dóra, F. Simon, and R. Moessner (2013), Phys. Stat. Sol. (RRL) **7**, 101.

Chamon, C., R. Jackiw, Y. Nishida, S.-Y. Pi, and L. Santos (2010), Phys. Rev. B **81**, 224515.

Chan, A., T. L. Hughes, S. Ryu, and E. Fradkin (2013), Phys. Rev. B **87**, 085132.

Chern, S.-S., and J. Simons (1974), Annals of Mathematics **99** (1), 48.

Choy, T.-P., J. M. Edge, A. R. Akhmerov, and C. W. J. Beenakker (2011), Phys. Rev. B **84**, 195442.

Das, A., Y. Ronen, Y. Most, Y. Oreg, M. Heiblum, and H. Shtrikman (2012), Nature Physics **8**, 887 EP .

Datta, S. (1997), *Electronic Transport in Mesoscopic Systems*, 1st ed. (Cambridge University Press).

Deng, M. T., C. L. Yu, G. Y. Huang, M. Larsson, P. Caroff, and H. Q. Xu (2012), Nano Letters **12** (12), 6414.

Diamantini, M. C., P. Sodano, and C. A. Trugenberger (1993), Phys. Rev. Lett. **71**, 1969.

Dirac, P. A. M. (1928), Proc. Roy. Soc. of London A **117** (778), 610.

Dirac, P. A. M. (1931), Proc. Roy. Soc. of London A **133** (821), 60.

Dittes, F.-M. (2000), Physics Reports **339** (4), 215 .

Dunne, G. V. (1999), in *Les Houches lecture series: Topological Aspects of Low Dimensional Systems*, edited by A. Comtet, T. Jolicoeur, S. Ouvry, and F. David, Chap. 3 (Springer Verlag Berlin Heidelberg).

Dyson, F. J. (1962), J. of Math. Phys. **3** (6), 1199.

Eddington, A. (1928), Proc. Roy. Soc. of London A **121** (788), 524.

Elliott, S. R., and M. Franz (2015), Rev. Mod. Phys. **87**, 137.

Faddeev, L., and R. Jackiw (1988), Phys. Rev. Lett. **60**, 1692.

Fidkowski, L., J. Alicea, N. H. Lindner, R. M. Lutchyn, and M. P. A. Fisher (2012), Phys. Rev. B **85**, 245121.

Fidkowski, L., and A. Y. Kitaev (2010), Phys. Rev. B **81**, 134509.

Flensberg, K. (2010), Phys. Rev. B **82**, 180516.

Freedman, M., A. Kitaev, M. Larsen, and Z. Wang (2003), Bull. Am. Math. Soc. **40** (1), 31.

Fu, L., and C. L. Kane (2008), Phys. Rev. Lett. **100**, 096407.

Fu, L., and C. L. Kane (2009), Phys. Rev. B **79**, 161408.

Fu, L., C. L. Kane, and E. J. Mele (2007), Phys. Rev. Lett. **98**, 106803.

Fulga, I. C., F. Hassler, and A. R. Akhmerov (2012), Phys. Rev. B **85**, 165409.

Fulga, I. C., F. Hassler, A. R. Akhmerov, and C. W. J. Beenakker (2011), Phys. Rev. B **83**, 155429.

Girvin, S. M., and A. H. MacDonald (1987), Phys. Rev. Lett. **58**, 1252.

Grigorio, L. S., M. S. Guimaraes, R. Rougemont, and C. Wotzasek (2011), Journal of High Energy Physics **2011** (8), 118.

Haberkorn, W., H. Knauer, and J. Richter (1978), Phys. Stat. Sol. A **47** (2), K161.

Haim, A., E. Berg, F. von Oppen, and Y. Oreg (2015), Phys. Rev. B **92**, 245112.

Haldane, F. D. M. (1981), J. Phys. C **14** (19), 2585.

Haldane, F. D. M. (1988), Phys. Rev. Lett. **61**, 2015.

Hall, E. H. (1879), Am. J. Math. **2** (3), 287.

Halperin, B. I. (1982), Phys. Rev. B **25**, 2185.

Halperin, B. I., Y. Oreg, A. Stern, G. Refael, J. Alicea, and F. von Oppen (2012), Phys. Rev. B **85**, 144501.

Hansson, T. H., M. Hermanns, S. H. Simon, and S. F. Viefers (2017), Rev. Mod. Phys. **89**, 025005.

Hasan, M. Z., and C. L. Kane (2010), Rev. Mod. Phys. **82**, 3045.

He, J. J., T. K. Ng, P. A. Lee, and K. T. Law (2014), Phys. Rev. Lett. **112**, 037001.

Henneaux, M., and C. Teitelboim (1986), Phys. Rev. Lett. **56**, 689.

Herring, C. (1937), Phys. Rev. **52**, 365.

Hsieh, D., D. Qian, L. Wray, Y. Xia, Y. S. Hor, R. J. Cava, and M. Z. Hasan (2008), Nature **452**, 970 EP .

Ivanov, D. A. (2001), Phys. Rev. Lett. **86**, 268.

Jackiw, R. (1993), arXiv preprint hep-th/9306075 .

Jotzu, G., M. Messer, R. Desbuquois, M. Lebrat, T. Uehlinger, D. Greif, and T. Esslinger (2014), Nature **515**, 237 EP .

Kallin, C. (2012), Rep. Prog. Phys. **75** (4), 042501.

Kane, C. L. (2013), in *Contemporary Concepts of Condensed Matter Science: Topological Insulators*, edited by M. Franz and L. W. Molenkamp (Elsevier Science).

Kane, C. L., and E. J. Mele (2005a), Phys. Rev. Lett. **95**, 146802.

Kane, C. L., and E. J. Mele (2005b), Phys. Rev. Lett. **95**, 226801.

Karlhede, A., S. Kivelson, and S. Sondhi (1993), in *Correlated Correlated electron systems: Proceedings of the 9th Jerusalem Winter School*, edited by V. J. Emery (World Scientific).

Kitaev, A. Y. (2001), Physics-Uspekhi **44** (10S), 131.

Kitaev, A. Y. (2003), Annals of Physics **303** (1), 2 .

Kitaev, A. Y. (2009), AIP Conference Proceedings **1134** (1), 22.

Kitagawa, T., E. Berg, M. Rudner, and E. Demler (2010), Phys. Rev. B **82**, 235114.

Kohmoto, M. (1985), Annals of Physics **160** (2), 343 .

König, M., S. Wiedmann, C. Brüne, A. Roth, H. Buhmann, L. W. Molenkamp, X.-L. Qi, and S.-C. Zhang (2007), Science **318** (5851), 766.

Kubo, R. (1957), J. Phys. Soc. Jpn. **12** (6), 570.

Kvorning, T., T. H. Hansson, A. Quelle, and C. M. Smith (2017), arXiv preprint arXiv:1709.00482 .

Kwon, H.-J., V. M. Yakovenko, and K. Sengupta (2004), Low Temp. Phys. **30** (7), 613.

Landau, L. (1930), Z. Phys. **64** (9), 629.

Landau, L. (1937), Phys. Z. Sowjetunion **11**, 26.

Landau, L., and E. Lifshitz (1980), *Statistical physics*, 3rd ed., Vol. 5 (Elsevier).

Laroche, D., D. Bouman, D. J. van Woerkom, A. Proutski, C. Murthy, D. I. Pikulin, C. Nayak, R. J. van Gulik, J. Nygård, P. Krogstrup, L. P. Kouwenhoven, and A. Geresdi (2017), arXiv preprint arXiv:1712.08459 .

Laughlin, R. B. (1981), Phys. Rev. B **23**, 5632.

Laughlin, R. B. (1983), Phys. Rev. Lett. **50**, 1395.

Laughlin, R. B. (1988), Nobel lecture: Nobel Media AB 2014 .

Lauterbur, P. C. (1973), Nature **242**, 190.

Law, K. T., P. A. Lee, and T. K. Ng (2009), Phys. Rev. Lett. **103**, 237001.

Leinaas, J. M., and J. Myrheim (1977), Il Nuovo Cimento B (1971-1996) **37** (1), 1.

Liu, J., A. C. Potter, K. T. Law, and P. A. Lee (2012), Phys. Rev. Lett. **109**, 267002.

Lutchyn, R. M., J. D. Sau, and S. Das Sarma (2010), Phys. Rev. Lett. **105**, 077001.

Mahaux, C., and H. A. Weidenmüller (1969), *Shell-Model Approach to Nuclear Reactions* (North-Holland, Amsterdam).

Majorana, E. (1937), Il Nuovo Cimento (1924-1942) **14** (4), 171.

Moore, J. E., and L. Balents (2007), Phys. Rev. B **75**, 121306.

Mourik, V., K. Zuo, S. M. Frolov, S. R. Plissard, E. P. A. M. Bakkers, and L. P. Kouwenhoven (2012), Science **336** (6084), 1003.

Nadj-Perge, S., I. K. Drozdov, B. A. Bernevig, and A. Yazdani (2013), Phys. Rev. B **88**, 020407.

Nadj-Perge, S., I. K. Drozdov, J. Li, H. Chen, S. Jeon, J. Seo, A. H. MacDonald, B. A. Bernevig, and A. Yazdani (2014), Science **346** (6209), 602.

Nakahara, M. (2003), *Geometry, topology and physics* (CRC Press).

Nayak, C., S. H. Simon, A. Stern, M. Freedman, and S. Das Sarma (2008), Rev. Mod. Phys. **80**, 1083.

Nazarov, Y., and Y. Blanter (2009), *Quantum Transport: Introduction to Nanoscience*, 1st ed. (Cambridge University Press).

Nielsen, H., and M. Ninomiya (1981), Physics Letters B **105** (2), 219 .

Nilsson, J., A. R. Akhmerov, and C. W. J. Beenakker (2008), Phys. Rev. Lett. **101**, 120403.

Niu, Q., D. J. Thouless, and Y.-S. Wu (1985), Phys. Rev. B **31**, 3372.

Oreg, Y., G. Refael, and F. von Oppen (2010), Phys. Rev. Lett. **105**, 177002.

Osca, J., D. Ruiz, and L. Serra (2014), Phys. Rev. B **89**, 245405.

Pientka, F., L. I. Glazman, and F. von Oppen (2014a), Phys. Rev. B **89**, 180505.

Pientka, F., G. Kells, A. Romito, P. W. Brouwer, and F. von Oppen (2012), Phys. Rev. Lett. **109**, 227006.

Pientka, F., Y. Peng, and F. von Oppen (2014b), in *Les Houches lecture series: Topological Aspects of Condensed Matter Physics*, edited by C. Chamon, M. O. Goerbig, R. Moessner, , and L. F. Cugliandolo, Chap. 9 (Oxford University Press).

Pisarski, R. D. (1986), Phys. Rev. D **34**, 3851.

Prange, R. E. (1981), Phys. Rev. B **23**, 4802.

Qi, X.-L., T. L. Hughes, and S.-C. Zhang (2008), Phys. Rev. B **78**, 195424.

Qi, X.-L., Y.-S. Wu, and S.-C. Zhang (2006), Phys. Rev. B **74**, 085308.

Read, N. (1989), Phys. Rev. Lett. **62**, 86.

Read, N., and D. Green (2000), Phys. Rev. B **61**, 10267.

Rex, S., and A. Sudbø (2014), Phys. Rev. B **90**, 115429.

Rokhinson, L. P., X. Liu, and J. K. Furdyna (2012), Nature Physics **8**, 795 EP .

Roth, A., C. Brüne, H. Buhmann, L. W. Molenkamp, J. Maciejko, X.-L. Qi, and S.-C. Zhang (2009), Science **325** (5938), 294.

Roy, R. (2009), Phys. Rev. B **79**, 195322.

Roy, R., and F. Harper (2017), Phys.

Rev. B **96**, 155118.
Ryu, S., J. E. Moore, and A. W. W. Ludwig (2012), Phys. Rev. B **85**, 045104.
Ryu, S., A. P. Schnyder, A. Furusaki, and A. W. W. Ludwig (2010), New J. Phys. **12** (6), 065010.
Sakurai, J., and J. Napolitano (2011), *Modern quantum mechanics* (Addison-Wesley).
Sato, M., and Y. Ando (2017), Rep. Prog. Phys. **80** (7), 076501.
Schnyder, A. P., S. Ryu, A. Furusaki, and A. W. W. Ludwig (2008), Phys. Rev. B **78**, 195125.
Senthil, T., and M. P. A. Fisher (2000), Phys. Rev. B **61**, 9690.
Shapiro, S. (1963), Phys. Rev. Lett. **11**, 80.
Sheng, D. N., Z. Y. Weng, L. Sheng, and F. D. M. Haldane (2006), Phys. Rev. Lett. **97**, 036808.
Spånslätt, C. (2015), *Topology in One-Dimensional Quantum Systems*, Lic. thesis (Stockholm University).
Stanescu, T. (2017), *Topological Quantum Matter & Quantum Computation*, 1st ed. (CRC Press).
Stone, M. (1991), Annals of Physics **207** (1), 38 .
Su, W. P., J. R. Schrieffer, and A. J. Heeger (1979), Phys. Rev. Lett. **42**, 1698.
Suddards, M. E., A. Baumgartner, M. Henini, and C. J. Mellor (2012), New J. Phys. **14** (8), 083015, (CC BY-NC-SA 3.0).
Takane, Y., and H. Ebisawa (1992), J. Phys. Soc. Jpn. **61** (5), 1685.
Takayama, H., Y. R. Lin-Liu, and K. Maki (1980), Phys. Rev. B **21**, 2388.
Tanaka, Y., and S. Kashiwaya (1995), Phys. Rev. Lett. **74**, 3451.
Tewari, S., and J. D. Sau (2012), Phys. Rev. Lett. **109**, 150408.
Thouless, D. J., M. Kohmoto, M. P. Nightingale, and M. den Nijs (1982), Phys. Rev. Lett. **49**, 405.
Tong, D. (2016), arXiv preprint arXiv:1606.06687 .
Tsui, D. C., H. L. Stormer, and A. C. Gossard (1982), Phys. Rev. Lett. **48**, 1559.
Volovik, G. (2003), *The Universe in a Helium Droplet* (Clarendon Press).
von Klitzing, K., G. Dorda, and M. Pepper (1980), Phys. Rev. Lett. **45**, 494.
von Neumann, J., and E. Wigner (1929), Phys.Z. **30**.
Wan, X., A. M. Turner, A. Vishwanath, and S. Y. Savrasov (2011), Phys. Rev. B **83**, 205101.
Watanabe, H., H. C. Po, M. P. Zaletel, and A. Vishwanath (2016), Phys. Rev. Lett. **117**, 096404.
Wen, X. G. (1990), Int. J. Mod. Phys. B **04** (02), 239.
Wen, X. G. (1992), Int. J. Mod. Phys. B **06** (10), 1711.
Wilczek, F. (1982), Phys. Rev. Lett. **49**, 957.
Witten, E. (2015), arXiv preprint arXiv:1510.07698 .
Xu, S.-Y., I. Belopolski, N. Alidoust, M. Neupane, G. Bian, C. Zhang, R. Sankar, G. Chang, Z. Yuan, C.-C. Lee, S.-M. Huang, H. Zheng, J. Ma, D. S. Sanchez, B. Wang, A. Bansil, F. Chou, P. P. Shibayev, H. Lin, S. Jia, and M. Z. Hasan (2015), Science **349** (6248), 613.
Yntema, G. (1955), Phys. Rev. **98**, 1144.
Yu, P. Y., and M. Cardona (2010), *Fundamentals of semiconductors*, 2nd ed. (Springer).
Zee, A. (1995), "Quantum hall fluids," in *Field Theory, Topology and Condensed Matter Physics*, edited by H. B. Geyer (Springer Berlin Heidelberg, Berlin, Heidelberg) pp. 99–153.
Zhang, H., C.-X. Liu, S. Gazibegovic, D. Xu, J. A. Logan, G. Wang,

N. van Loo, J. D. S. Bommer, M. W. A. de Moor, D. Car, R. L. M. Op het Veld, P. J. van Veldhoven, S. Koelling, M. A. Verheijen, M. Pendharkar, D. J. Pennachio, B. Shojaei, J. S. Lee, C. J. Palmstrom, E. P. Bakkers, S. Das Sarma, and L. P. Kouwenhoven (2017), arXiv preprint arXiv:1710.10701 .

Zheludev, N. (2007), Nature Photonics **1** (4), 189.